Oceanographic Conditions on St. Anns Bank from 2011 to 2017

Chantelle Layton, Dave Hebert, and Roger Pettipas

Fisheries and Oceans Canada
Bedford Institute of Oceanography
P.O. Box 1006
Dartmouth, Nova Scotia
Canada B2Y 4A2

2020

Canadian Technical Report of
Hydrography and Ocean Sciences 333

Fisheries and Oceans Canada | Pêches et Océans Canada

Canada

Canadian Technical Report of Hydrography and Ocean Sciences

Technical reports contain scientific and technical information of a type that represents a contribution to existing knowledge but which is not normally found in the primary literature. The subject matter is generally related to programs and interests of the Oceans and Science sectors of Fisheries and Oceans Canada.

Technical reports may be cited as full publications. The correct citation appears above the abstract of each report. Each report is abstracted in the data base *Aquatic Sciences and Fisheries Abstracts.*

Technical reports are produced regionally but are numbered nationally. Requests for individual reports will be filled by the issuing establishment listed on the front cover and title page.

Regional and headquarters establishments of Ocean Science and Surveys ceased publication of their various report series as of December 1981. A complete listing of these publications and the last number issued under each title are published in the *Canadian Journal of Fisheries and Aquatic Sciences*, Volume 38: Index to Publications 1981. The current series began with Report Number 1 in January 1982.

Rapport technique canadien sur l'hydrographie et les sciences océaniques

Les rapports techniques contiennent des renseignements scientifiques et techniques qui constituent une contribution aux connaissances actuelles mais que l'on ne trouve pas normalement dans les revues scientifiques. Le sujet est généralement rattaché aux programmes et intérêts des secteurs des Océans et des Sciences de Pêches et Océans Canada.

Les rapports techniques peuvent être cités comme des publications à part entière. Le titre exact figure au-dessus du résumé de chaque rapport. Les rapports techniques sont résumés dans la base de données *Résumés des sciences aquatiques et halieutiques*.

Les rapports techniques sont produits à l'échelon régional, mais numérotés à l'échelon national. Les demandes de rapports seront satisfaites par l'établissement auteur dont le nom figure sur la couverture et la page de titre.

Les établissements de l’ancien secteur des Sciences et Levés océaniques dans les régions et à l'administration centrale ont cessé de publier leurs diverses séries de rapports en décembre 1981. Vous trouverez dans l'index des publications du volume 38 du *Journal canadien des sciences halieutiques et aquatiques*, la liste de ces publications ainsi que le dernier numéro paru dans chaque catégorie. La nouvelle série a commencé avec la publication du rapport numéro 1 en janvier 1982.

Canadian Technical Report of
Hydrography and Ocean Sciences 333

2020

OCEANOGRAPHIC CONDITIONS ON ST. ANNS BANK FROM 2011 TO 2017

by

Chantelle Layton, Dave Hebert, and Roger Pettipas

Ocean and Ecosystem Sciences Division,
Fisheries and Oceans Canada
Bedford Institute of Oceanography
P.O. Box 1006
Dartmouth, Nova Scotia
Canada, B2Y 4A2

Cat. No. Fs 97-18/333E-PDF ISBN 978-0-660-34935-0 ISSN 1488-5417

Correct Citation for this publication:

Layton, C., Hebert, D., and Pettipas R.2020. Oceanographic Conditions on St. Anns Bank from 2011 to 2017. Can. Tech. Rep. Hydrogr. Ocean Sci. 333: viii + 86 p.

CONTENTS

List of Tables

List of Figures

ABSTRACT

Layton, C., Hebert, D., and Pettipas R.2020. Oceanographic Conditions on St. Anns Bank from 2011 to 2017. Can. Tech. Rep. Hydrogr. Ocean Sci. 333: viii + 86 p.

St. Anns Bank, a region off Scatarie Island, Nova Scotia, was designated as an Area of Interest (AOI) in 2011. In response, a sampling program in the AOI began in fall 2011, facilitated by the Atlantic Zone Monitoring Program (AZMP). Observations were made in accordance to the AZMP station occupation structure; a selected transect of stations that includes CTD profiles, water samples, and net tows. In addition, these observations were supplemented with moorings equipped with various combinations of CTDs, temperature recorders, and acoustic Doppler current profilers. Here, a brief discussion on data collected during the hydrographic surveys is presented, along with time-series analysis of the mooring observations which includes water column temperature variability, near-bottom hydrographic variability, as well as temporal and spatial velocity variability.

RÉSUMÉ

Layton, C., Hebert, D., and Pettipas R.2020. Oceanographic Conditions on St. Anns Bank from 2011 to 2017. Can. Tech. Rep. Hydrogr. Ocean Sci. 333: viii + 86 p.

Le banc de Sainte-Anne, une région au large de l'île Scatarie, en Nouvelle-Écosse, a été désignée zone d'intérêt en 2011. Due à cela, un programme d'échantillonnage dans cette zone a débuté à l'automne 2011, facilité par le Programme de monitorage de la zone Atlantique (PMZA). Les observations ont été faites conformément à la structure d'occupation des stations PMZA; un transect de stations qui comprend des profils CTD, des échantillons d'eau et des filets. De plus, ces observations ont été complétées par des mouillages équipés de diverses combinaisons de CTDs, de capteurs de température et de courantomètres à effet Doppler. Ici, une brève discussion sur les données recueillies lors des relevés hydrographiques est présentée, ainsi qu'une analyse des séries temporelles provenant des observations des mouillages qui comprend la variabilité de la température dans colonne d'eau, la variabilité hydrographique prés du fond, ainsi que la variabilité temporelle et spatiale de la vitesse des courants.

1 Introduction

In June 2011, St. Anns Bank, an area off the coast of the most eastern tip of Cape Breton Island, Nova Scotia, was designated as an Area of Interest (AOI). The choice of this region was the result of a network-planning exercise using the MARXAN analytical tool for the eastern Scotian shelf region (Kenchington, 2013). The AOI spanned over 5,100 km^2 which encompasses three benthic habitat types, inshore bank, shelf, and slope/channel with the intention to protect ecosystem types that represent the broader region of eastern Scotian shelf and biological features within the region (Kenchington, 2013). The area was designated as a Marine Protected Area (MPA) in June 2017 with re-defined boundaries which includes four zones; one core protection zone and three adaptive management zones. In total, the MPA contributes approximately 4,364 km^2 (0.08%) to the 2020 Marine Conservation Targets (Government of Canada, 2018).

Prior to its designation as an MPA, a monitoring framework for the region was proposed by Kenchington (2013) with 62 suggested indicators. A review on the monitoring framework was conducted and the list was pared down to 51 indicators: nine background indicators, four sub-groups of effective indicators, four related to the benthic environment, eight related to fish and fishery resources, four related to marine mammals, seabird, and reptiles, and three in the category of other, and 23 activity and threat indicators (DFO, 2014). This report will focus on one of the background indicators: "temperature, salinity, oxygen concentration, light levels, chlorophyll, pigments, nutrients and zooplankton within the AOI and both upstream and downstream, as measured on the Atlantic Zone Monitoring Program (AZMP) Cabot Strait and Louisbourg lines, plus an additional line in the AOI" (DFO, 2014). Historically, sampling in the AOI was scarce. In order to fill the sampling gap, a transect of five hydrographic stations perpendicular to the local bathymetry were added to AZMP seasonal spring and fall shelf surveys. These stations were sampled using the full standard AZMP sampling suite. In addition, moorings were also deployed in order to obtain multi-year continuous hydrographic and velocity time-series.

This report will address the background indicators defined for the monitoring of the St. Anns Bank MPA. First, a detailed account of all data collected during AZMP seasonal surveys from 2011 to 2017 will be summarized. Then a synthesis of these data, which includes CTD sections and zooplankton abundance/biomass, will be presented. Finally, the mooring observations will be used to summarize the water column temperature and near bottom hydrographic variability, and the spatial-temporal velocity variability.

2 Data

2.1 Hydrographic Surveys

A transect of five stations across the shelf, labelled STAB1 to STAB5 with STAB1 being nearest to the shore, were sampled twice a year during the spring (April) and the fall (September)(Figures 1 and 2). Based on the AOI region, stations were chosen to be cross-slope in the middle of the defined boundaries. Upon finalizing the MPA, the boundaries were re-defined, and now stations lie along the northwest boundary of the MPA, with STAB1 and STAB2 in the most near-shore adaptive zone, STAB3 and STAB4 along the northwest boundary of the MPA core, and STAB5 located along the most northern boundary of the MPA core (Figure 1). At each station, a full water column CTD, equipped with additional instruments to measure dissolved oxygen, fluorescence, and

photo-synthetically active radiation (PAR), profile was acquired. Niskin bottle water samples were taken at nominal depths for nutrients analysis, calibration for salinity and oxygen, chlorophyll and accessory pigment analysis (HPLC), and particulate organic carbon/nitrogen (POC/PON). The nominal water depths, as applicable to the total depth of each station are: near-surface, 10, 20, 30, 40, 50, 60, 80, 100, 250 m, and near bottom. The fluorescence, PAR, HPLC and POC/PON, all of which are ancillary measurements, will not be reported here. In addition, station occupations included a vertical ring net tow with a 202 μm mesh net for zooplankton identification, abundance, and wet and dry weight biomass.

2.2 Moorings

Mooring deployments began in April 2012 and the final moorings were recovered in November 2017. The temporal-spatial coverage of moored measurements varied between the years (Figure 2). One mooring location, STAB-C, was repeated each year on the 100 m isobath, specifically in 114 m of water, between STAB3 and STAB4 along the northwest boundary of the MPA core. Sampling began in April 2012 with six month mooring deployments between April and September for 2012 and 2013, as there were some concerns with ice. Beginning in April 2014, year long deployments began. The mooring deployed in April 2014 failed pre-maturely, and was replaced in September 2014. At this time, mooring turnaround occurred in September until the final recovery in November 2017. In September 2015, four additional moorings (STAB-I, O, S, N) were deployed in the region for 12 months in order to determine how representative the single mooring (STAB-C) described dynamics in the region. A mooring (STAB-I) was deployed inshore of STAB-C, between STAB2 and STAB3 on the boundary of the MPA core and near shore adaptive zone in 70 m of water. Another mooring (STAB-O) was deployed offshore from STAB-C, between STAB4 and STAB5 along the northwest boundary of the MPA core in 240 m of water. To examine the downstream slope dynamics from St.Anns Bank, a mooring, STAB-S, was placed on the 100 m isobath, in 100 m of water parallel to the transect. Another mooring, STAB-N, was deployed downstream of STAB-I along the 100 m isobath, but a bit deeper in 130 m of water, in a region where a fraction of Nova Scotia current flows onto the shelf break, just west outside the boundaries of the MPA.

Moorings were equipped with a combination of instruments which included CTDs, ADCPs, and temperature recorders. All moorings deployed had one of two schematics. The first schematic includes a CTD and an ADCP mounted near the bottom, this is the setup for a majority of the moorings. The second schematic includes temperature recorders, set at 5 m and then every 5 m to 40 m, then every 10 m to 60 m and then every 25 m down to 90 m, where a few were equipped with pressure sensors. Refer to Figure 3 for schematics of the moorings along the transect line for years 2012, 2013, 2015, and 2016.

2.3 Mooring Data Return

2.3.1 STAB-C

At STAB-C, two moorings were deployed adjacent to each other, initially during the spring cruise and recovered during the fall cruise during the same year, however, starting fall 2014, moorings were deployed for a full year. One mooring was equipped with a CTD and an ADCP moored 2 m and 10 m above the seafloor respectively. The second mooring was configured as a thermistor chain. This two mooring configuration was consistent for all years with the exception of 2012.

In 2012, one mooring was deployed with two spar buoy's adjacent instead of one adjacent mooring as in the previous paragraph. The mooring was equipped with a SeaBird SBE 37-SM microCAT CTD and a Teledyne WorkHorse Sentinel 300 kHz ADCP (Tables 2 and 3). Note that all other CTD and ADCP moorings were equipped with the instruments noted unless specified. The two spar buoys were equipped with temperature recorders (Figure 3). One had two temperature recorders both of which had pressure sensors, at nominal depths of 3 and 50 m, and the other spar mooring with instruments at nominal depths of 25 and 75 m (Table 4). All instruments in 2012 gave 100% data return. The temperature recorders were attached to a 165 m buoyant rope which was free to float towards the surface and this results in pressure and temperature variation (Figure 4). The temperature recorder pressure readings at a nominal depth of 3 m indicated an average moored depth of 2 m, and excursions exceeding 3 m did not occur due to the amount of buoyancy (Figure 4). Similarly, the temperature recorder at a nominal depth of 50 m indicated an average moored depth of 37 m, and exceeded 3 m from this depth 41.9% of the time (Figure 5). For the second spar buoy, the instrument at a nominal depth of 25 m indicated an average moored depth of 19 m and exceeded 3 m from this depth 26.6% of the time (Figure 6). Finally, for the instrument moored at a nominal depth of 75 m the pressure readings indicate an average moored depth of 52 m and exceeded this depth 53.6% of the time (Figure 7).

In 2013, the mooring equipped with the CTD and ADCP gave 100% data return. The thermistor chain was equipped with 10 temperature recorders and 2 temperature recorders equipped with pressure sensors (Table 4). Upon recovery, the near surface, 2 m, instrument was damaged and did not record data past July 22, 2013. As in 2012, variation in pressure and temperature were observed as not enough buoyancy was added to prevent knockdown. Vertical excursion of the temperature recorder moored at a nominal depth of 12 m, where pressure readings indicate an average moored depth of 16 m, exceeded 3 m 11.8 % of the time (Figure 8). For the instrument at 49 m, with an average moored depth of 53 m, vertical excursions exceeded 3 m 3.9 % of the time (Figure 9).

In 2014, the mooring equipped with the CTD and ADCP was deployed in the spring, but the ADCP failed pre-maturely, and only recorded values until July 20, 2014 (Table 3), the CTD gave 100% data return (Table 2). During the fall cruise, this mooring was recovered and replaced with a mooring which had the same schematic. The mooring was intended on being recovered in spring 2015, but was recovered during fall 2015. The battery of the ADCP died 14 days prior to recovery (Table 3). The CTD gave 100% data return (Table 2). The thermistor chain mooring deployed in the spring was equipped with 12 instruments at the same depths as 2013, but the mooring was lost.

In 2015, a mooring was deployed during the fall cruise, which was equipped with a CTD and an ADCP. The ADCP gave 100% data return (Table 3), but the conductivity cell on the CTD failed in early March 2016, giving roughly 50% data return, the temperature and pressure sensor functioned properly and gave 100% data return (Table 2). The thermistor chain was equipped with 11 temperature recorders, 1 temperature recorder equipped with a pressure sensor, and 1 CTD (Table 4). Of the successfully recovered instruments, two were equipped with pressure sensors. The CTD was moored at 7 m, and vertical excursions of the instrument exceeding 3 m occurred 3.1% of the time (Figure 10). The second instrument equipped with a pressure sensor was moored at 10 m, vertical excursions exceeding 3 m occurred 2.8 % of the time (Figure 11). Events of decreased

pressure occurred from December 2015 to mid February 2016, with a significant event occurring near the end of January 2016, where the instrument dips below 25 m which is due to a velocity event. Other knockdown events occur at the beginning of April 2016 and September 2016.

In 2016, a mooring equipped with a CTD and an ADCP was deployed during the fall cruise and recovered during the following fall cruise in November 2017. The mooring was successfully recovered and gave 100% data return (Table 2, 3). The thermistor chain was equipped with 12 instruments, but 2 were lost when recovered. Of the recovered instruments there were 6 temperature recorders, 3 temperature recorders equipped with pressure sensors, and 1 CTD. The CTD moored at 7 m had vertical excursions exceeding 3 m occurred 5.7% of the time (Figure 12). At 8 m, vertical excursions exceeding 3 m occurred 6.6 % of the time (Figure 13), at 48 m 6.8 % of the time (Figure 14), and at 89 m, 2.2% of the time (Figure 15). Sporadic knockdown events occurred between mid-November 2016 and mid-March 2017. A few significant events occurred near the end of December 2016, where the instrument dips below 40 m, which are most likely due to high velocities.

2.3.2 STAB-I

At STAB-I, year-long mooring deployments began in fall 2015. The schematic is the same as STAB-C with a single CTD and ADCP. The mooring deployed in 2015 was successfully recovered and gave 100% data return. The mooring deployed in fall 2016 did not release upon recovery. Months later, it was found washed ashore and only the ADCP data was able to be recovered, and gave 100% data return.

2.3.3 STAB-O

At STAB-O, year long mooring deployments began in fall 2015, with a CTD and here, a Teledyne QuarterMaster 150 kHz ADCP. The mooring deployed in 2015 was successfully recovered and gave 100% data return. The mooring deployed in 2016 was also successfully recovered and gave 100% data return.

2.3.4 STAB-S

At STAB-S, deployments, mooring schematics, and instruments are the same as STAB-I. The mooring deployed in fall 2015 was successfully recovered and gave 100% data, as with the mooring deployed in fall 2016.

2.3.5 STAB-N

At STAB-N, deployments, mooring schematics, and instruments are the same as STAB-I. The mooring deployed in fall 2015 was successfully recovered and gave 100% data, as with the mooring deployed in fall 2016.

3 Discussion

3.1 Hydrographic Survey's

3.1.1 CTD and Water Samples

Stratification along the St. Anns Bank transect varies. During sampling in the fall, the water column is stratified with a warm, 8.6 to 17.2 °C, and fresh, 29 to 30.9, mixed layer overriding a

cold, 0.7 to 4.6 °C, intermediate layer (Figure 16). Below the cold intermediate layer, which just pertains to STAB5, yearly observations have little variability with temperatures between 5.4 to 7.7°C and salinity ranging from 34.5 to 34.9. Observations in 2017 were made roughly two months later than normal, therefore the inclusion of these data in the analysis is omitted, but the data is presented for completeness (Figure 16).

There is inter-annual variability. Compared to years 2012 to 2016, the stratification along the transect is different for 2011. Near surface temperatures were the coolest, and the cold intermediate layer temperature signature is not prevalent at STAB1 and STAB2 (Figures 16 and 17). For 2012 and 2013, temperature, salinity, and oxygen properties are similar with the relatively warm and fresh surface layer extending across the transect, as well as the cold intermediate layer (Figures 18 and 19). Below the surface mixed layer, there is an oxygen maximum in depths corresponding to the cold intermediate layer. Transect water properties for 2014 and 2015 are similar, except for the near surface temperatures. Near surface temperatures for 2014 were the second coolest (Figure 20) whereas 2015 has the warmest, freshest, and thickest surface mixed layer (Figure 21). Below the mixed layer, both 2014 and 2015 have the coldest intermediate layers along with the most prominent maxima in oxygen (Figures 20 and 21). Hydrographic properties for 2016 were similar to 2012 and 2013, with the exception of oxygen, which varies longitudinally (Figure 22).

In the spring, the warm and fresh surface layer is replaced by a relatively cold, -1.6 to 1.5 °C, and relatively salty, 30.6 to 32.3, layer (Figure 24). In general, less salty waters are found at STAB1 and STAB2. Below this layer, the water properties are similar to those in the fall, with temperature ranging from 4.4 to 8°C and salinity ranging from 33.9 to 34.9. There is not as much inter-annual variability along the transect compared to the fall, with temperature, salinity, and oxygen being similar across the transect for all years, with the exception of 2017 where surface waters are warmer (Figures 25, 26, 27, 28, and 29). The surface and mid-water depth oxygen levels are much higher in the spring than in the fall for all years. Due to sampling timing, there is the potential to capture the spring bloom. There is some evidence that the spring bloom, or remnants of the event, was captured in 2013, 2014, and 2015. (Figures 25, 26, and 27).

Building climatology values for the 30-year base period of 1981 to 2010 for St. Anns Bank was evaluated. Historically, this region is under sampled. For calculating monthly climatology values, the total number of profiles during the sampled months, April and September, are seven for both months. Thus, it was determined to not be enough data to create a meaningful climatology.

3.1.2 Zooplankton Abundance and Biomass

Zooplankton species counts from the 202 μm ring net tows from near bottom to the surface were found following the standard protocol (Mitchell et al., 2002). Following the standard specie abundance reporting for the Maritimes region, taxonomic names were combined into the following categories; *Calanus finmarchicus*, *Pseudocalanus*, copepods, non-copepods. The non-copepods were then categorized into 10 groups; amphipoda, bivalva, chaetognatha, cirripedia, echinodermata, euphausiacea, gastropoda, larvacea, ostacoda, and polychaeta.

Zooplankton weights, dry and wet, were measured using the samples obtained from the 202μm rings net tows using the standard protocol which were converted to biomass (Mitchell et al., 2002).

Across the transect, for the entire time-series, there is a slight increase in *Calanus finmarchicus* abundances cross-slope with lower abundance at STAB1 (Figure 30). For the other standard

reported zooplankton abundance categories, there is no significant temporal or spatial trend, but copepods are predominately more abundant than non-copepods.

For the non-copepods, presence for a majority of the reported species occur intermittently, with no temporal and spatial trend for amphipoda, echinodermata, euphausiaces, and polychaeta (Figure 31). There is temporal dependence for bivalva and cirripedia, where they are predominately found during the fall and spring respectively. Chaetognatha abundance was present during all hydrographic survey's at STAB4, and intermittently at all other stations. Gastropoda was consistently present at almost all stations for the time-series. When larvacea was present, it was present across the entire transect. Ostracoda was the least present non-copepod reported, but when measured, it was predominately found at STAB5.

In general, zooplankton dry biomass was temporally variable, with biomass being higher during the spring (Figure 32). This trend was predominant for STAB1, STAB2, and STAB4. Biomass at STAB5 is the most variable with no temporal trend.

3.2 Moorings

3.2.1 Water Column Temperature Variability

Profile measurements indicate that as fall progresses into winter, the warm surface mixed and cold intermediate layers breakdown to a single layer, thus resulting in a two-layer stratification system. Based on the location of the mooring and the temperature recorder depth, the deep water temperature variability cannot be commented on, and the discussion on the breakdown and formation of the cold intermediate layer will be brief.

In 2012, six months of vertically evenly spaced measurements of temperature were obtained, which can give some insight on the transition from spring through to summer, and early fall conditions. As noted in Section 2.3.1, these measurements were subject to knockdown events, therefore, the raw data indicating, for example, warm temperature spikes at 75 m should be taken with caution. Instead, the filtered low-passed data will be focused on, but variations in the temperature signal are still taken with caution (Figure 33). At the beginning of the time-series, the water-column is fairly uniform in temperature. The near surface waters warm at an average linear rate of 0.17°C/day until reaching a maximum temperature in August, when waters begin to cool again and remain constant for the remainder of the time-series (mid-October). Measurements at 25 m are regarded with caution, but suggest that waters at these depths warm as well. At depth, 50 m and 75 m, waters remain nearly constant, but suggest slight warming from 1°C in late April to 4°C in mid October.

In 2013, six months of full water column temperature measurements were obtained, which again, will give insight about temperature transitions from spring to summer (Figure 34). At the beginning of the time-series, moored temperature suggests a surface mixed layer. Beginning in early May, surface waters, down to 39 m, begin to warm, and temperatures at and below 49 m stay constant. Compared to the profile measurements, these depths correspond to the near surface thermocline and cold intermediate layer respectively. Due to instrument failure in late July 2013, the near surface temperature maximum is not known, but measurements at 12 m suggest sometime in August. By mid-August temperature beings to cool. In September, at and below 19 m, temperatures are similar in structure to that in May, but the near surface waters are still relatively warm. Between July and October, there were seven events of sudden warming, followed by cooling in depth ranges of the thermocline.

In 2015, the mooring was deployed in late September, so only 3 months of data was obtained for this year, but provides continuous measurements through to the next year (Figure 35). Compared to measurements made in 2012 and 2013 (Figures 33 and 34), these observations will give insight about the temperature throughout fall and winter. At the beginning of the time series, in late September, and also seen in the end of the time series from 2012 and 2013, measurements at and below 10 m to 30 m are in the thermocline, and 60 m to 90 m pertain to the cold intermediate layer. The near surface waters, 10 m to 30 m, cool until late February 2016. Using measurements at 10 m, near surface waters cool at an average linear rate of -0.11 °C/day. During mid-October 2015, there appears to be an event which mixes the upper 30 m, resulting in a surface mixed layer by the end of October, and persists until mid-May 2016. During this time period, late September to January, measurements at 60 m to 90 m have little variation. From February to May 2016, the near surface water temperature remains constant, around 0°C, as with measurements from 60 m to 90 m, remaining around 1°C. By early May, near surface waters begin to warm at a linear rate of 0.17°C/day as inferred from observations at 10 m, and stratify again. During the near surface warming, similar to 2013 measurements, there are events of sudden warming then cooling particularly around the beginning of July and in September. Near surface temperatures appear to reach a maximum by mid-August, and then begin to cool. From May to December, observations from 60 m to 90 m again remain constant (Figure 36). Beginning in September, the near surface waters (8 m) cool at a linear rate of -0.1°C/day (Figure 36). As seen in previous years, there are events of sudden warming and cooling in the near surface waters until mid-December when the water column becomes completely mixed. In the cold intermediate layer depths, temperature remains fairly constant until beginning of December, where it warms by 2°C. From mid-December 2016 to mid-February 2017, water column temperature continues to cool, then stay constant around 0°C until mid-April. From mid-April until early August, the water column begins to stratify with the near-surface waters warming, particularly at 8 m, which warms at a rate of 0.18°C/day. Observations related to the cold intermediate layer remain fairly constant after mid-April. There are multiple sudden warming followed by cooling events, particularly in early August, early September, and throughout the end of September through to November.

3.2.2 Near-bottom Hydrography Variability

Across the STAB transect, the bottom hydrography at each mooring site is expected to be different at each location, as the CTD data has already suggested. The near-bottom moored measurements summarize bottom hydrography fluctuations at a finer temporal scale than hydrographic surveys.

3.2.2.1 STAB-C

At STAB-C, the near bottom CTD profile measurements at the near-bottom moored depths (Table 2) along the STAB transect indicate relatively colder and fresher, and thus less dense waters during spring sampling and relatively warmer and saltier, and thus more dense waters during fall sampling. Between May and mid-October 2012, waters remain fairly constant with an average temperature around 2.8°C and a salinity of 33.1, with an event that occurs in August where temperature and salinity increases (Figure 37). Throughout the time series, waters stay along the same mixing line (Figure 38). Here, define the mixing line to be the expected water properties when the cold

intermediate layer waters, here being relatively cold and fresh, mix with the deeper relatively warm and salty water.

From the thermistor chain mooring in 2013, the deepest recorder, at 89 m indicates an increase in water temperature from mid-April (0°C) to late September (2°C) (Figure 34). For the moored CTD around 105 m, the trend is similar where initial values in mid-April are near 0°C (Figure 37). Throughout the time-series, between April to September, temperature increases, which is coherent with salinity, and thus density. This trend is interspersed with a few warming events, particularly in May and in August, but waters stay along the same mixing line (Figure 38).

In late March 2014, year-long mooring deployments began. Between March and October, conditions are similar to the previous two years, where again, there is an event during August where temperature and salinity values increase (Figure 37). Beginning in November 2014, temperature and salinity are no longer coherent, where waters are relatively warmer and fresher than those found along the mixing line (Figure 38). These waters persist until February 2015, where waters then continue to cool until an annual minimum value in April 2015, and waters return to the mixing line. From April to May, waters begin to warm and become more salty. Waters remain fairly constant again from May until October. From the temperature recorder measurements at 90 m, it indicates slight warming from about 2°C in October 2015, to about 4°C by January 2016. From here, waters cool down to 2°C by February, and remains constant until April when temperature slowly increases until reaching a maximum again of about 3°C in September. The temperature remains constant until middle of December, where it warms up to 4.5°C, then cools to 1°C by April 2017, with a small warming event in March 2017. After that, waters remain constant. The temperature variations at 105 m are similar to the nearby temperature recorder measurements at 89 m. Similar to 2014, relatively warmer and fresher waters arrive in November 2015, and persist until about February 2016. Around this time, the conductivity cell failed, therefore, no comments can be made on the salinity variations, however, they are probably similar to previous years. As in 2014 and 2015, a different water mass is present beginning in mid-October 2016, and persists until roughly March 2017. After March, conditions are similar to previous years.

3.2.2.2 STAB-I

At STAB-I, there was only one year of near-bottom moored CTD measurements, October 2015 to October 2016. Overall, waters are less dense than the bottom waters at STAB-C, as expected, where waters are relatively colder and fresher, but experience similar events (Figure 39). Between mid-October 2015 to January 2016, waters are relatively warmer and more fresh than the average background values (Figure 40). During December 2015, waters begin to cool, until around March 2016 where waters remain around 0° and a salinity of 31.5 until May. Then waters increase to 2°C and salinity of 31, and remain constant until the end of the time series.

3.2.2.3 STAB-O

At STAB-O, near bottom hydrography properties are fairly constant throughout the time-series, as expected from the CTD profiles where water properties around 235 m have no temporal variation between spring and fall (Figure 41). The same is true for the higher temporal resolution data, where waters are relatively warmer and saltier, and thus more dense than those at STAB-C (Figures 41

and 42).

3.2.2.4 Downstream

Downstream from the STAB transect, the two moorings are placed roughly along the same isobath as STAB-C. At STAB-S, similar to STAB-C, beginning in December 2015 waters deviate from the mixing line and are relatively warmer and more fresh, which persists until roughly March 2016 (Figures 43 and 44). From March to December, waters remain fairly constant. As at STAB-C, the same event in December 2016 occurs and persists until March 2017. However, here, waters were warmer than the event seen in the previous year (Figure 44). At STAB-N, near bottom hydrography temporal properties are nearly identical to that of STAB-S (Figures 45 and 46).

3.2.3 Temporal Velocity Variability

For the analysis, all moored ADCP measurements were rotated in an x-y Cartesian coordinate system. The angle for measurements made along the STAB transect was estimated from a standardized major axis regression of the hydrographic stations using the "sma" function from the R package "sma" (Warton et al., 2012). Resulting angle put the positive along-isobath axis 48.9° counterclockwise of true east, roughly southeast, and the positive cross-isobath axis 41.1° counterclockwise of true east, roughly northeast. For the moorings not located on the transect, STAB-S and STAB-N, the angle was estimated using their locations and put the positive along-isobath axis -161.1° clockwise of true east, roughly southwest, and the positive cross-isobath axis -71.1° clockwise of true east, roughly southeast. Using station and mooring coordinates to calculate the rotating angles was chosen over using the mean flow direction or local bathymetry in order to easily make an inter-comparison of direction variability between moorings.

3.2.3.1 STAB-C

From the literature (*e.g.* Brickman et al. (2016)) it is expected that flow is predominately along-isobath, or southeast, with a positive along-isobath velocity component in the rotated x-y Cartesian coordinate system. In 2012, the progressive vector diagram indicates varying flow direction throughout the water-column, but is primarily southeast (Figures 47 and 48). Near the surface, flow is intensified and is primarily southeast. As depth increases, the net flow direction becomes more cross-isobath, or northeast. Throughout most of the water column, 12 m to 92 m, between May and June, flow goes from southeast to southwest direction, then northeast. At the beginning of June, flow resumes southeast. In the upper half of the water column, 12 m to 40 m, from mid-June to beginning of September, there are alternating patterns of the dominant flow components. At depth, between 60 m to 104 m, there are periods of reversal flow, near the end of June to beginning of July, during August, and in the middle of August.

In 2013, again, flow is intensified near the surface and primarily southeast for the six months that measurements were obtained (Figures 49 and 50). Near the beginning of the time-series, late April, until middle of May, flow is reversed. As a function of depth, near the surface, flow is more cross-isobath with the along-isobath component being twice as large in magnitude, and at depth, the along-isobath component is dominant. Until July, flow is predominately southeast, then flow is predominately in the southwest direction near the surface at 14 m to 90 m for a few weeks. From

July to the end of September, flow is southeast, then flow reverses and is in the northwest direction around 30 m to the bottom, and then tends towards the northeast direction as a function of depth. No measurements were taken from September to December.

In 2014, flow is primarily southeast (Figure 51). At the beginning of the time-series, in April, flow is in the northwest direction until the beginning of May, when flow reverses and resumes southeast (Figure 52). In the middle of May, flow reverses again until roughly the beginning of June, when flow returns to southeast. For both of these events, flow is intensified at the surface. The first mooring deployed failed in July and was replaced at the beginning of October. In mid-October, flow is predominately in the southwest direction in the upper 40 m (Figure 53). Flow then transitions to northwest, and the proceeds southeast by the beginning of November. During December, the dominant velocity component alternates.

In 2015, flow is predominately southeast and surface intensified, with no significant events observed (Figures 53,54, and 55). In 2016, flow again is southeast throughout most of the year (Figures 55, 56, and 57). In May, from 60 m to 100 m, flow alternates between northeast and northwest direction, and then returns to southeast by mid June. In 2017, flow is similar to 2016, with a predominant southeast, and surface intensified flow (Figure 57). At depth, between 60 m and 101 m, beginning in May, flow alternates between southeast flow to northwest flow until mid August, after then, flow continues southeast until the end of sampling.

In general, flow is surface intensified. Surface intensified flow reversal events are most likely to happen between the end of April and June, as observed in four of the six years that data was collected between 2012 and 2017. Other events occur between June and September with a few occurring in the later months. Between December and March, the along-isobath velocity component is intensified throughout the water column, and occurs at all three of the years when sampling occurred.

Tidal analysis was completed on ADCP time-series from each mooring deployment for STAB-C as there were breaks in the time-series and the sampling rate and bin depths between each deployment varied. A more careful approach could be taken to match up the time-series, but analysis here is sufficient for data presentation. Output from tidal analysis includes the amplitude of the major and minor axis, with the major always being positive, and the sign of the minor indicating the rotational sense with positive indicating the ellipse traces counter-clockwise and negative clockwise. Other parameters includes ellipse orientation, which is the angle measured counter-clockwise from 0° east to the major axis, and phase which is the timing of high water referenced to astronomic positions over Greenwich meridian. For brevity, the results for three major tidal constituents, K1, M2, and O1 are presented. For the K1 tidal constituent the major axis is roughly uniform throughout the water column (Figure 58). The minor axis is negative, and as depth increases, becomes more positive. The orientation is slightly more in the negative cross-isobath direction, with the angle being 100°, which translates to -80° in reference to the rotated x-y Cartesian system. For the M2 constituents, Figure 59, the major amplitude has a mid-depth minimum, and a maximum near the bottom, similar for the minor axis, with it always being negative, so again, a counter-clockwise tendency. The orientation is nearly along-isobath, 150° or -30° in the referenced x-y coordinate system. For the O1 constituent the major amplitude tends to be smaller at depth (Figure 60). The minor is nearly zero throughout the water-column, but is slightly negative at the surface and positive at depth. The orientation is similar to K1, with

it begin roughly 100° or -80° at the surface, and 50° or -130° near the bottom.

3.2.3.2 STAB-I

Similar to STAB-C, the expected average velocity direction at STAB-I is southeast. During 2015, the first mooring at this location was deployed during the fall at the end of September. From the beginning of the measurements to the end of December, direction is primarily southeast, with no significant events (Figures 54 and 61). Flow is surface intensified, with one high magnitude event beginning near the end of October and lasting until the beginning of November. In 2016, flow again is southeast with no significant events (Figures 56, 61, and 62). In 2017, flow direction, is again, mainly southeast (Figure 62). From April to August, at depth, between 47 m and 55 m, flow is more northeast, then in September, flow returns to southeast until the end of the mooring deployment.

3.2.3.3 STAB-O

As for STAB-I, the first mooring deployed in this location was in late September and again, the expected velocity direction is southeast (Figures 54 and 56). For the sampling portion in 2015, there are alternating flow directions, from southeast, to northeast, and is most prevalent between 26 m to 90 m (Figure 63). In 2016, flow is primarily southeast, but there are a number of events where flow deviates from southeast (Figures 63 and 64). Between 26 m to 110 m, significant event occurred during February when flow is southwest. During May, flow reverses again, but now between 26 m to 150 m until the middle of June, when flow returns to the southeast direction. Around the end of July until the beginning of August, flow reverses again, but through the entire water column, it then returns southeast for the remainder of the year. During the middle of December, a high velocity magnitude event occurs from 19 m to 103 m. In 2017, flow is primarily southeast, but from April to June, dominant flow components alternate, primarily between 19 m to 119 m (Figure 64). Then for the remainder of the mooring deployment, flow is in the southeast direction.

3.2.3.4 STAB-S

At STAB-S, the temporal coverage is similar to that of STAB-I and STAB-O. At this mooring location, the dominant flow direction is southwest, with the flow being surface intensified, and as a function of depth tends towards the northwest direction as depth increases, and is prevalent for the entire time series (Figures 54, 56, and 65). There are a few significant flow direction changes. From 11 m to 30 m in August 2016, flow goes from southwest towards more southeast, which is prevalent until October 2016 (Figure 66). The same event occurs in 2017, but last longer, to the end of October.

3.2.3.5 STAB-N

The temporal coverage for STAB-N is the same as the other moorings, STAB-I, STAB-O, and STAB-S. In general, the dominant flow direction is southwest with the flow being surface intensified, and as depth increases, flow tends towards the northwest direction with reference to the surface measurements (Figures 54, 56, and 67). Throughout the entire time-series, there are few

events where flow deviated from its average direction. During 2015, the dominant flow component alternates from the end of October to the middle of November. Near the end of the time-series, in 2017, flow direction changes from southwest to northeast from April to August, and then resumes southwest (Figure 68).

3.2.4 Spatial Velocity Variability

3.2.4.1 STAB transect

Due to the temporal coverage of STAB-I and STAB-O, discussion on the spatial variability will only be from October 2015 to October 2017. Across the transect, flow is intensified at the surface, with the direction of the flow tending towards the southeast direction as depth increases (Figures 54 and 56). Large magnitude events, particularly in November 2015 to April 2016 seen at STAB-I, appear to be coherent with measurements made in the top 50 m of the water-column at STAB-C, but this feature is not seen in measurements made at STAB-O. In December 2016, the maximum velocity magnitude event is seen at all three mooring locations, and measurements appear to be coherent, with the event spanning through the entire water column. In summary, based on graphical analysis of the velocity data along the STAB transect, measurements appear to be coherent, and thus there is little spatial variability.

3.2.4.2 Downstream of STAB transect

Discussion on the spatial variability for the moorings downstream from the STAB transect will cover the same temporal time scale, October 2015 to October 2017. Both moorings, for the entire time series, exhibit surface intensified flow and the direction tends towards the northwest direction to 80 m then towards southwest to about 100 m. In terms of the spatial variability, both capture the same events, and graphically, the measurements appear to be coherent, but with measurements at STAB-S being more cross-isobath than those exhibited at STAB-N.

3.2.4.3 Seasonal

The ADCP measurements at each mooring site was broken up into seasonal time-series where winter is defined as January to March, spring from April to June, summer from July to September, and fall from October to December. For each season, average along- and cross-isobath velocity profiles were calculated. At STAB-C, the average spring and summer profiles for all available years are similar, and compared to fall and winter the magnitude is smaller (Figure 69). During the fall and winter, the magnitude of the velocity is greater, with velocity direction being slightly in the negative cross-isobath, or southwest, direction. Velocity magnitude is largest in winter 2016 and fall 2016, which is expected due to events of nearly a month's duration. At STAB-I, compared to STAB-C, seasonal profiles are similar, but the magnitude during fall 2015 is greater (Figures 70). For STAB-O, the seasonal trend is similar to STAB-C, with magnitude being greater during fall and winter, and less in spring and summer (Figure 71). Below about 100 m, for all seasons, velocity at depth is primarily southeast. As seen at STAB-C and STAB-I, maximum magnitude values occur during winter 2016 and fall 2016, primarily due to events lasting for weeks at a time.

At the two mooring locations downstream from the moorings on the transect line, seasonal trends are similar, but the direction of the flow is different. Along the transect, average seasonal

flow tended to be slightly in the negative cross-isobath, or southwest, direction, but here flow is more in the positive cross-isobath, or southeast, direction (Figures 72 and 73). As for the transect moorings, the down-slope moorings still suggest slower flow during spring and summer with maximum magnitude values occurring during the fall and winter. The maximum flow seen across the STAB transect during winter 2016 and fall 2016 is not as apparent down-slope. It is suggested at STAB-N, but is constrained to the top 80 m, where as at STAB-C and STAB-O, it is apparent throughout the entire water-column, 105 m and 235 m respectively.

3.2.5 Transport

In order to address the question of whether or not a single mooring could encapsulate dynamics across the transect line, an analysis on the transport was conducted. This involved using ADCP data from STAB-I, STAB-C, and STAB-O when the time series overlapped, which was between October 2015 to November 2017.

The along-isobath velocity at each mooring location was vertically binned to 10m bins from the surface to the bottom and temporally averaged over a month in order to mask any correlation to tidal signals. The depth integrated along-isobath velocity was calculated for each site and is defined as $\bar{U}_C$ for STAB-C, $\bar{U}_I$ for STAB-I, and $\bar{U}_O$ for STAB-O. These were used to calculated the total transport. A linear regression was done on the depth integrated velocity against all three mooring locations. There was a high correlation for both STAB-C and STAB-O, and moderate correlation for STAB-I (Figure 74). The total transport calculated using one mooring agrees well with the total transport calculated using three moorings. In general, there is less transport during the summer, between 0.1 to 0.2 Sv, and higher during the winter between 0.3 to 0.8 Sv, with near 0 Sv, and at time negative, transport during the spring. Based on this analysis, if only mooring can be deployed along the transect, either STAB-C or STAB-O would be a suitable choice in order to capture dynamics, and the transport calculation could be corrected for using the resulting linear regression results.

4 Acknowledgements

The authors would like to thank all sea-going, field operations, and data management staff at the Bedford Institute of Oceanography, as well as the officers and crew of the Canadian Coast Guard who have supported this data collection throughout the years. We would also like to thank the reviewers, Andrew Cogswell and Zeliang Wang, who provided comments and suggested edits that improved the document.

REFERENCES

Brickman, D., Wang, Z., and DeTracey, B. (2016). Variability of current streams in atlantic canadian waters: A model study. *Atmosphere-Ocean*, 54(3):218–229.

DFO (2014). *Review of a Monitoring Framework for the St. Anns Bank Area of Interest*. Number 2013/028. Fisheries and Oceans Canada Canadian Science Advisory Secretariate Science Response.

Government of Canada (2018). St. Anns Bank Marine Protected Area (MPA).

Kenchington, T. J. (2013). *A Monitoring Framework for the St. Anns Bank Area of Interest*. Number 2013/117. Canadian Science Advisory Secretariate Research Document.

Mitchell, M. R., Harrison, G., Pauley, K., Gagné, A., Maillet, G., and Strain, P. (2002). *Atlantic zonal monitoring program sampling protocol*. Canadian Technical Report of Hydrography and Ocean Sciences 223.

Warton, D. I., Duursma, R. A., Falster, D. S., and Taskinen, S. (2012). smatr 3 - an R package for estimation and inference about allometric lines. *Methods in Ecology and Evolution*, 3:257–259.

5 Figures

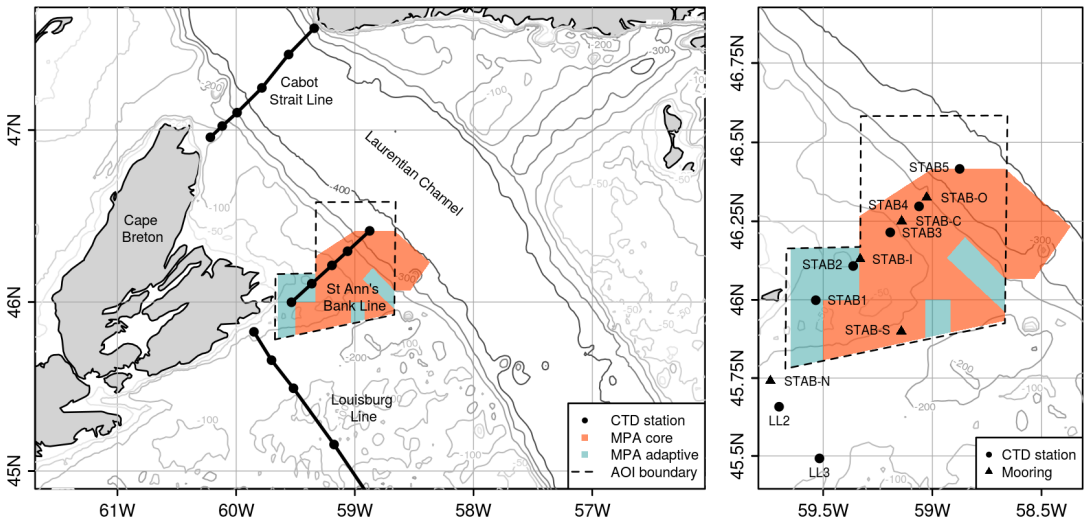

Figure 1: Map of St. Anns Bank study region. (Left) The St. Anns Bank transect is indicated by a black line and sampling stations indicated with black dots, with the MPA core protection zone indicated in orange, and the MPA adaptive management zones indicated in blue. The AOI boundary lines are indicated by a dashed line for context. Also, nearby AZMP core transects, the Cabot Strait and Louisbourg lines, are indicated for context. (Right) Detailed spatial coverage of sampling efforts from 2012 to 2017 in St. Anns Bank. CTD stations are indicated by a black circle, and mooring locations with a black triangle.

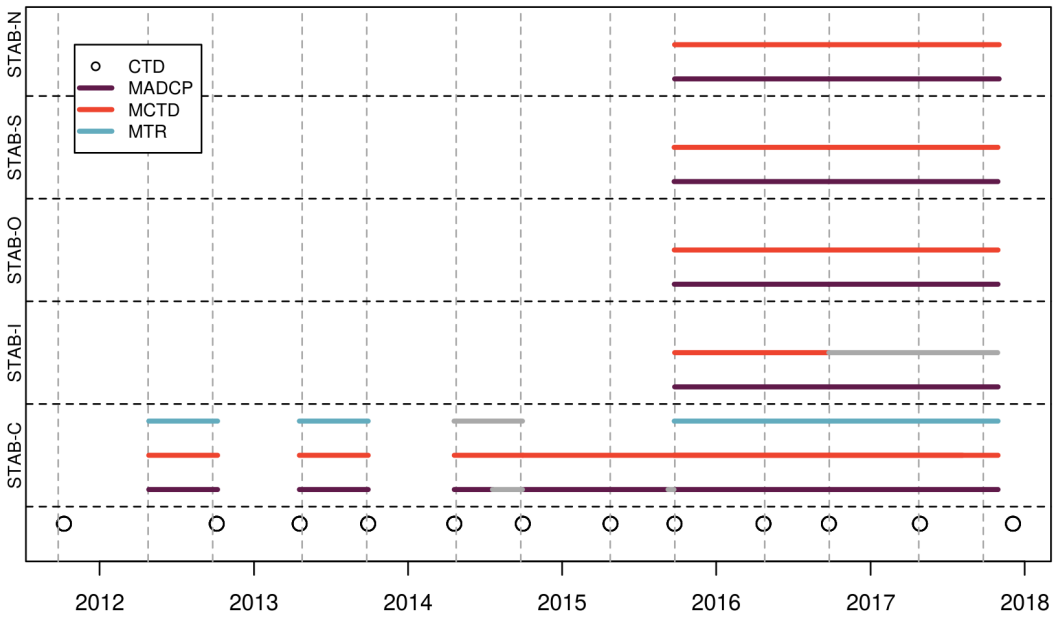

Figure 2: Temporal coverage of hydrographic surveys and moorings. Conductivity-temperature-depth (CTD) profiles are indicated by circles and moored instruments for each mooring location are indicated by a line (see Figure 1 for spatial coverage of locations). Moored instruments include moored Acoustic Doppler current profiler (MADCP), moored CTD (MCTD), and moored temperature recorders (MTR). Horizontal grey lines indicate where sampling was anticipated, but instruments were either lost or damaged. Vertical dashed grey lines indicate the 25th of April and September for each year.

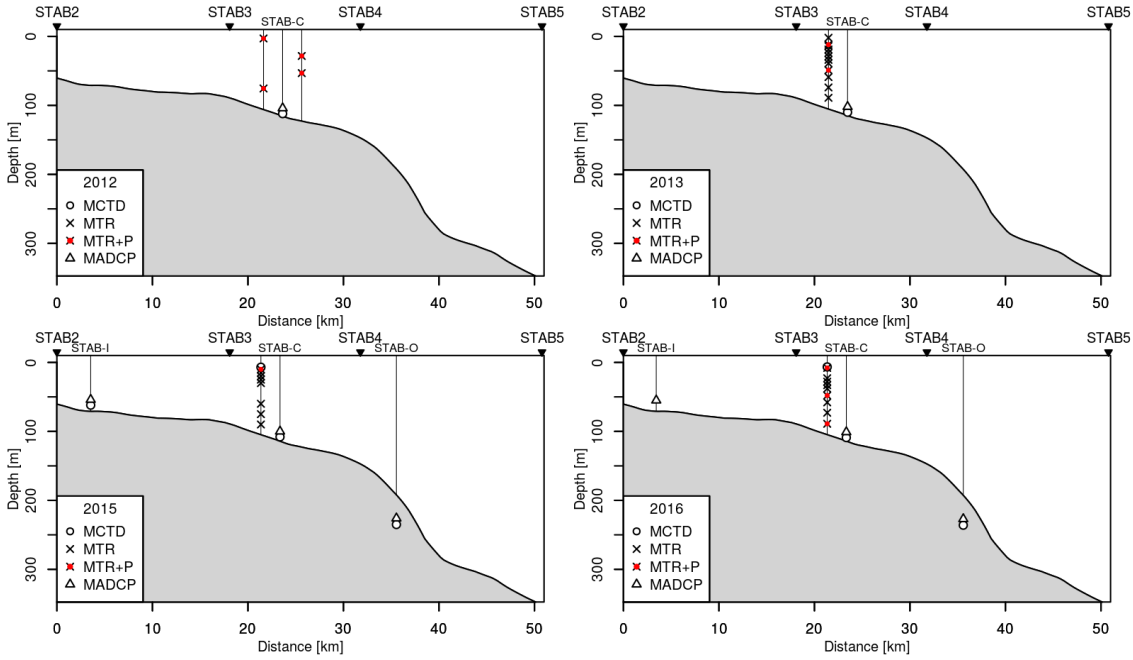

Figure 3: Schematics of moorings along the STAB transect for (top-left) 2012, (top-right) 2013, (bottom-left) 2015, and (bottom-right) 2016, as indicated in the legend for each plot. Note that mooring schematics for 2014 is omitted here, but the successfully recovered mooring had a CTD and ADCP moored near the bottom at STAB-C. Discrepancy between the cross-sectional bathymetry and the moored depth of the instruments at STAB-O is due to the resolution of the bathymetry data. Locations of the spar buoys and the thermistor chain moorings (see text) are offset for visualization.

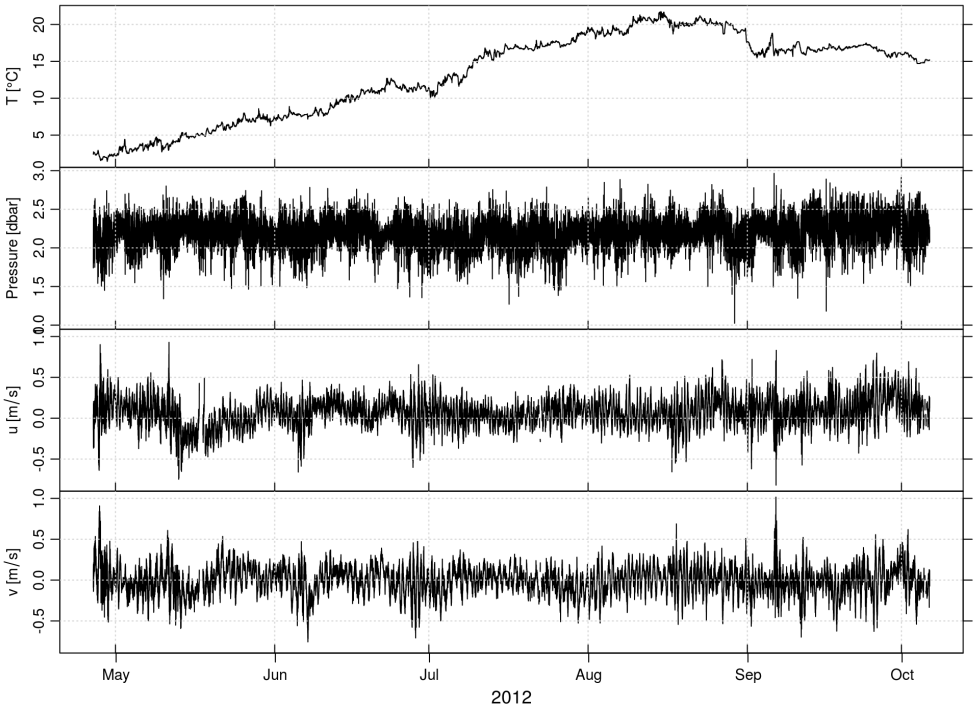

Figure 4: From top to bottom: time-series plot of temperature and pressure from a temperature logger at a nominal depth of 2 m, along-isobath and cross-isobath velocity components inferred from ADCP measurements at the 12 m bin for STAB-C in 2012.

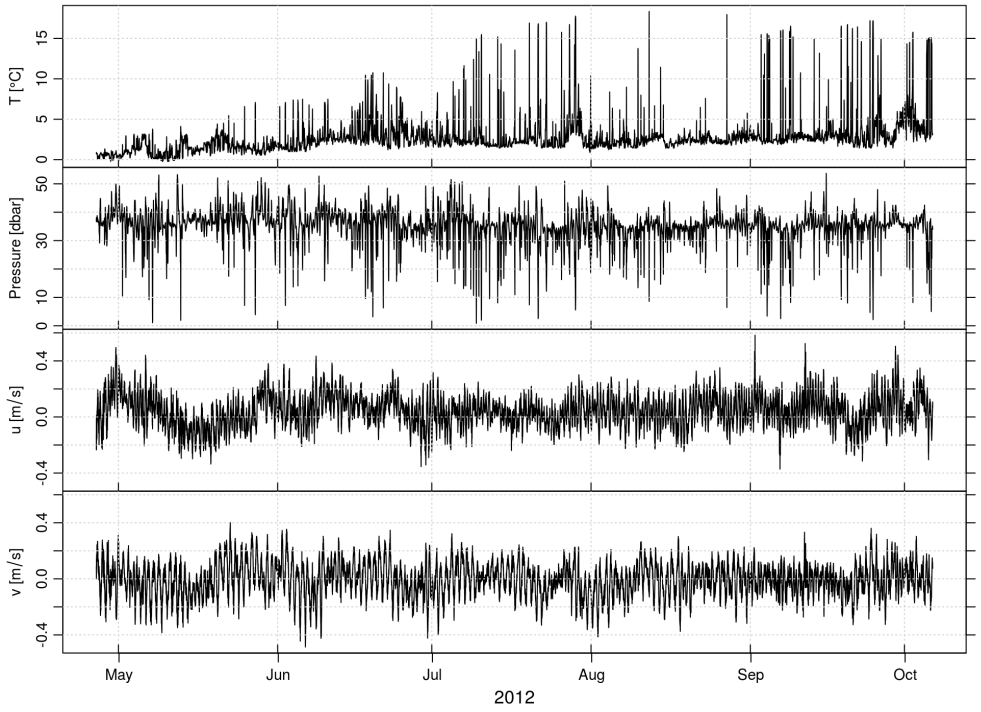

Figure 5: From top to bottom: time-series plot of temperature and pressure from a temperature logger at a nominal depth of 50 m, along-isobath and cross-isobath velocity components inferred from ADCP measurements at the 36 m bin for STAB-C in 2012.

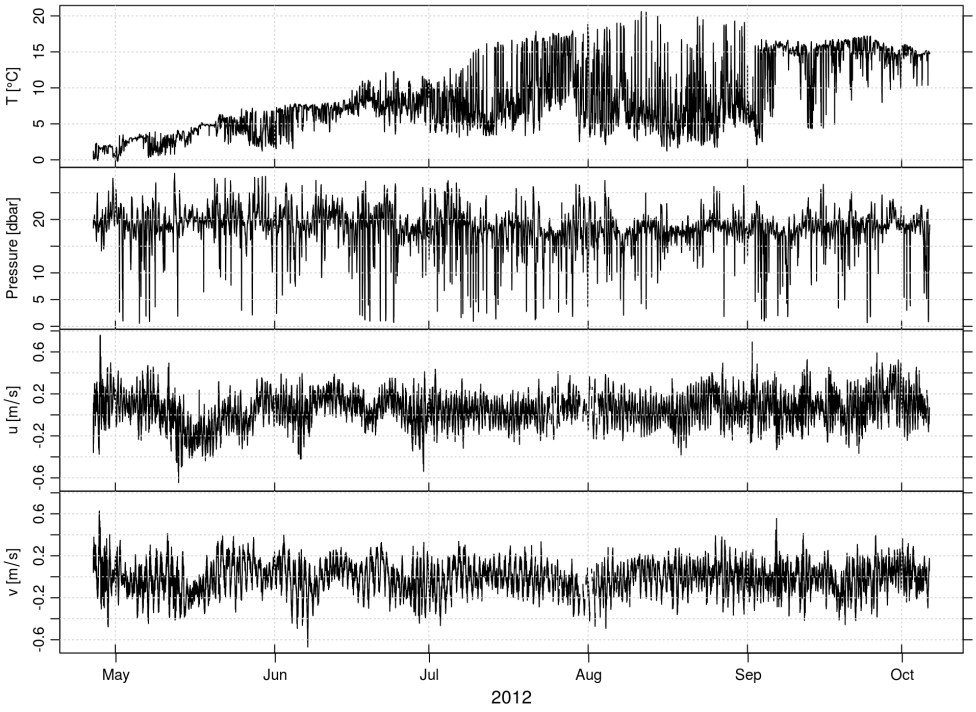

Figure 6: From top to bottom : time-series plot of temperature and pressure from a temperature logger at a nominal depth of 25 m, along-isobath and cross-isobath velocity components inferred from ADCP measurements at the 20 m bin for STAB-C in 2012.

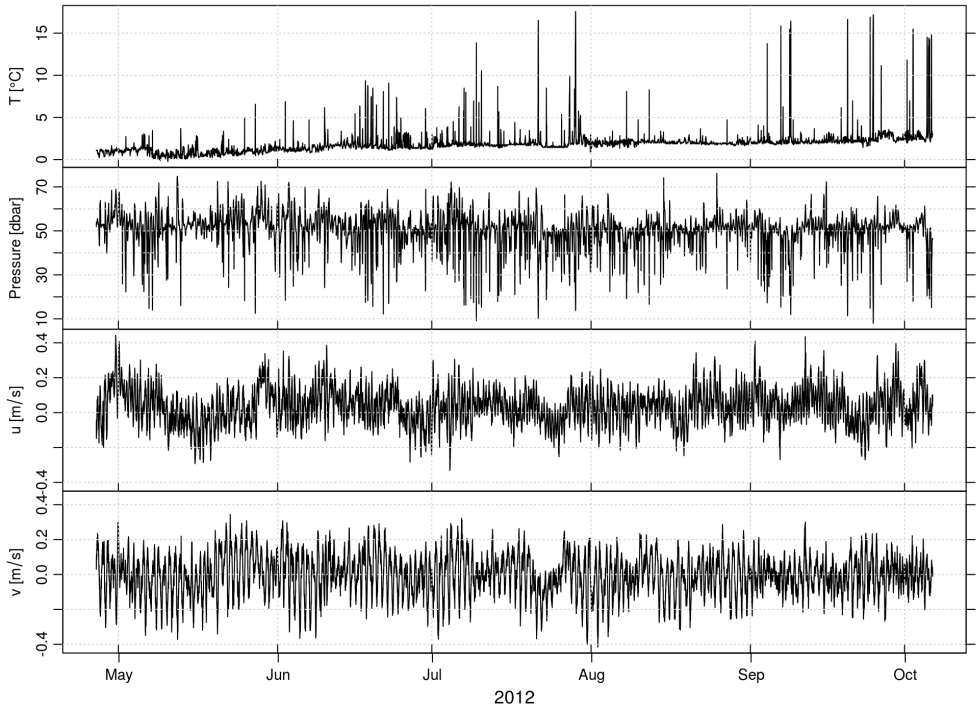

Figure 7: From top to bottom : time-series plot of temperature and pressure from a temperature logger at a nominal depth of 75 m, along-isobath and cross-isobath velocity components inferred from ADCP measurements at the 52 m bin for STAB-C in 2012.

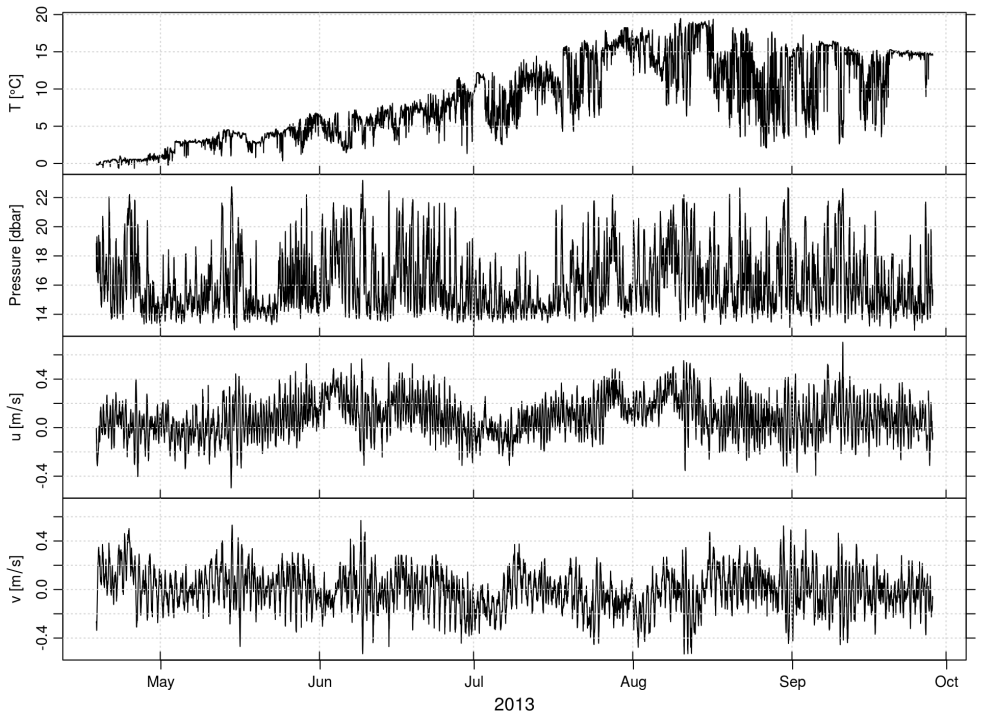

Figure 8: From top to bottom : time-series plot of temperature and pressure from a temperature logger at a nominal depth of 12 m, along-isobath and cross-isobath velocity components inferred from ADCP measurements at the 14 m bin for STAB-C in 2013.

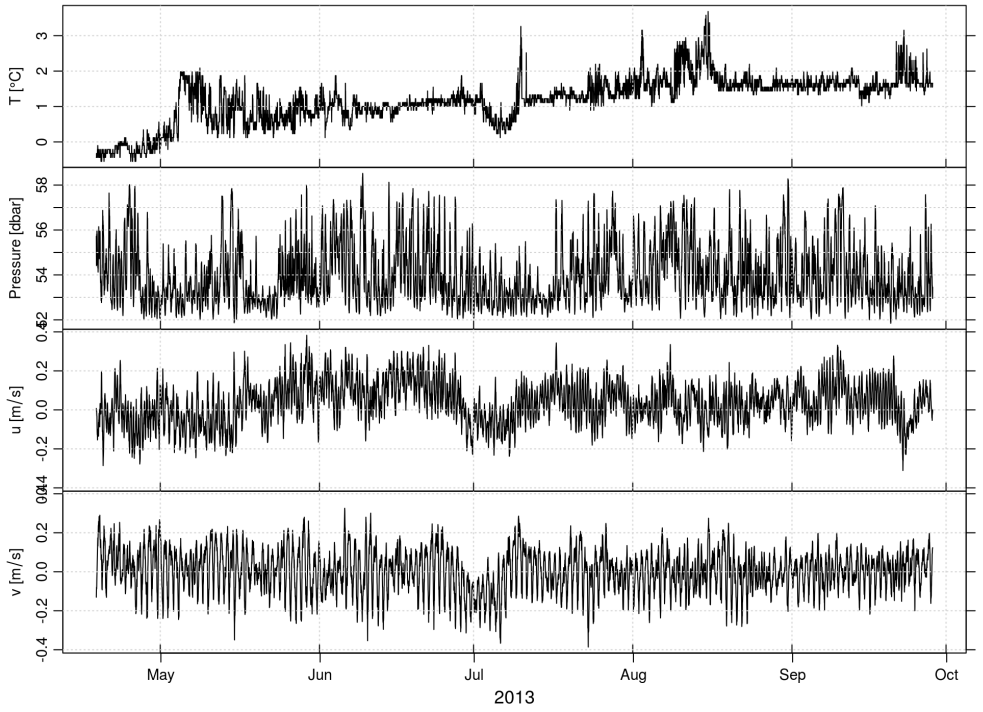

Figure 9: From top to bottom : time-series plot of temperature and pressure from a temperature logger at a nominal depth of 49 m, along-isobath and cross-isobath velocity components inferred from ADCP measurements at the 54 m bin for STAB-C in 2013.

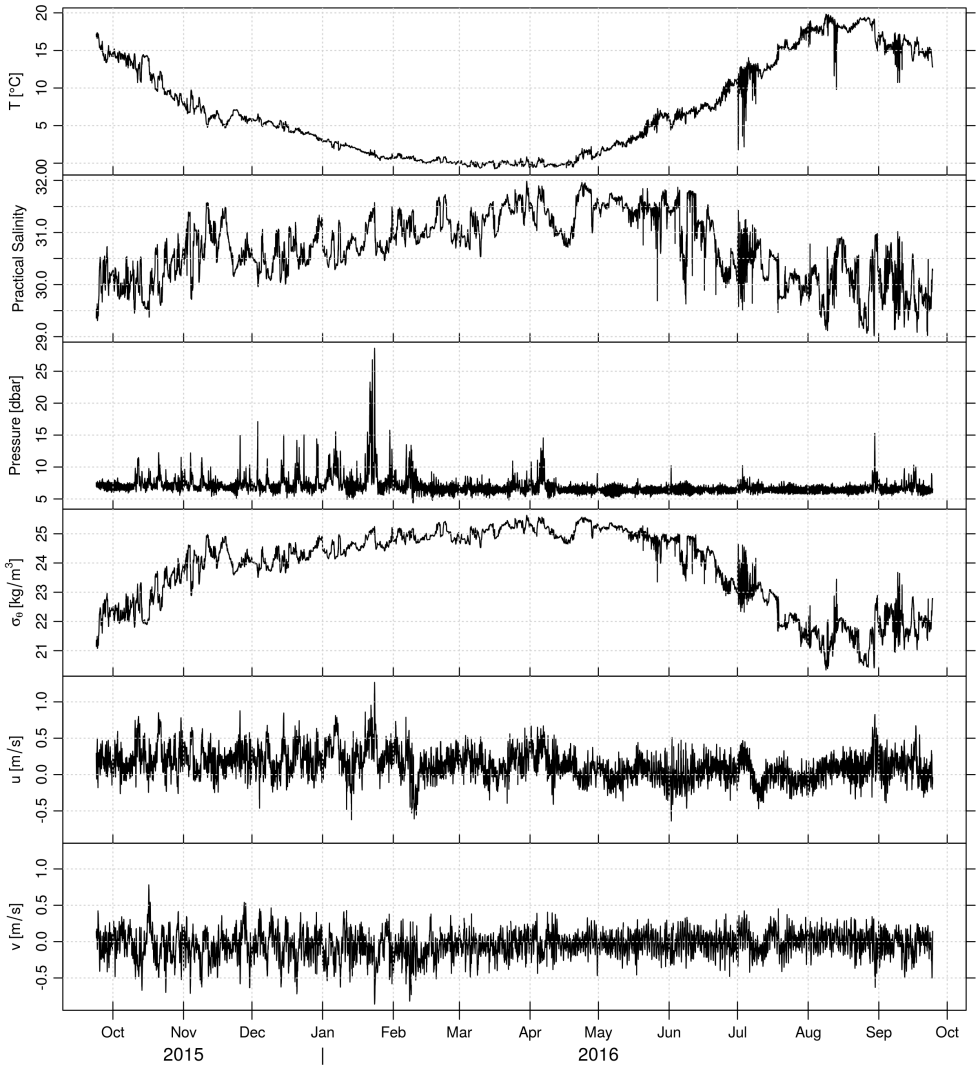

Figure 10: From top to bottom : time-series of moored temperature, salinity, pressure, and density from a CTD at a nominal depth of 7 m, along-isobath and cross-isobath velocity components inferred from ADCP measurements at the 12 m bin for STAB-C during fall 2015 to fall 2016.

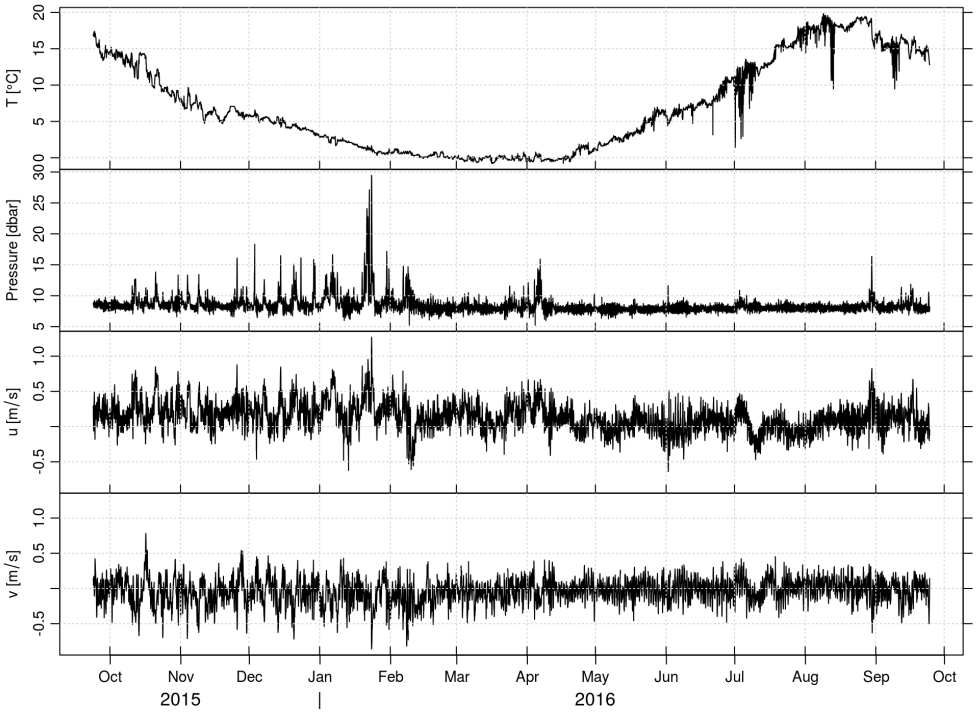

Figure 11: From top to bottom : time-series plot of temperature and pressure from a temperature logger at a nominal depth of 10 m, along-isobath and cross-isobath velocity components inferred from ADCP measurements at the 12 m bin for STAB-C during fall 2015 to fall 2016.

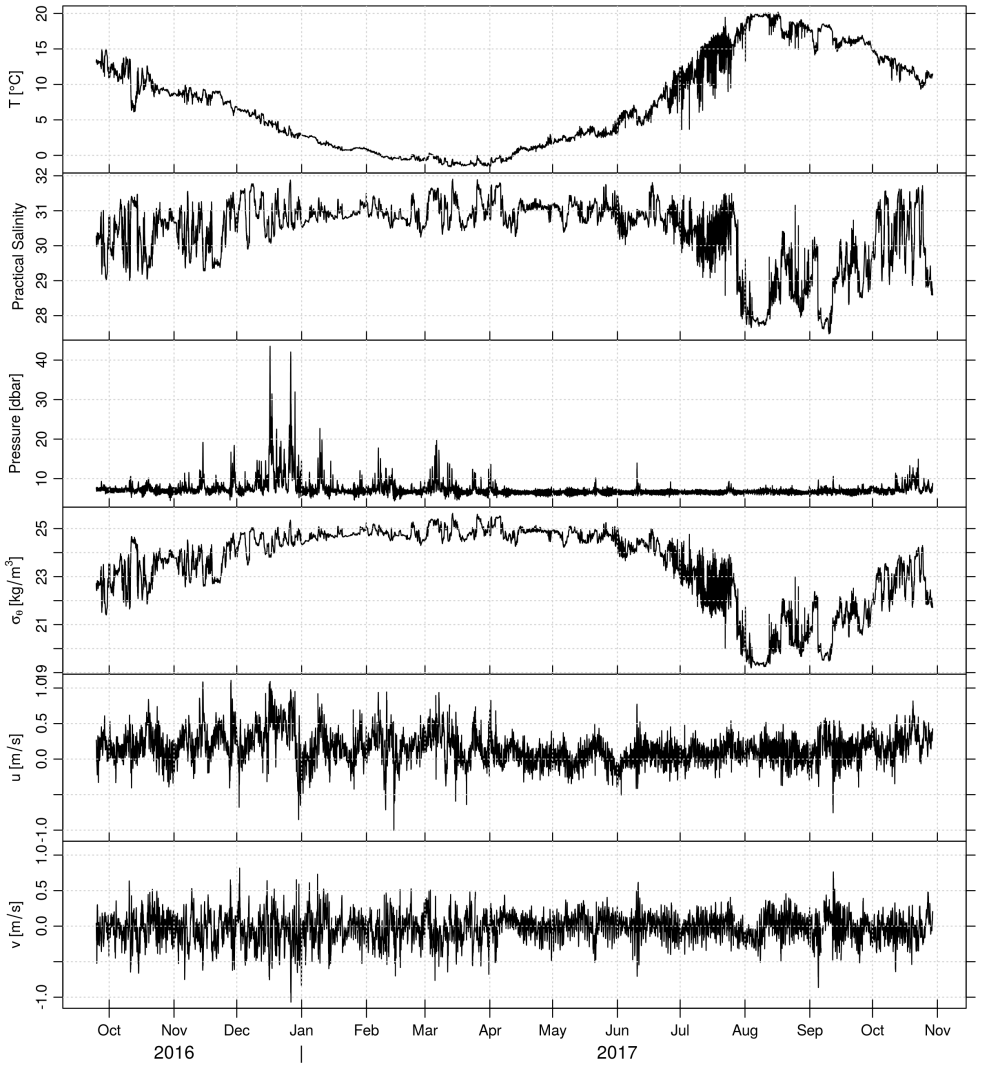

Figure 12: From top to bottom : time-series of moored temperature, salinity, pressure, and density from a CTD at a nominal depth of 6.6 m, along-isobath and cross-isobath velocity components inferred from ADCP measurements at the 13 m bin for STAB-C during fall 2016 to fall 2017.

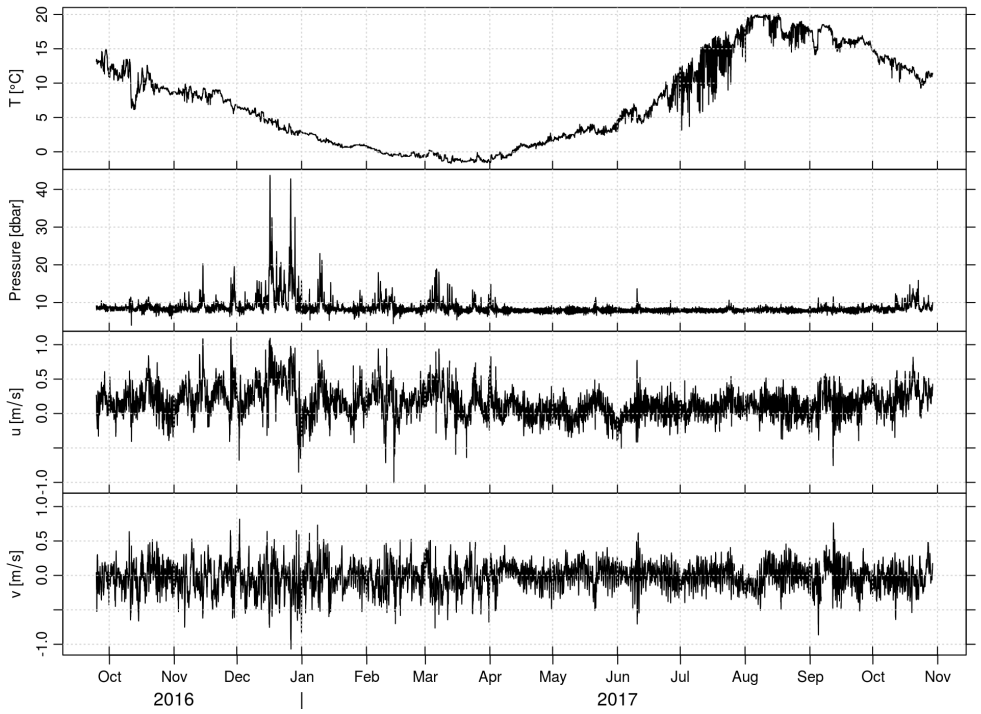

Figure 13: From top to bottom : time-series plot of temperature and pressure from a temperature logger at a nominal depth of 8 m, along-isobath and cross-isobath velocity components inferred from ADCP measurements at the 13 m bin for STAB-C during fall 2016 to fall 2017.

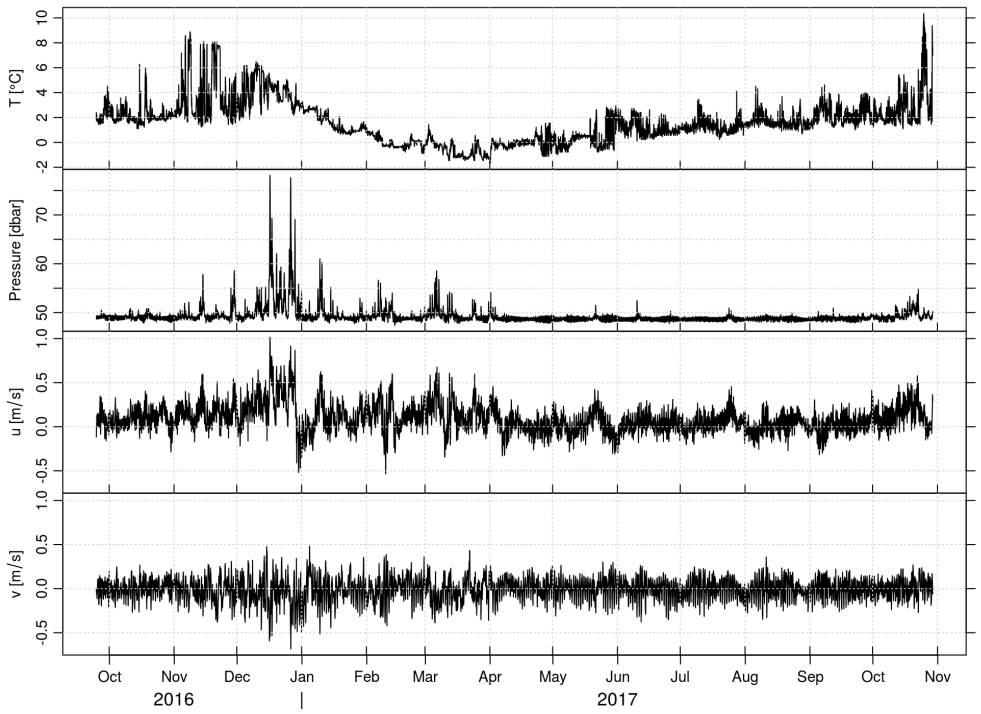

Figure 14: From top to bottom : time-series plot of temperature and pressure from a temperature logger at a nominal depth of 48 m, along-isobath and cross-isobath velocity components inferred from ADCP measurements at the 49 m bin for STAB-C during fall 2016 to fall 2017.

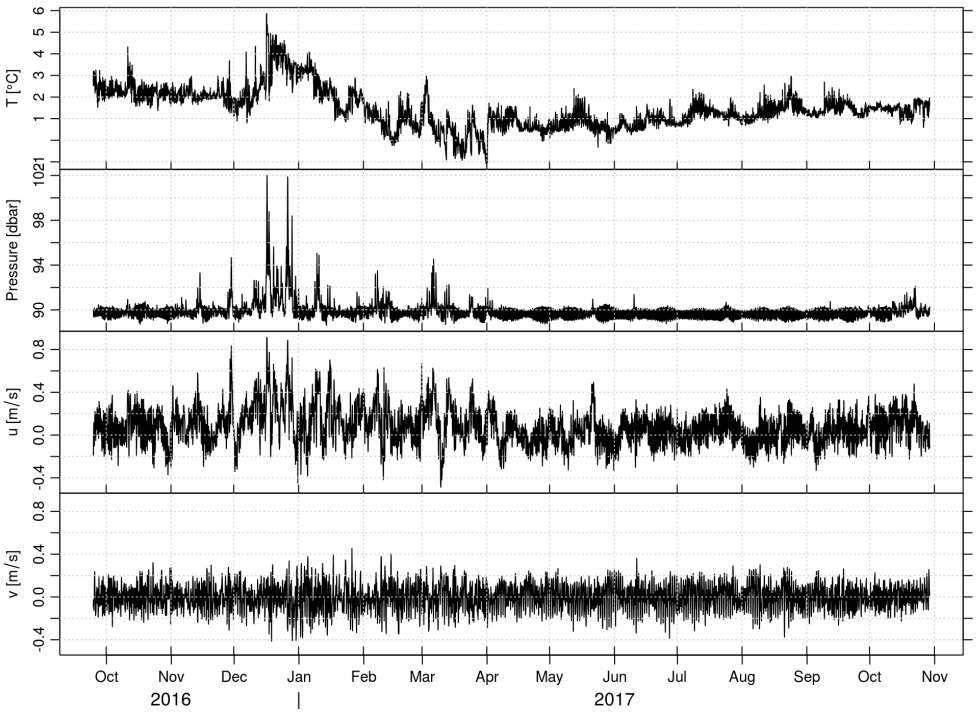

Figure 15: From top to bottom : time-series plot of temperature and pressure from a temperature logger at a nominal depth of 89 m, along-isobath and cross-isobath velocity components inferred from ADCP measurements at the 89 m bin for STAB-C during fall 2016 to fall 2017.

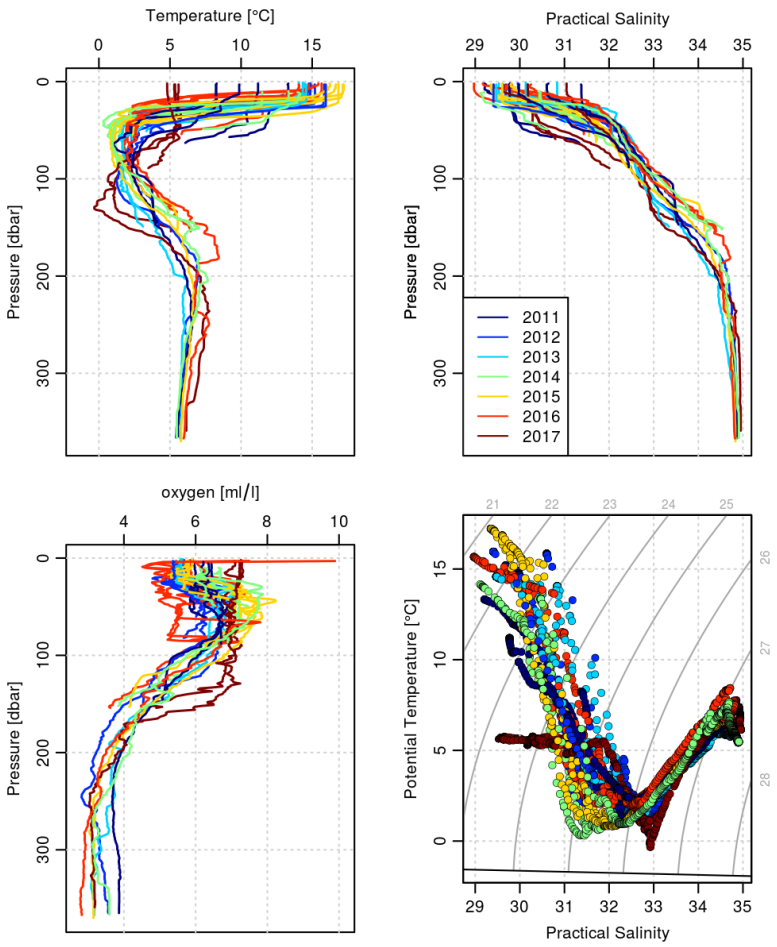

Figure 16: Profile plots of temperature (top-left), salinity, (top-right), and oxygen (bottom-left), temperature - salinity diagram (bottom-right) using CTD profiles data taken in St. Anns Bank during the fall hydrographic survey. Note that data from 2017 was taken two months later than normal. These data are omitted from analysis, but presented here for completeness.

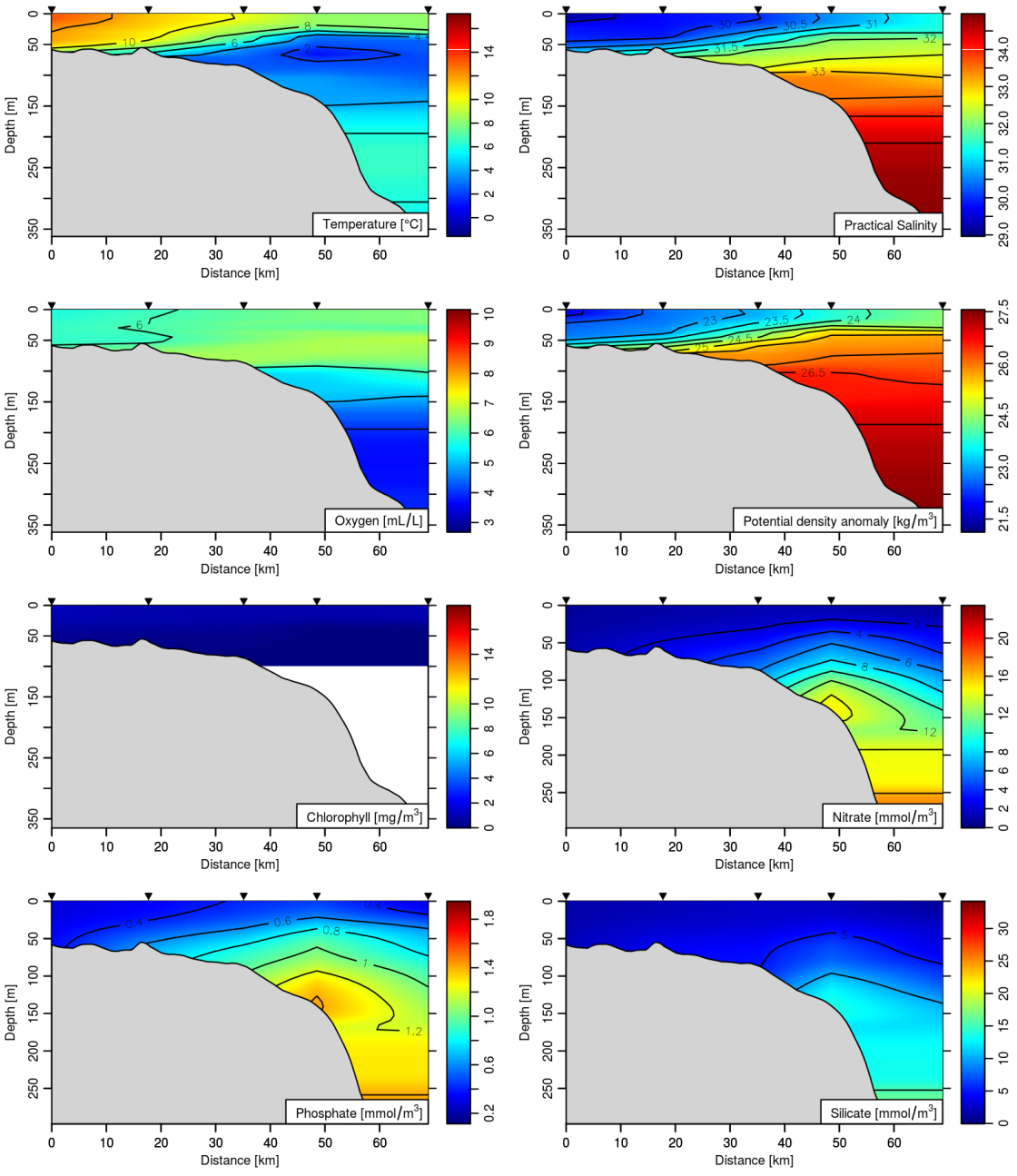

Figure 17: Section plots of temperature, salinity, oxygen, and density as measured by the CTD and chlorophyll, nitrate, phosphate, and silicate as measured by water samples from the fall 2011 hydrographic survey.

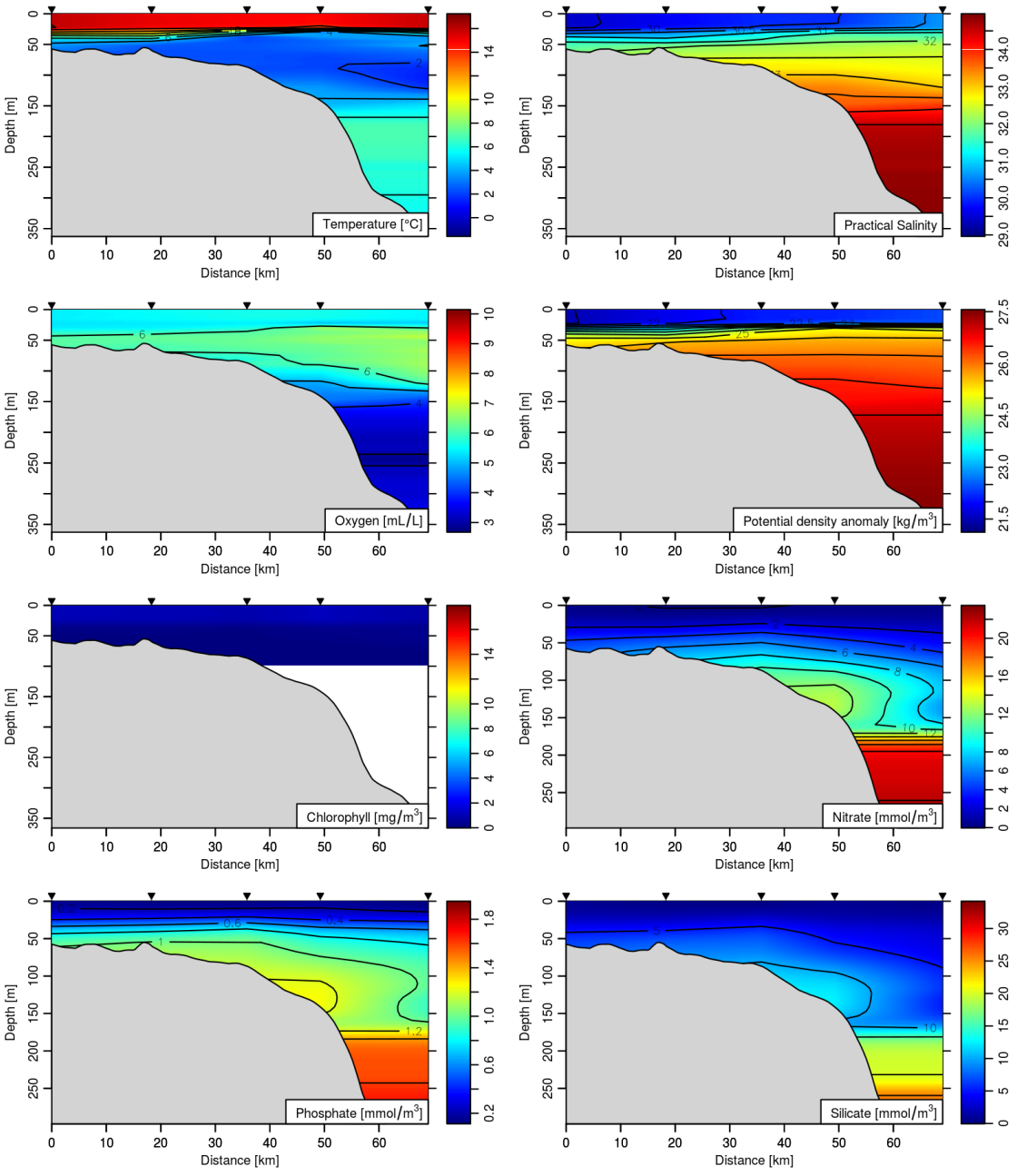

Figure 18: Section plots of temperature, salinity, oxygen, and density as measured by the CTD and chlorophyll, nitrate, phosphate, and silicate as measured by water samples from the fall 2012 hydrographic survey.

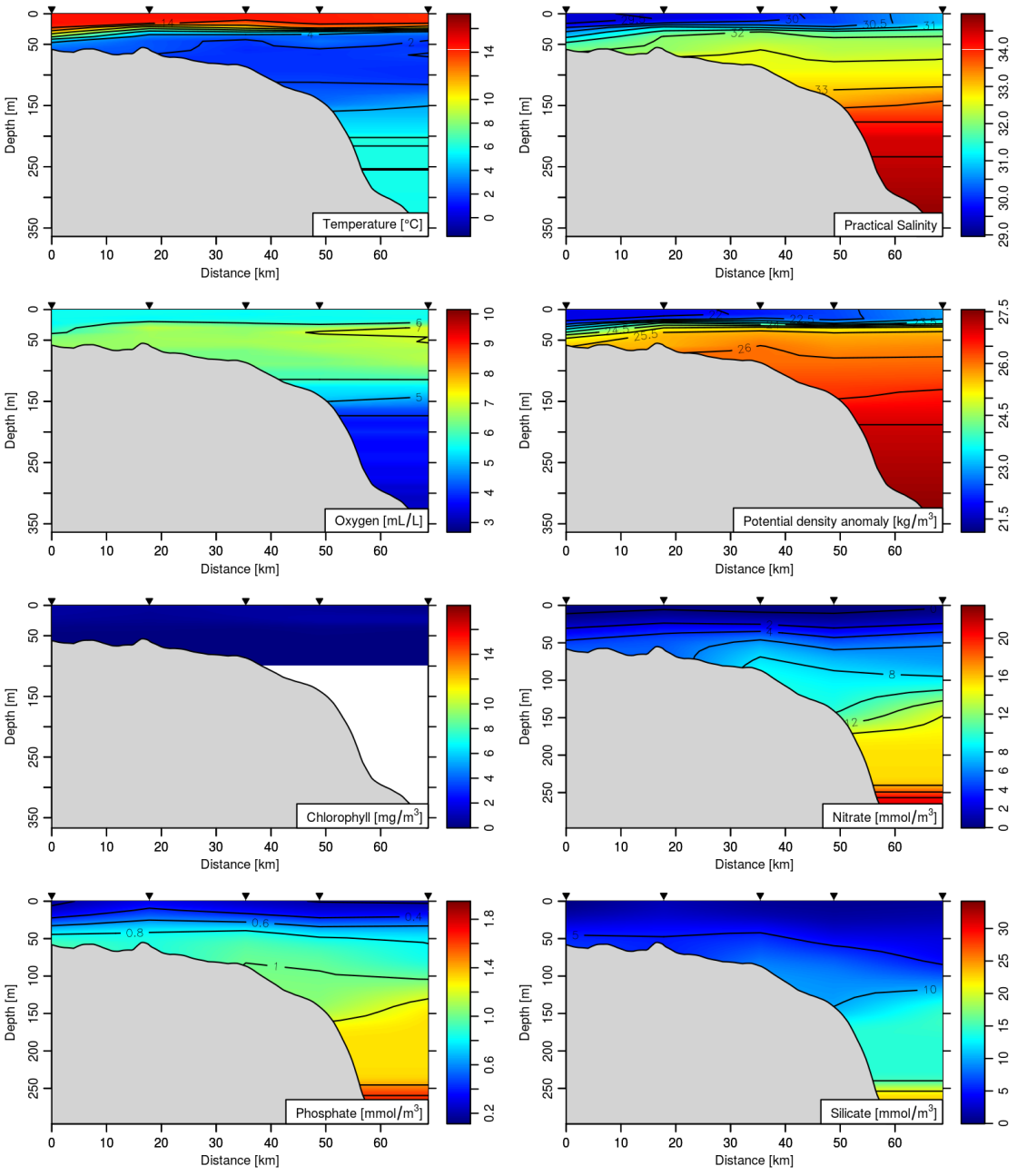

Figure 19: Section plots of temperature, salinity, oxygen, and density as measured by the CTD and chlorophyll, nitrate, phosphate, and silicate as measured by water samples from the fall 2013 hydrographic survey.

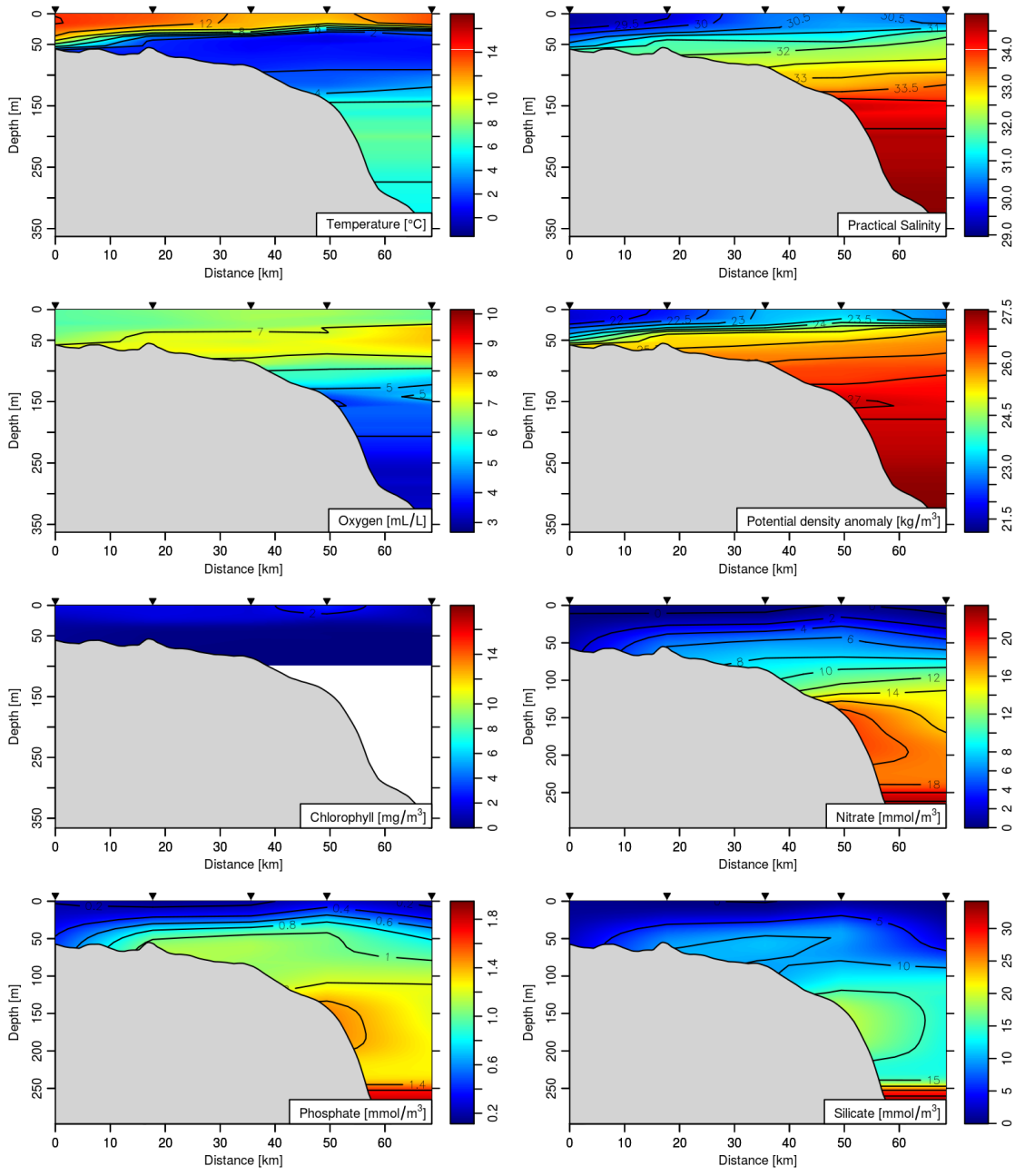

Figure 20: Section plots of temperature, salinity, oxygen, and density as measured by the CTD and chlorophyll, nitrate, phosphate, and silicate as measured by water samples from the fall 2014 hydrographic survey.

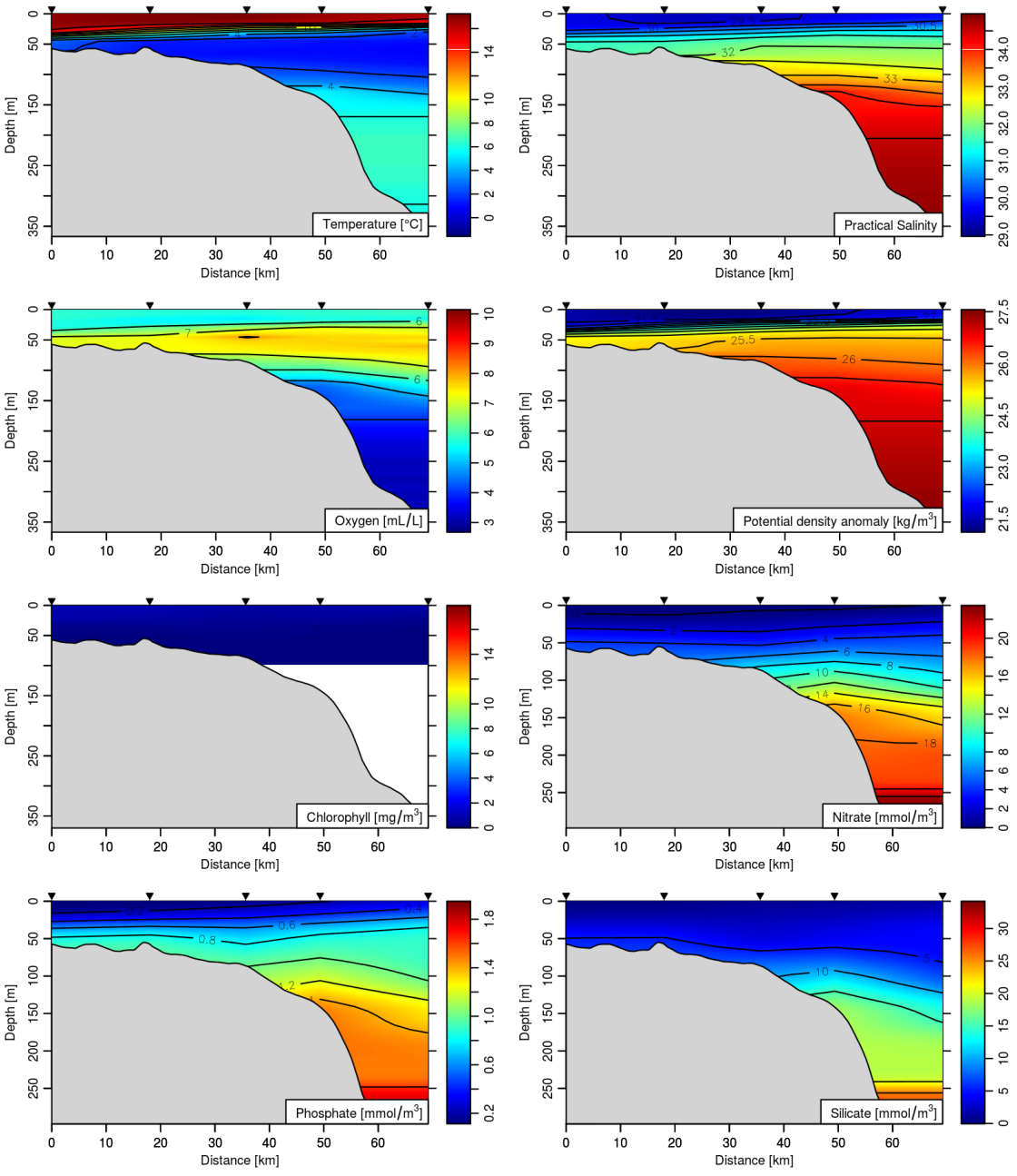

Figure 21: Section plots of temperature, salinity, oxygen, and density as measured by the CTD and chlorophyll, nitrate, phosphate, and silicate as measured by water samples from the fall 2015 hydrographic survey.

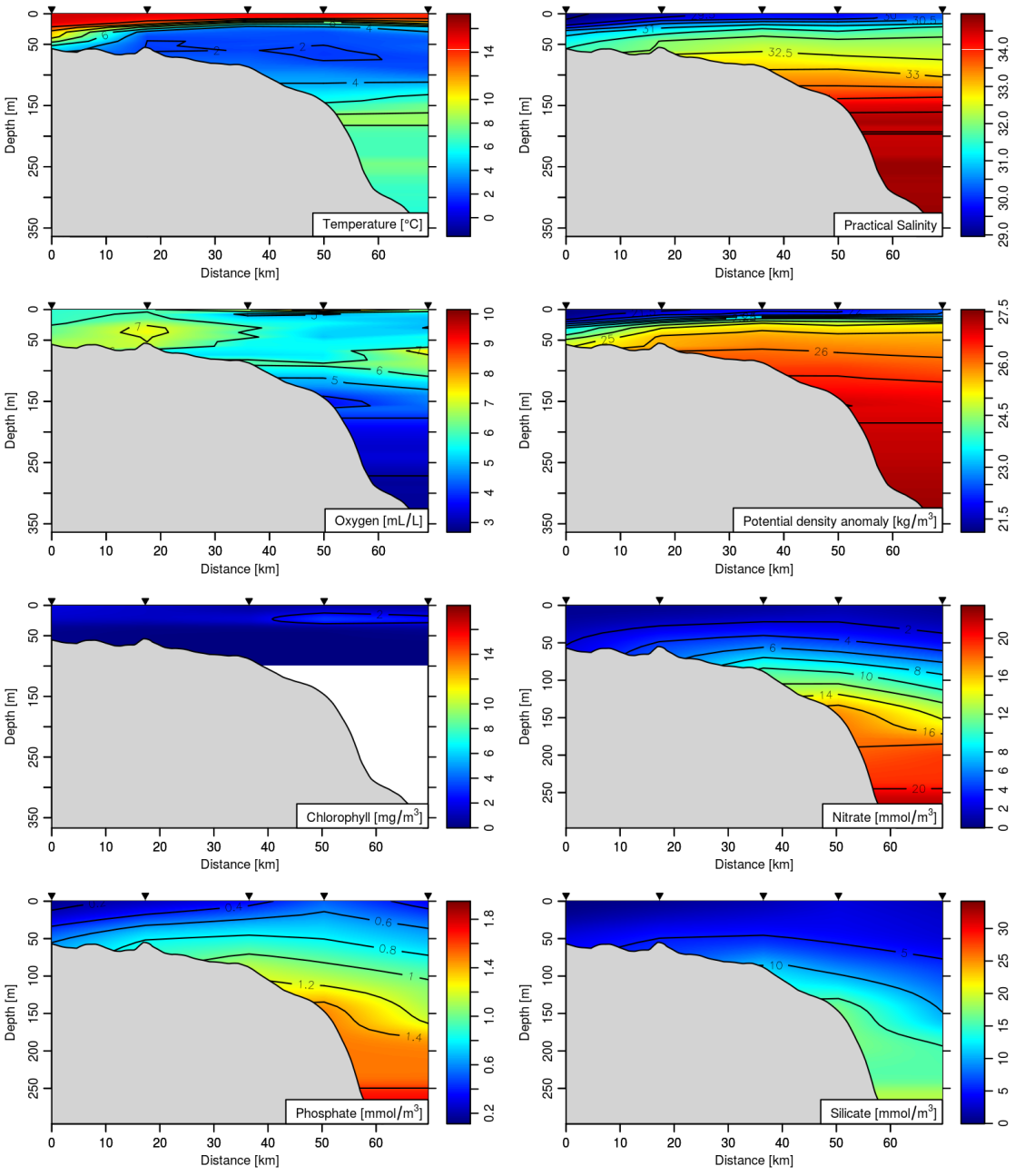

Figure 22: Section plots of temperature, salinity, oxygen, and density as measured by the CTD and chlorophyll, nitrate, phosphate, and silicate as measured by water samples from the fall 2016 hydrographic survey.

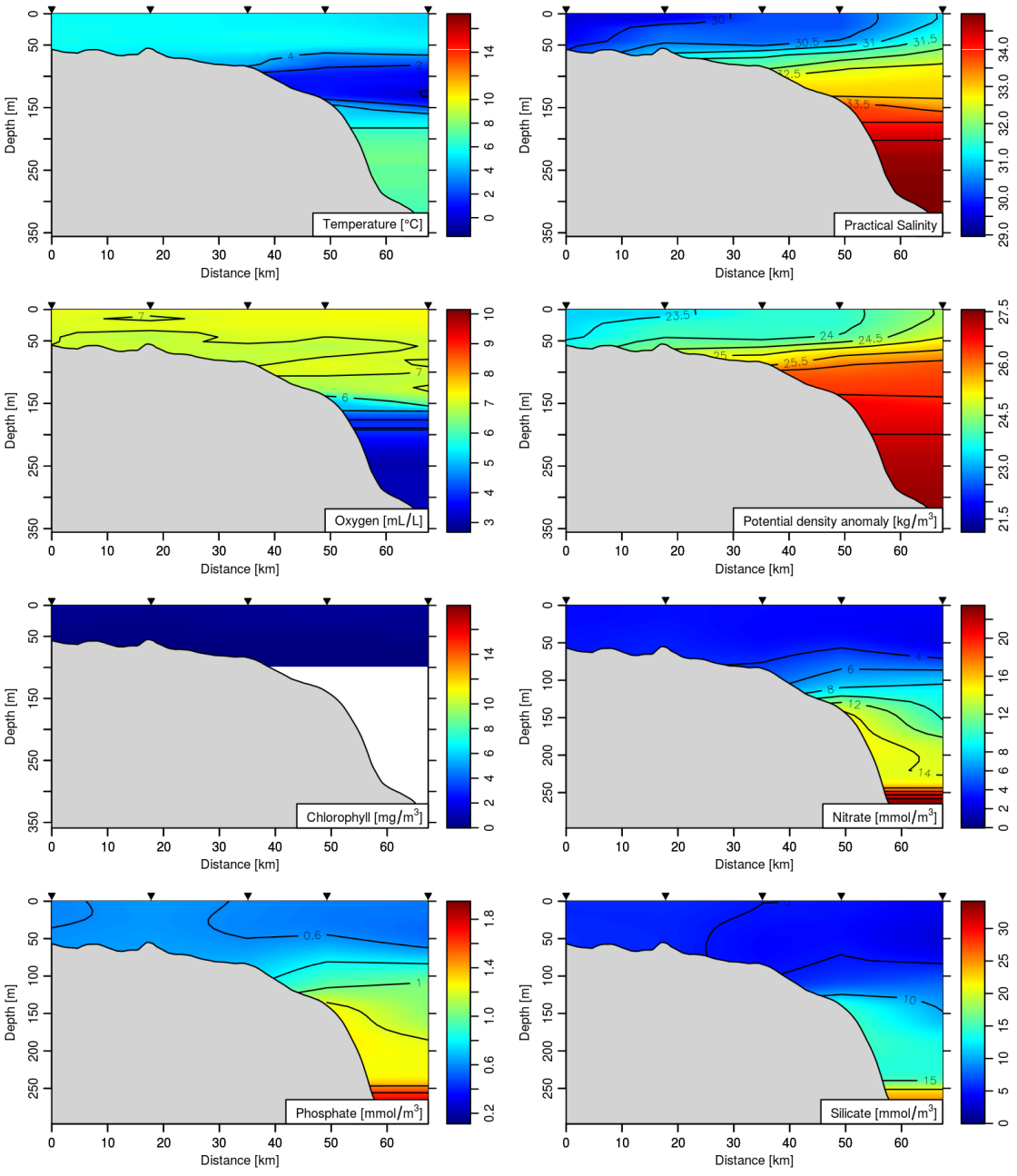

Figure 23: Section plots of temperature, salinity, oxygen, and density as measured by the CTD and chlorophyll, nitrate, phosphate, and silicate as measured by water samples from the fall 2017 hydrographic survey.

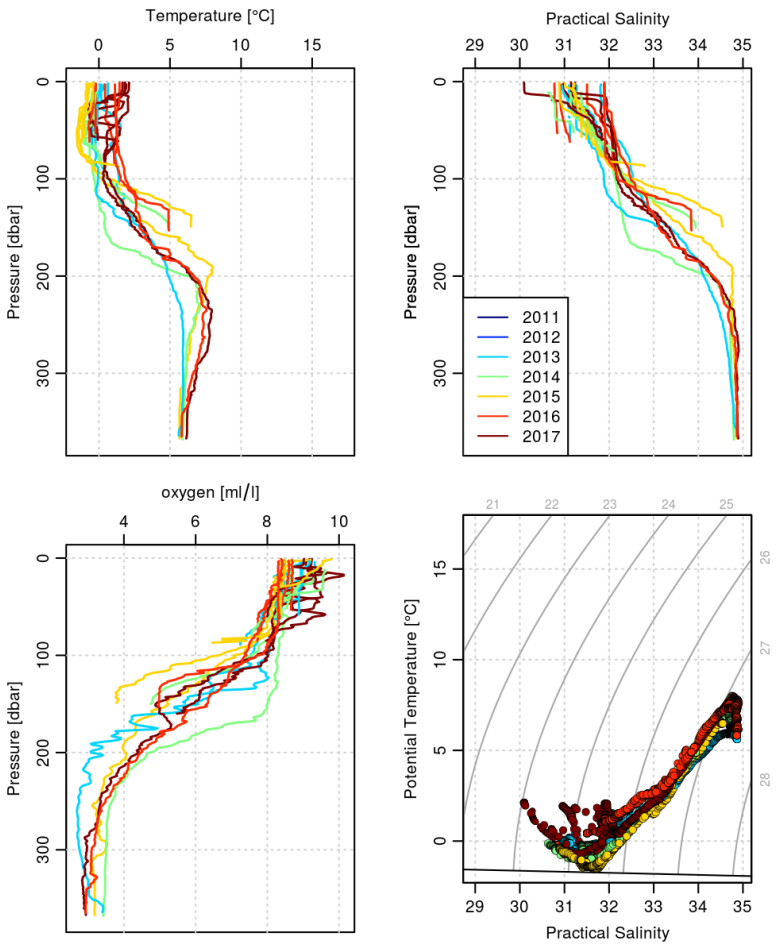

Figure 24: Profile plots of temperature (top-left), salinity, (top-right), and oxygen (bottom-left), temperature - salinity diagram (bottom-right) using CTD profiles data taken in St. Anns Bank during the spring hydrographic survey.

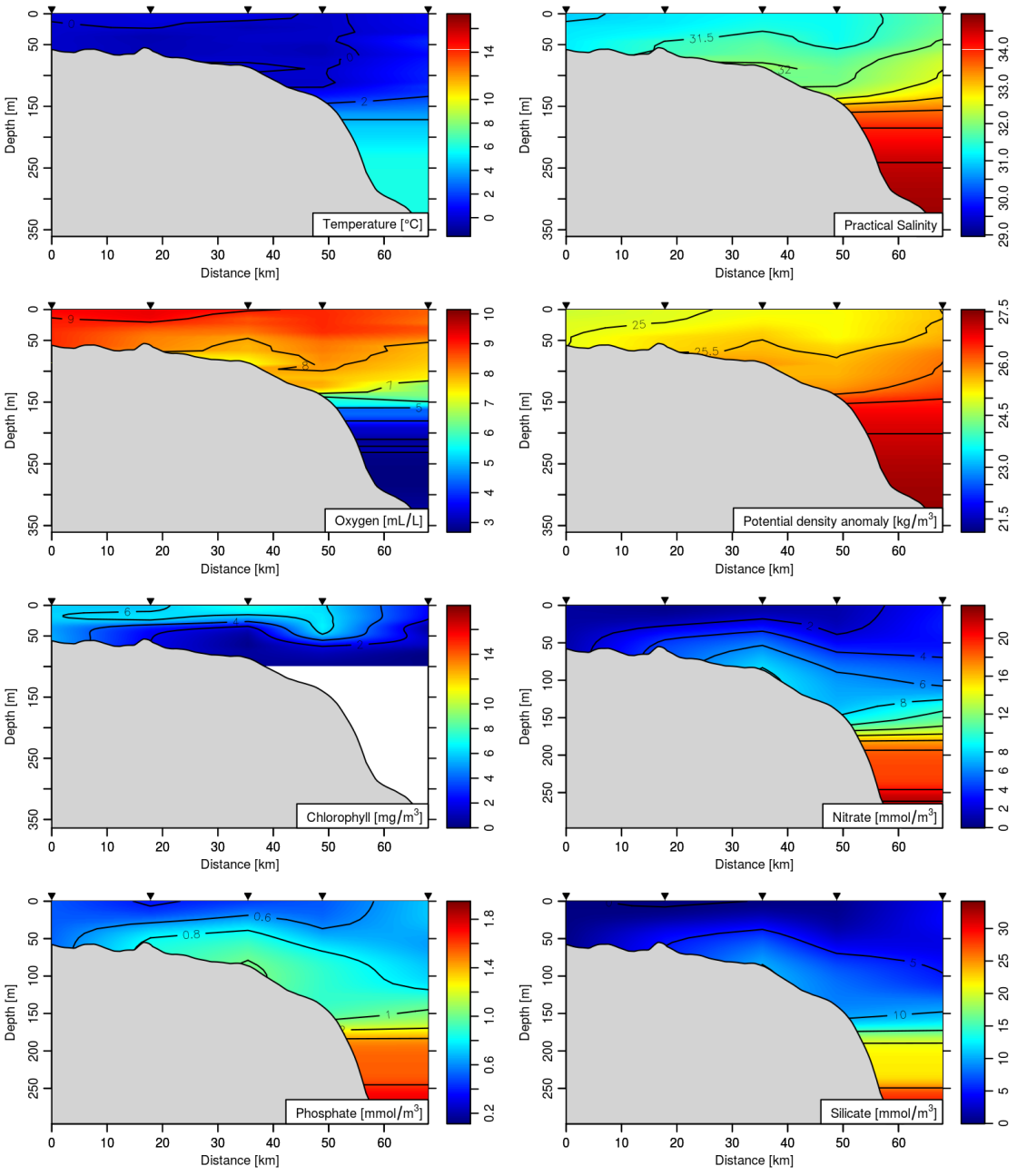

Figure 25: Section plots of temperature, salinity, oxygen, and density as measured by the CTD and chlorophyll, nitrate, phosphate, and silicate as measured by water samples from the spring 2013 hydrographic survey.

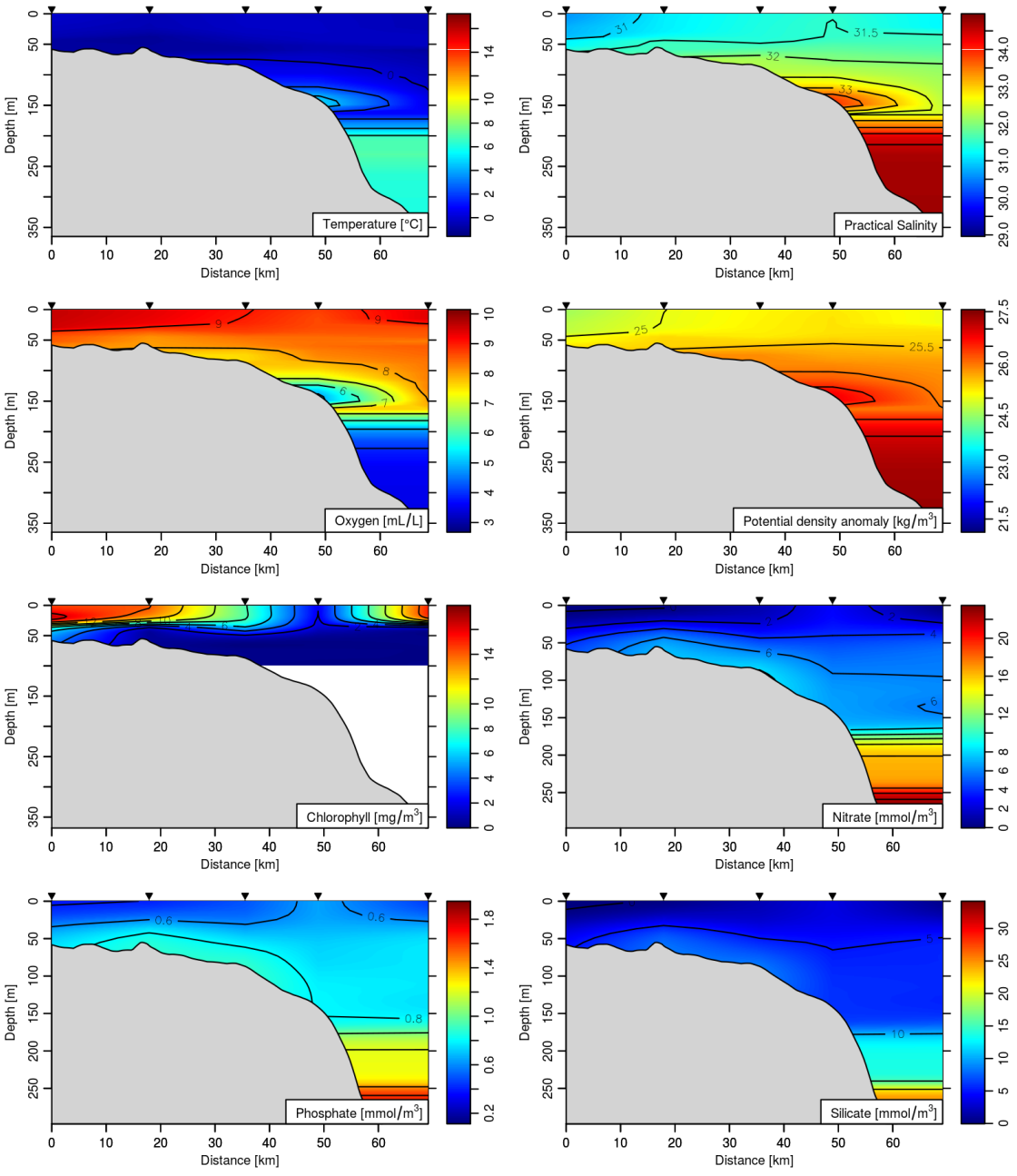

Figure 26: Section plots of temperature, salinity, oxygen, and density as measured by the CTD and chlorophyll, nitrate, phosphate, and silicate as measured by water samples from the spring 2014 hydrographic survey.

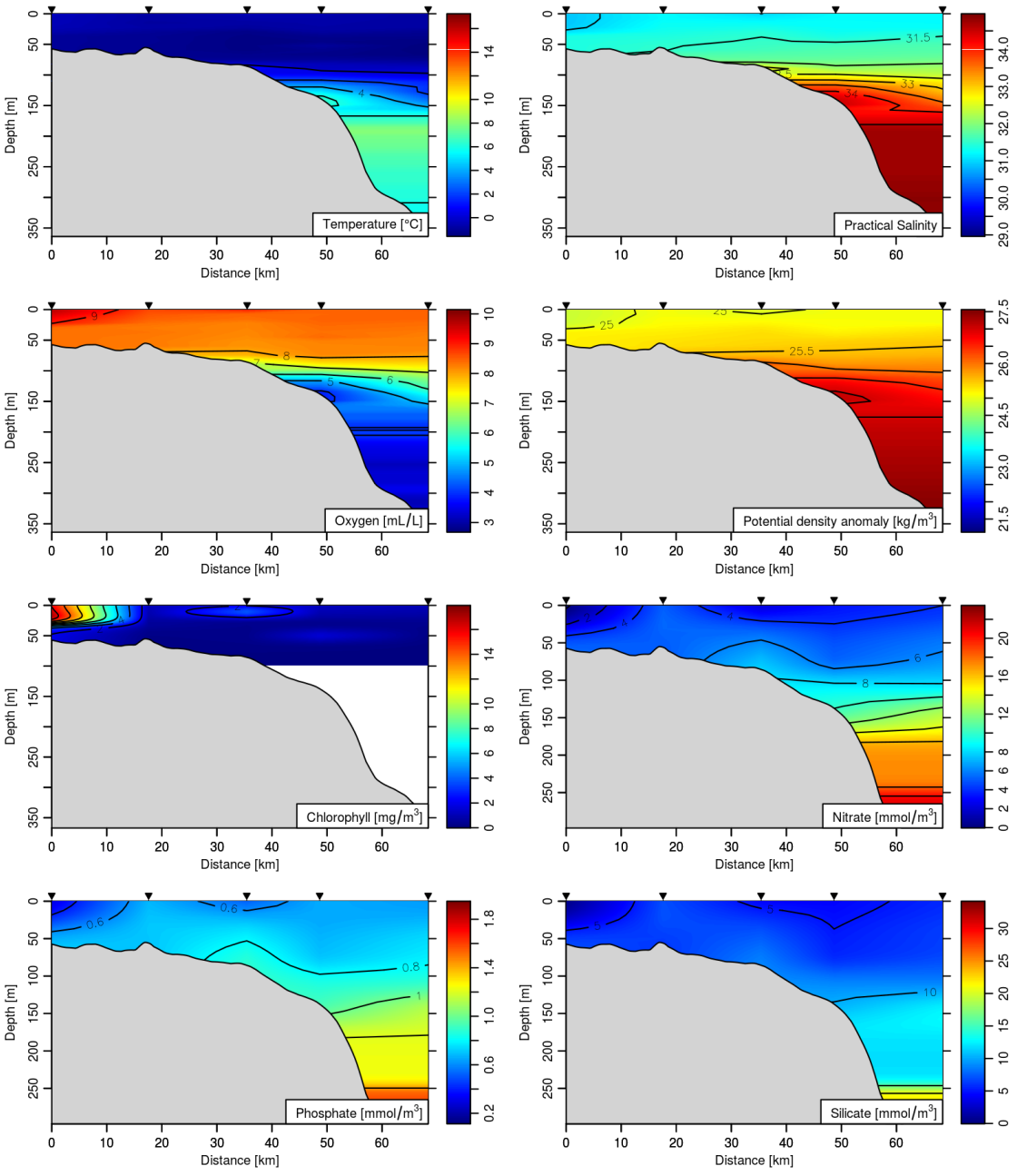

Figure 27: Section plots of temperature, salinity, oxygen, and density as measured by the CTD and chlorophyll, nitrate, phosphate, and silicate as measured by water samples from the spring 2015 hydrographic survey.

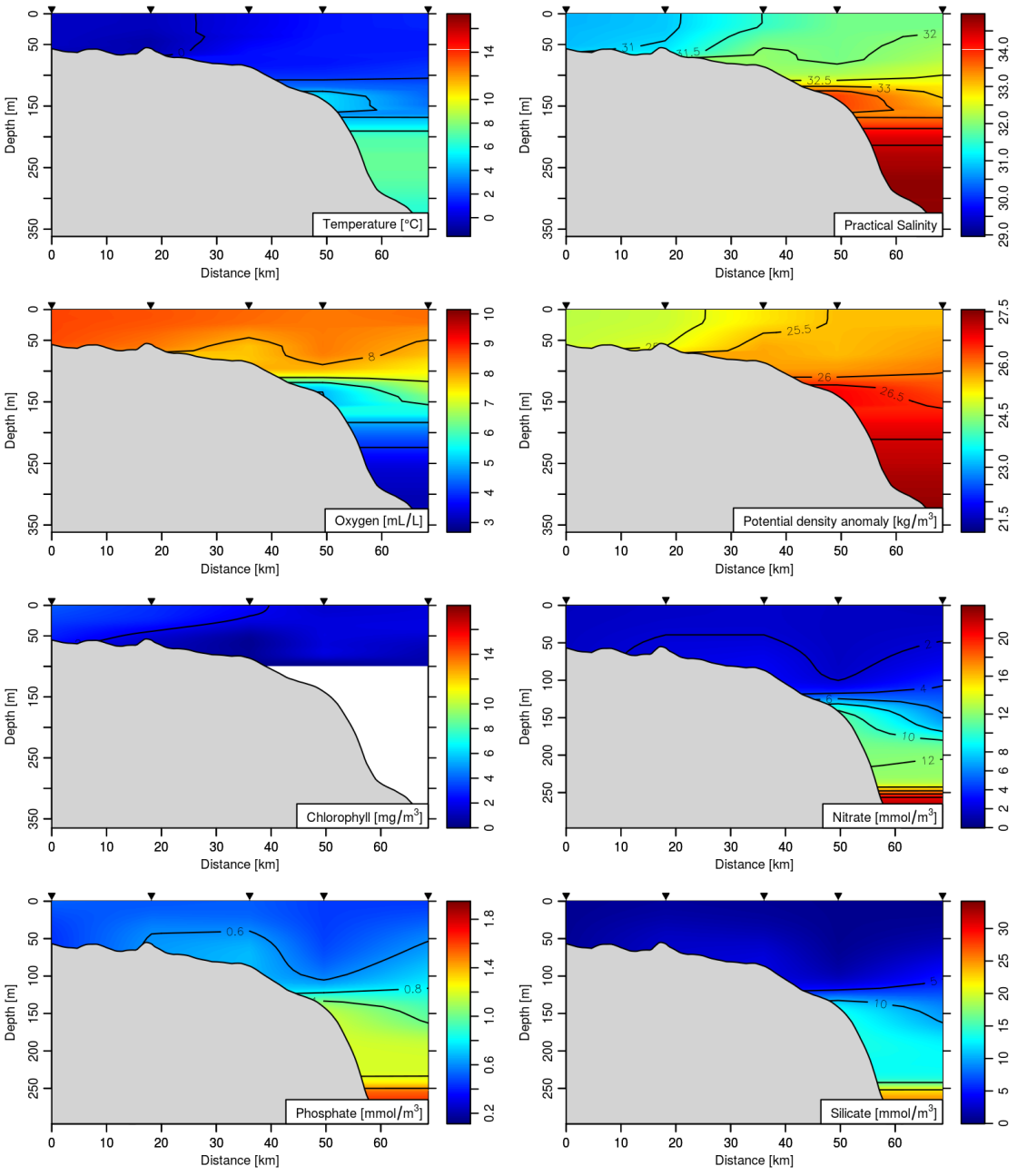

Figure 28: Section plots of temperature, salinity, oxygen, and density as measured by the CTD and chlorophyll, nitrate, phosphate, and silicate as measured by water samples from the spring 2016 hydrographic survey.

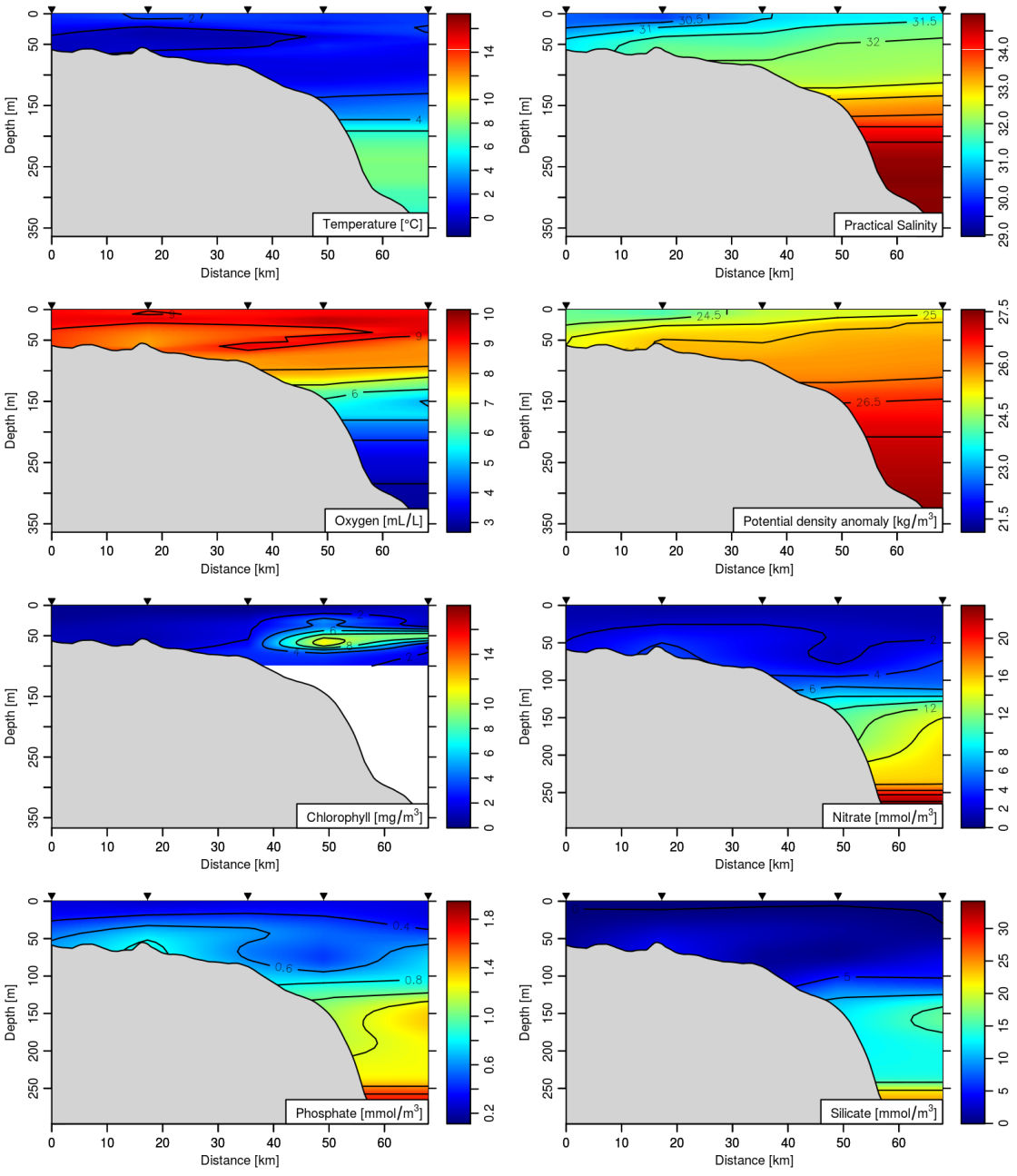

Figure 29: Section plots of temperature, salinity, oxygen, and density as measured by the CTD and chlorophyll, nitrate, phosphate, and silicate as measured by water samples from the spring 2017 hydrographic survey.

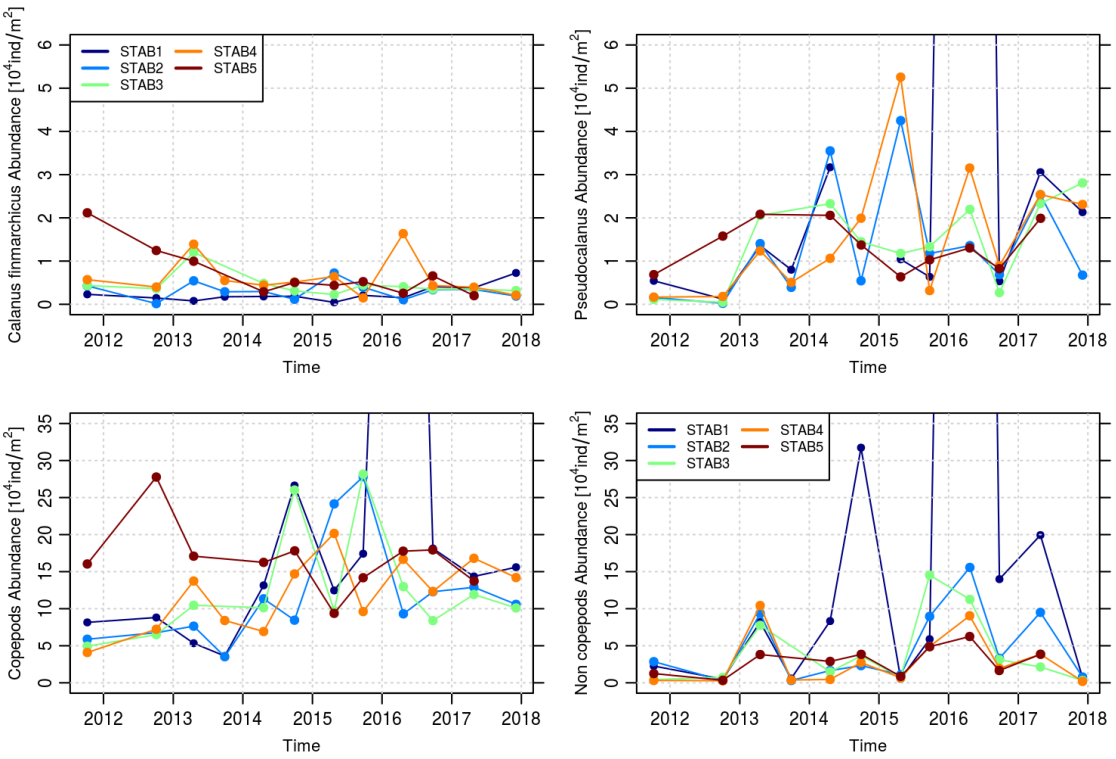

Figure 30: Dominant zooplankton species abundance at each station location along the STAB transect for (top-left) *Calanus finmarchicus*, (top-right) *Pseudocalanus*, (bottom-left) copepods, and (bottom-right) non-copepods. Note the varying y-axis scales.

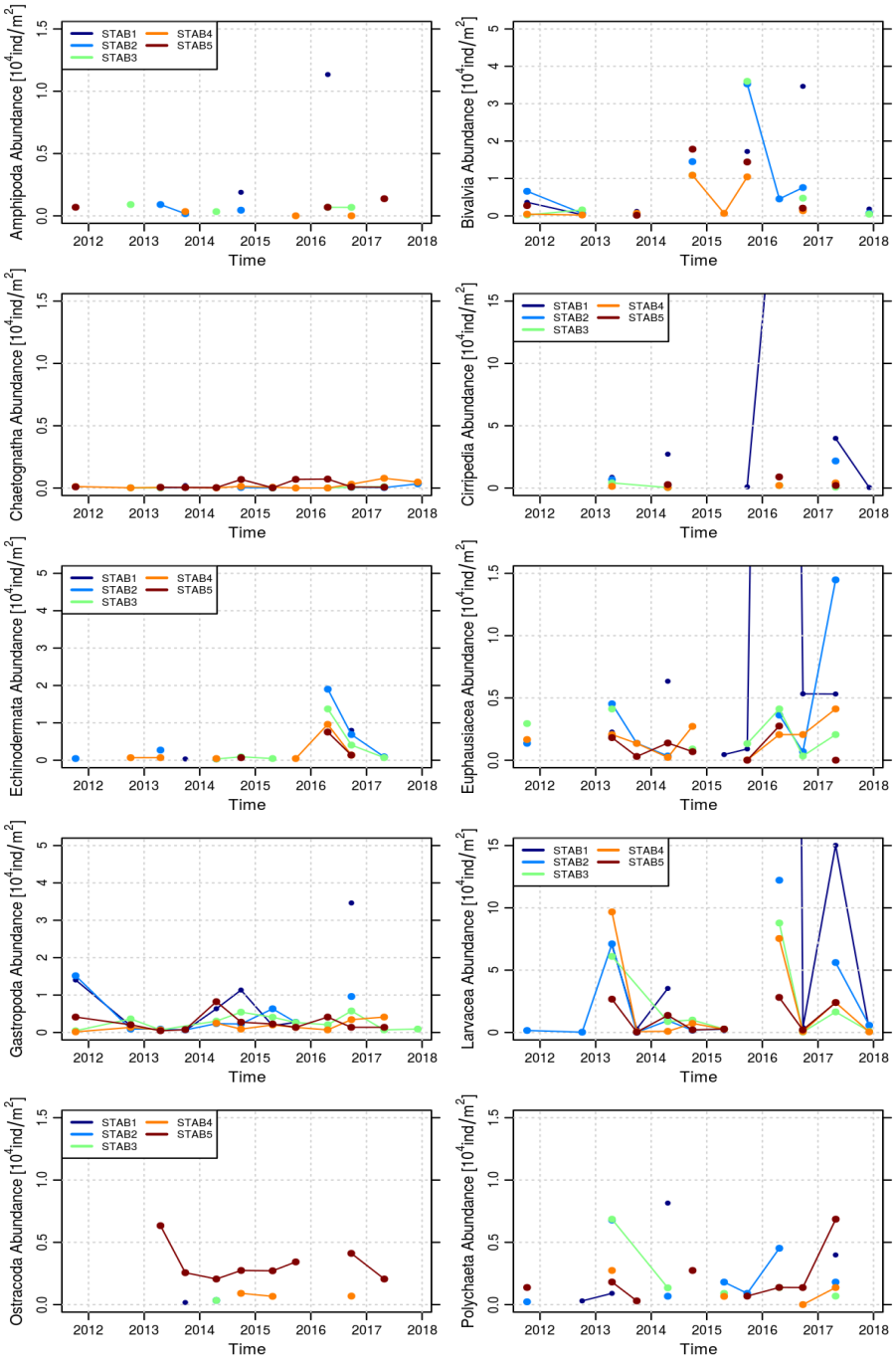

Figure 31: Dominant non-copepod species abundance at each station along the STAB transect. Note the varying y-axis scales.

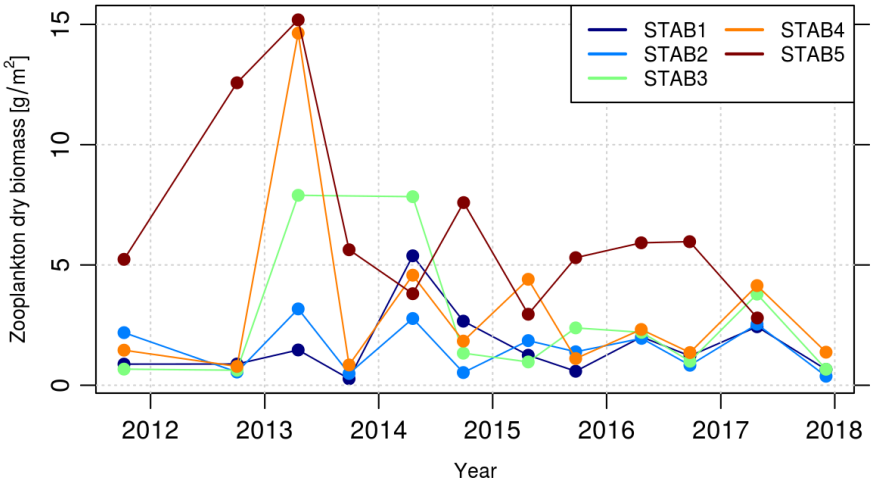

Figure 32: Total zooplankton dry biomass at each station along the STAB transect.

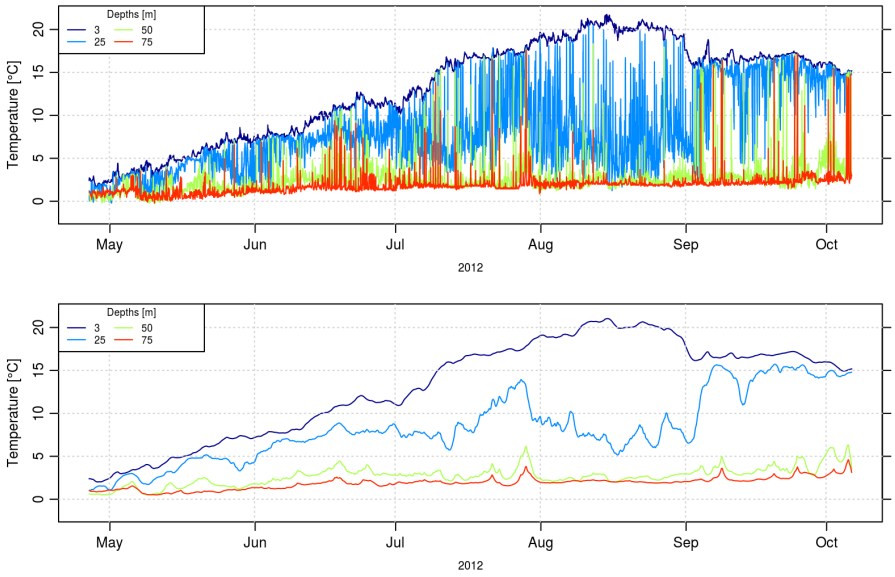

Figure 33: Time-series from temperature recorders of the raw (top) and low-pass filtered (bottom) at STAB-C in 2012.

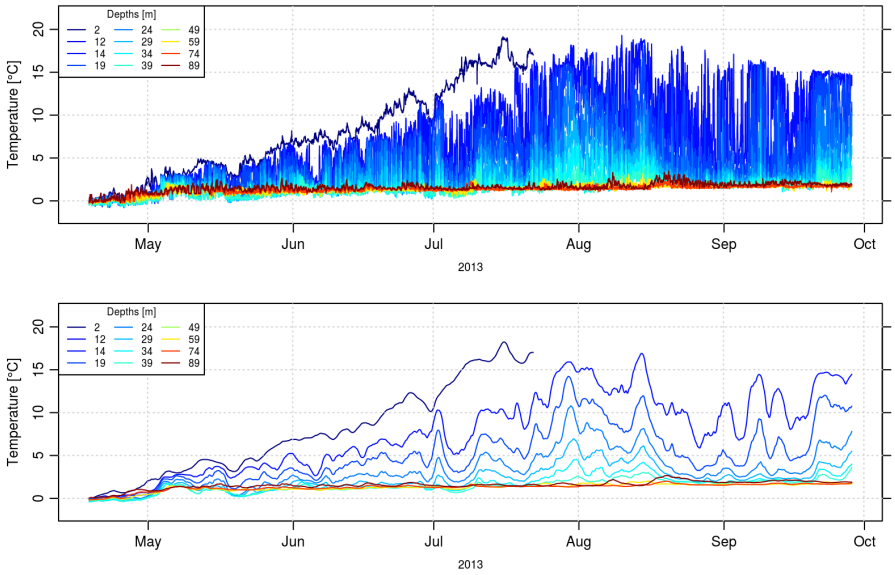

Figure 34: Time-series from temperature recorders of the raw (top) and low-pass filtered (bottom) at STAB-C in 2013.

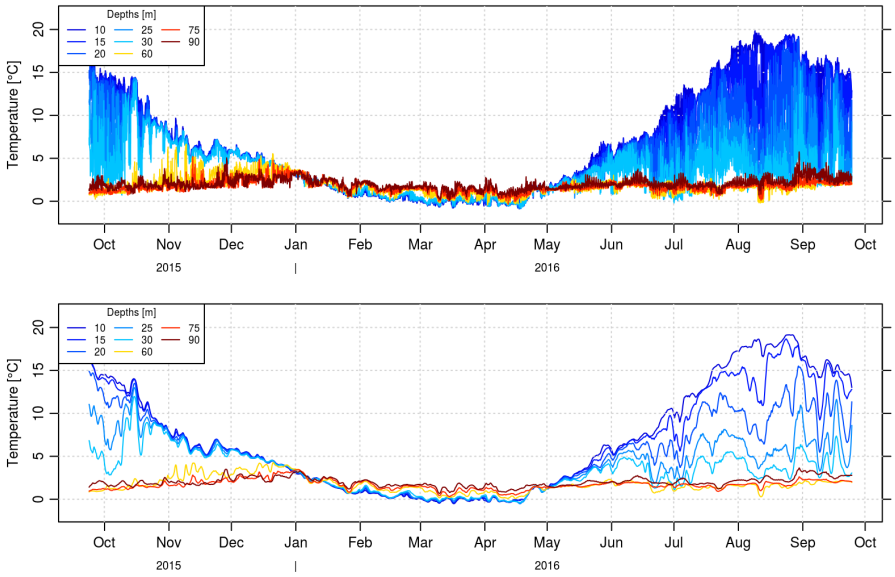

Figure 35: Time-series from temperature recorders of the raw (top) and low-pass filtered (bottom) at STAB-C from fall 2015 to fall 2016.

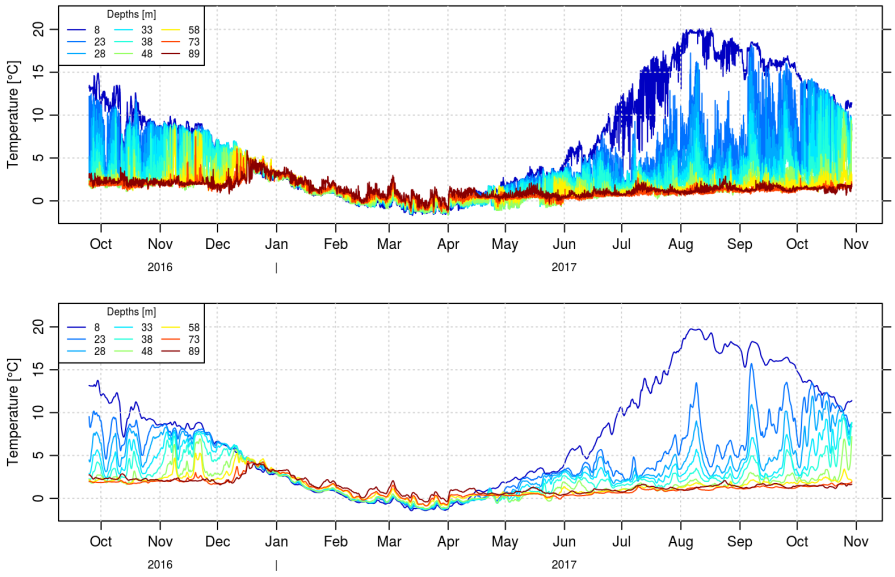

Figure 36: Time-series from temperature recorders of the raw (top) and low-pass filtered (bottom) at STAB-C from fall 2016 to fall 2017.

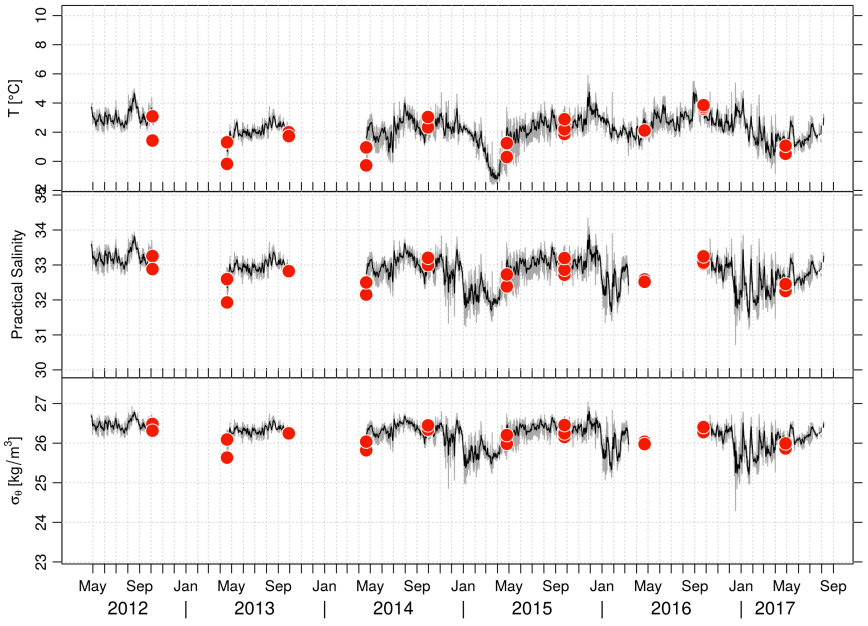

Figure 37: Time-series from a moored CTD placed near the bottom, about 100 m, at the repeated mooring location, STAB-C. From top to bottom, temperature, salinity, and density. Grey lines indicate raw data and black is the low-passed data. Red dots indicate measurements made by CTD profiles across the transect at the instrument moored depth.

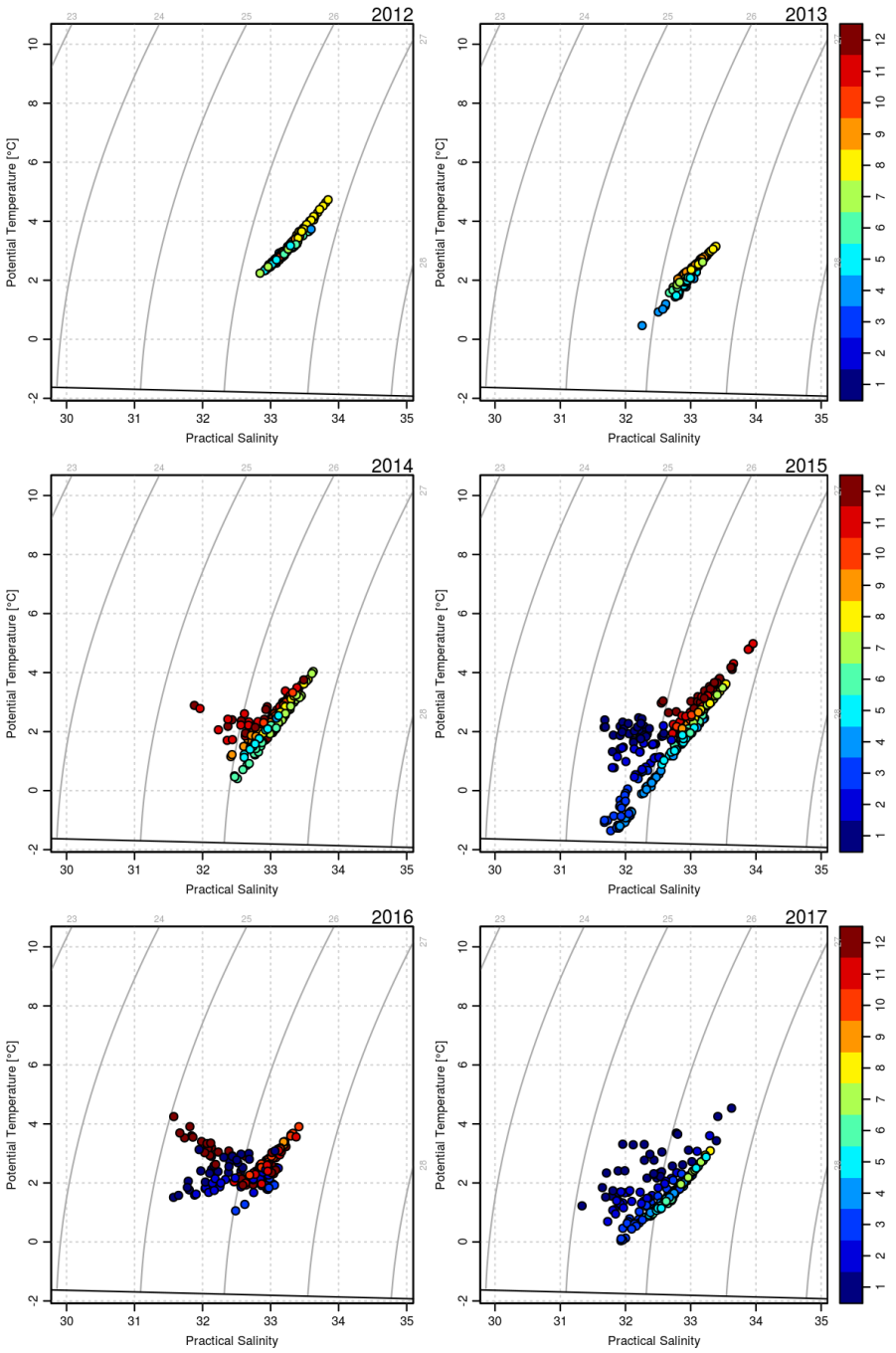

Figure 38: Temperature-salinity diagram of daily average moored near-bottom, around 100 m, measurements at STAB-C for each sampling year, from 2012 to 2017, colour coded by month where 1 refers to January, and 12 refers to December.

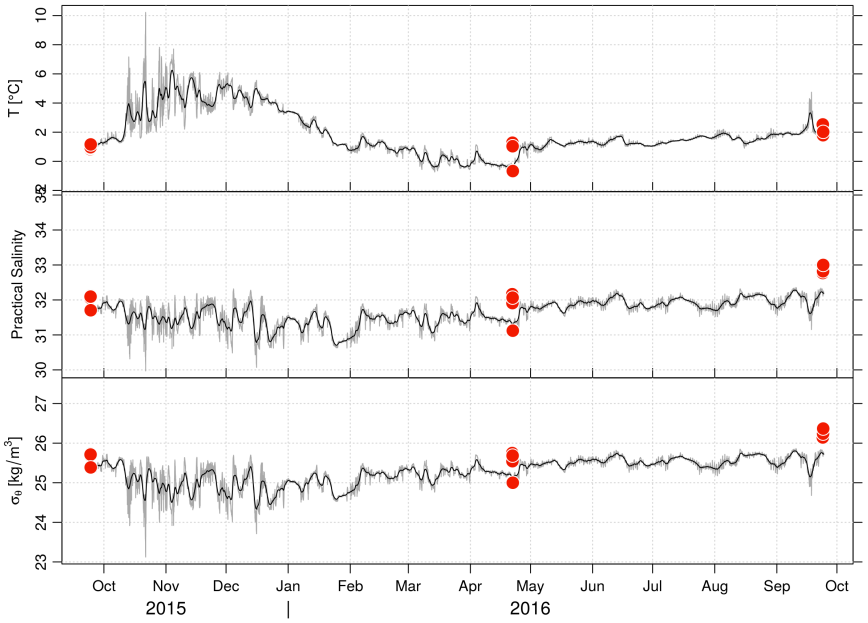

Figure 39: Time-series from moored CTD placed near the bottom, around 60 m, at STAB-I which is located between STAB2 and STAB3. From top to bottom, temperature, salinity, and density. Grey lines indicate raw data and black is the low-passed data. Red dots indicate measurements made by CTD profiles across the transect at the instrument moored depth.

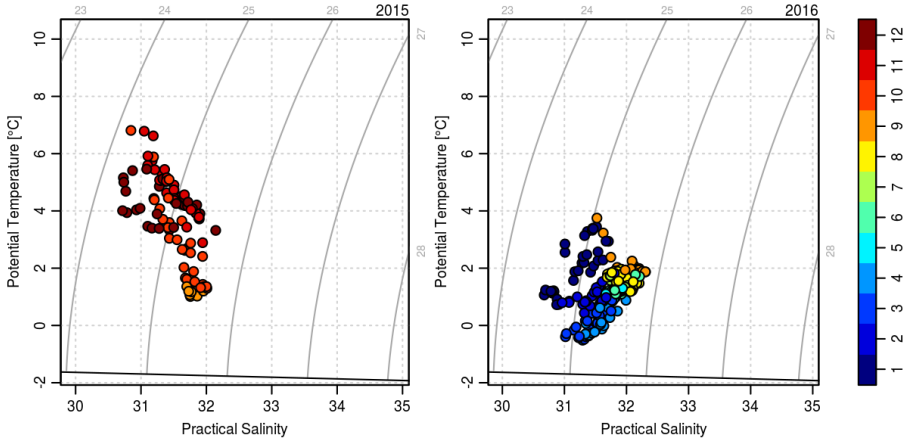

Figure 40: Temperature-salinity diagram of daily average moored near-bottom, around 60 m, measurements at STAB-I for each sampling year, from 2015 to 2016, colour coded by month where 1 refers to January, and 12 refers to December.

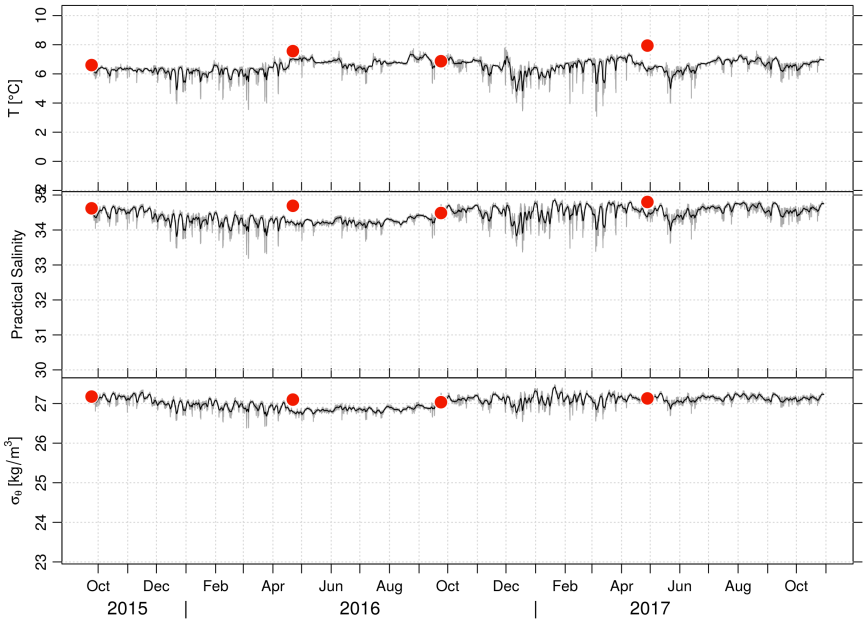

Figure 41: Time-series from moored CTD placed near the bottom, around 235 m, at STAB-O which is located between STAB4 and STAB5. From top to bottom, temperature, salinity, and density. Grey lines indicate raw data and black is the low-passed data. Red dots indicate measurements made by CTD profiles across the transect at the instrument moored depth.

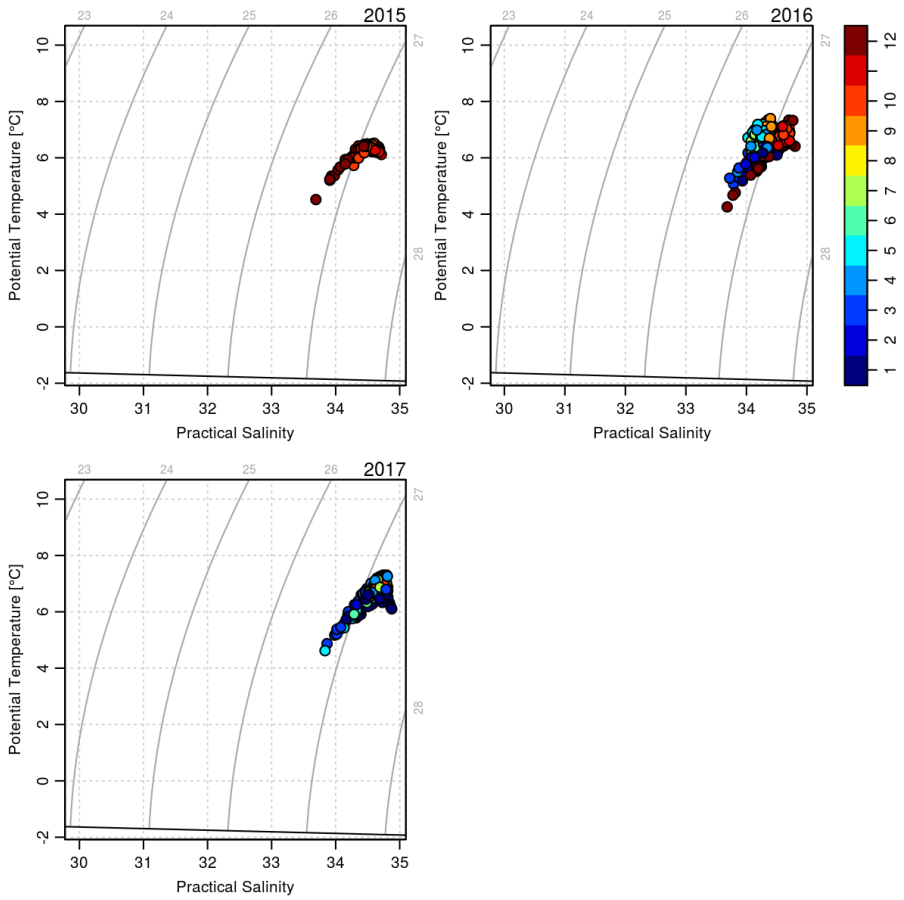

Figure 42: Temperature-salinity diagram of daily average moored near-bottom, around 235 m, measurements at STAB-O for each sampling year, from 2015 to 2017, colour coded by month where 1 refers to January, and 12 refers to December.

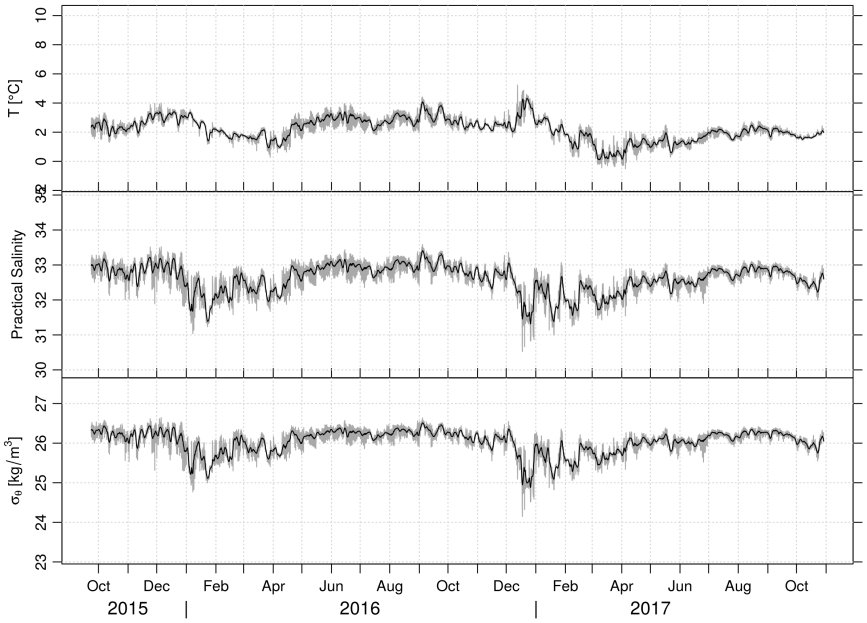

Figure 43: Time-series from moored CTD placed near the bottom, around 110 m, at the mooring downstream of the STAB transect, STAB-S. From top to bottom, temperature, salinity, and density. Grey lines indicate raw data and black is the low-passed data.

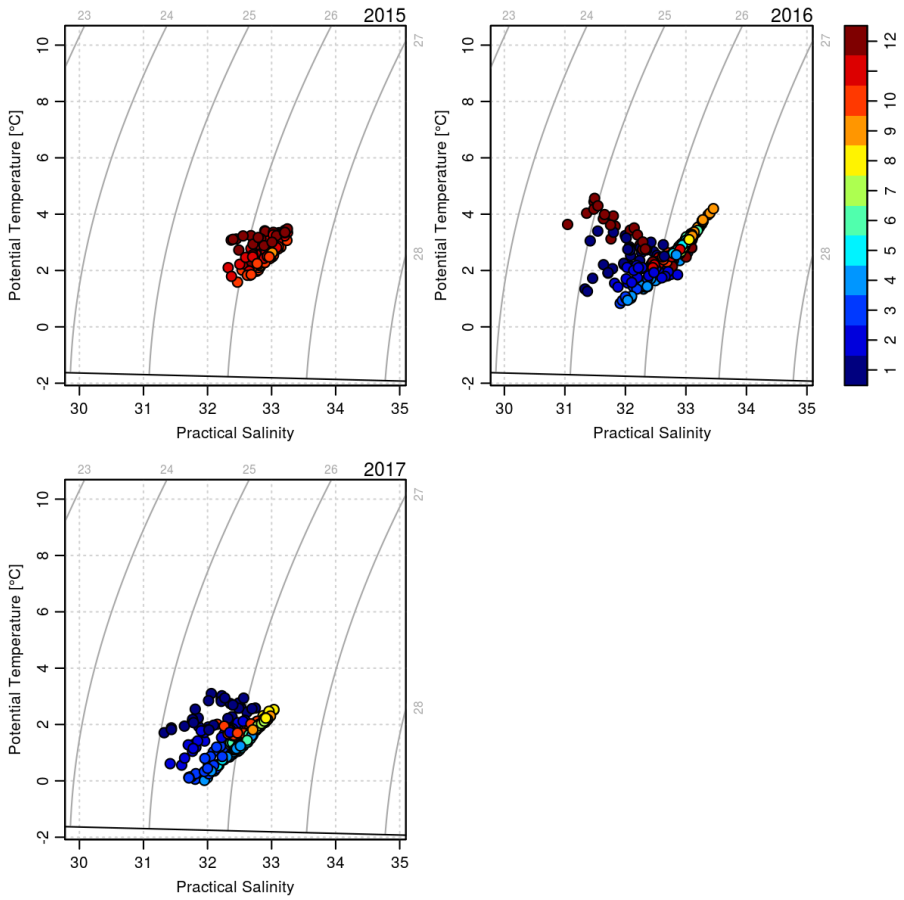

Figure 44: Temperature-salinity diagram of daily average moored near-bottom, around 110 m, measurements at STAB-S for each sampling year, from 2015 to 2017, colour coded by month where 1 refers to January, and 12 refers to December.

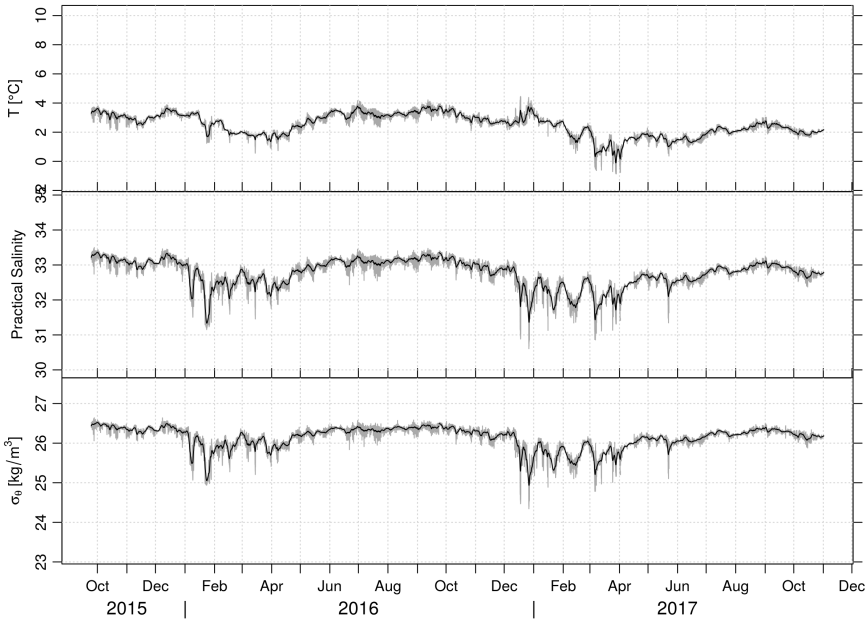

Figure 45: Time-series from moored CTD placed near the bottom, around 125 m, at the mooring, STAB-N, which is downstream of STAB-S. From top to bottom, temperature, salinity, and density. Grey lines indicate raw data and black is the low-passed data.

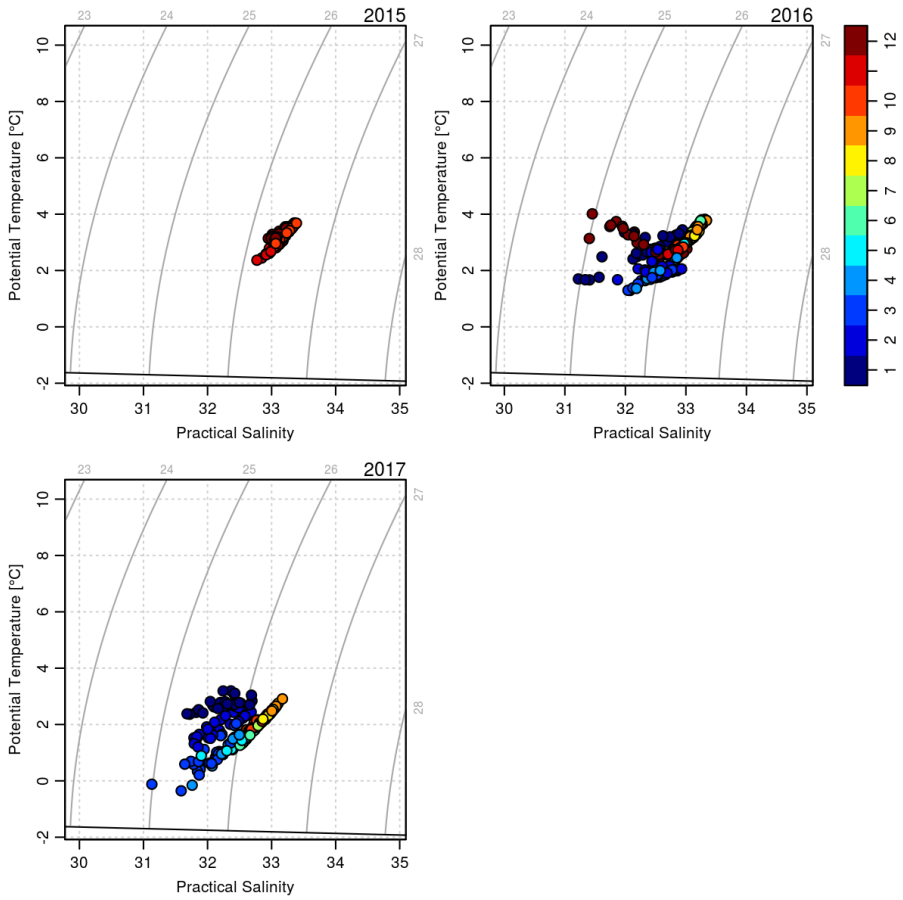

Figure 46: Temperature-salinity diagram of daily average moored near-bottom, around 125 m, measurements at STAB-N for each sampling year, from 2015 to 2017, colour coded by month where 1 refers to January, and 12 refers to December.

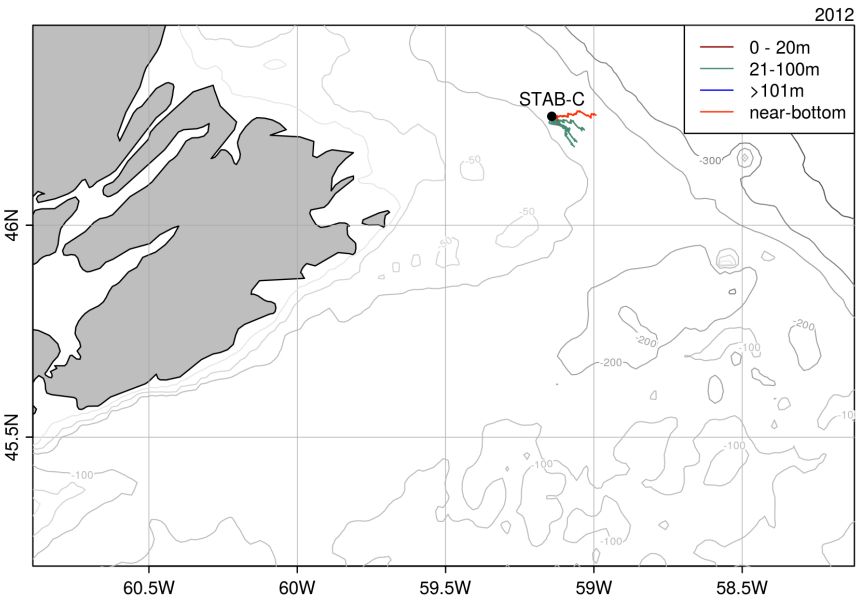

Figure 47: Scaled progressive vectors for all moorings deployed in 2012.

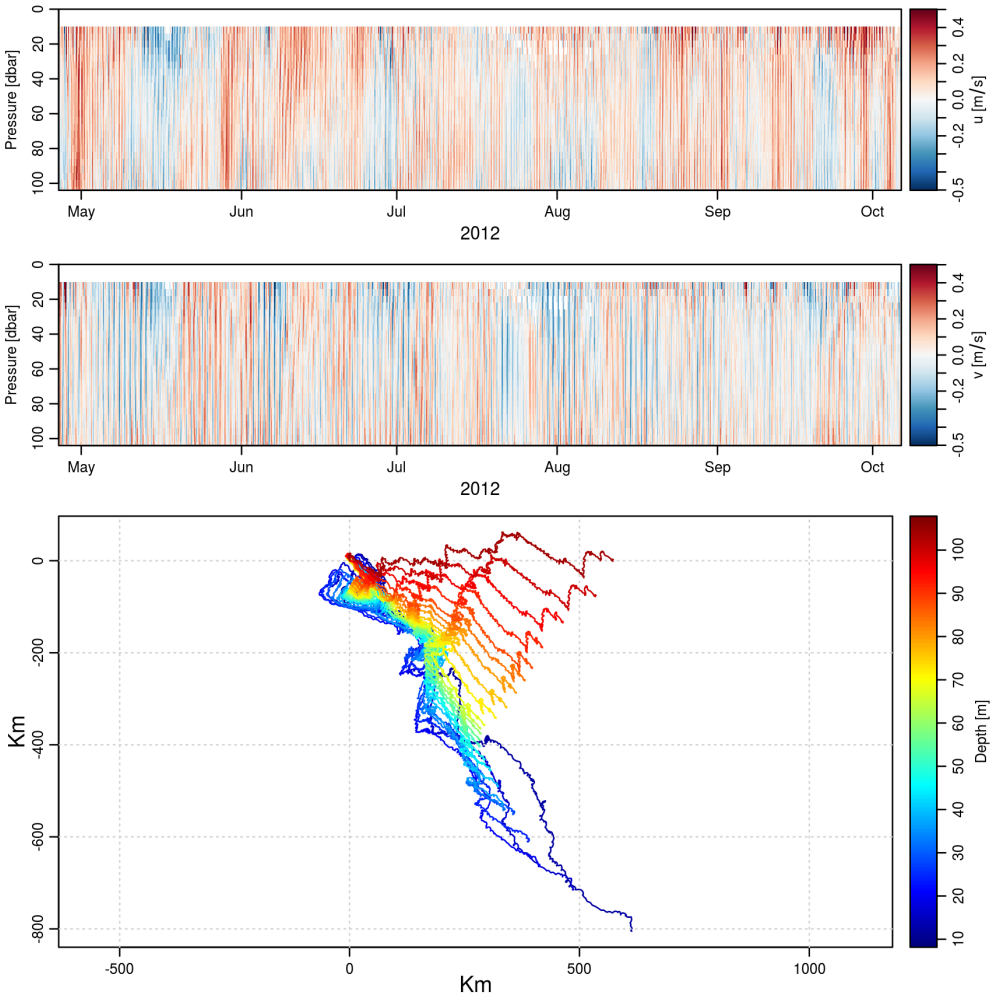

Figure 48: Velocity measurements at STAB-C in 2012, (top) along-isobath, (middle) cross-isobath, and (bottom) a progressive vector diagram from the ADCP measurements.

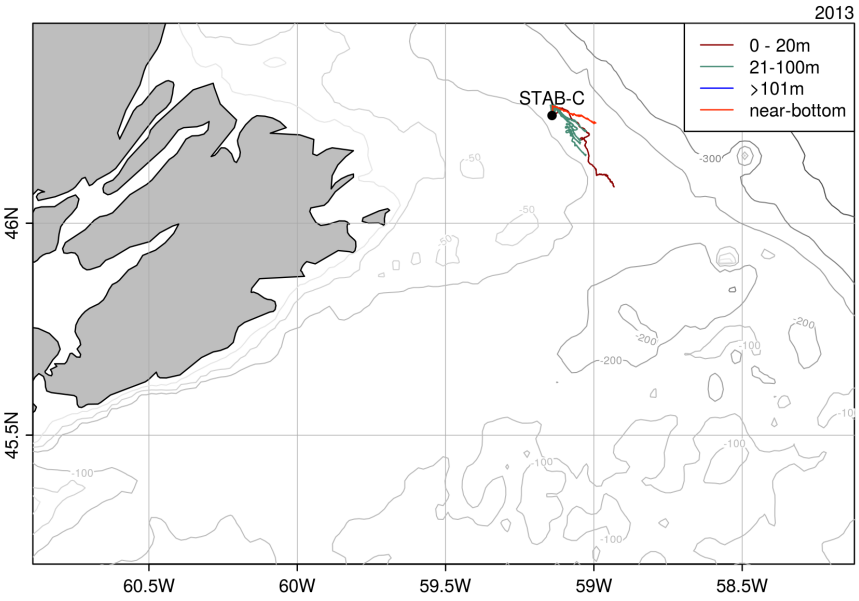

Figure 49: Scaled progressive vectors for all moorings deployed in 2013.

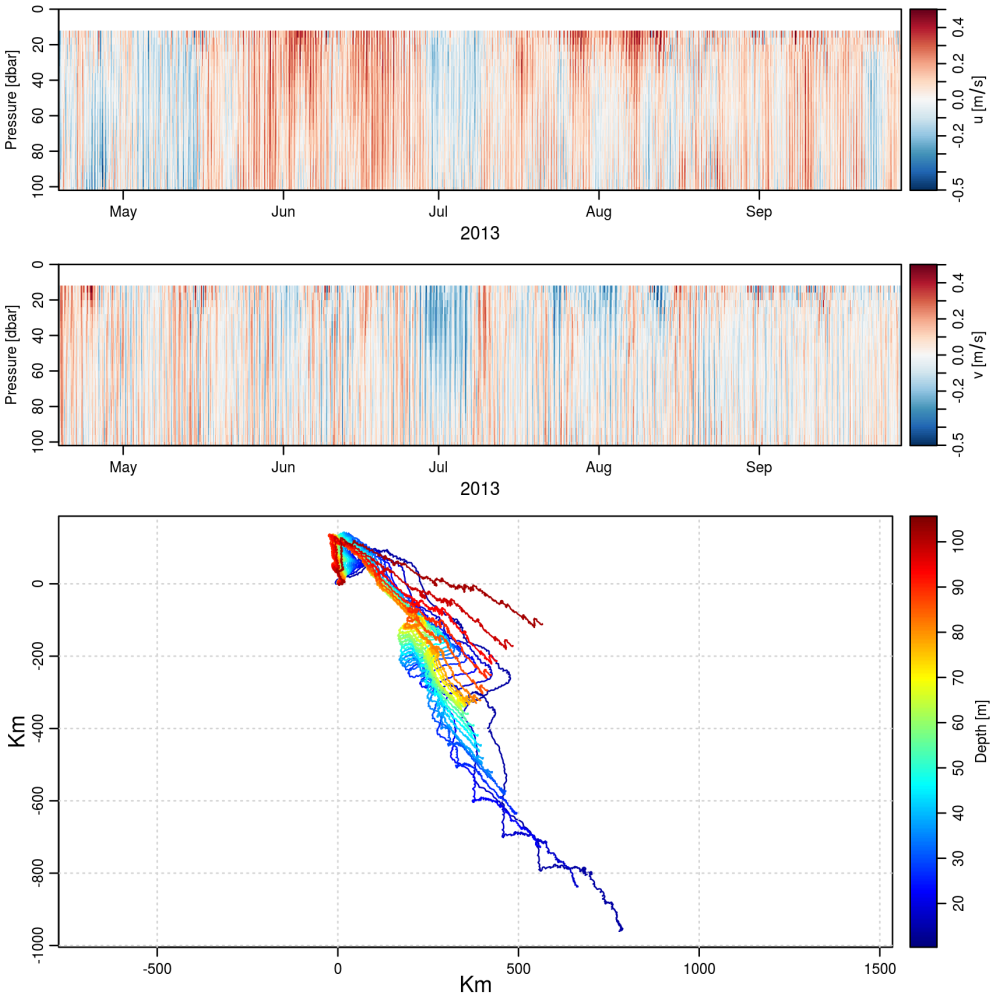

Figure 50: Velocity measurements at STAB-C in 2013, (top) along-isobath, (middle) cross-isobath, and (bottom) a progressive vector diagram from the ADCP measurements.

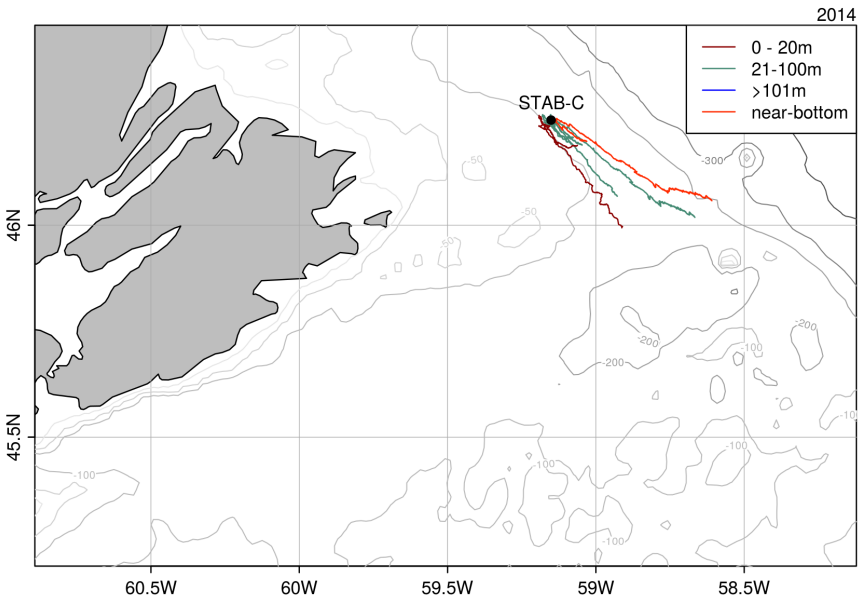

Figure 51: Scaled progressive vectors for all moorings deployed in 2014. Note that there were two separate mooring deployments at STAB-C during this year.

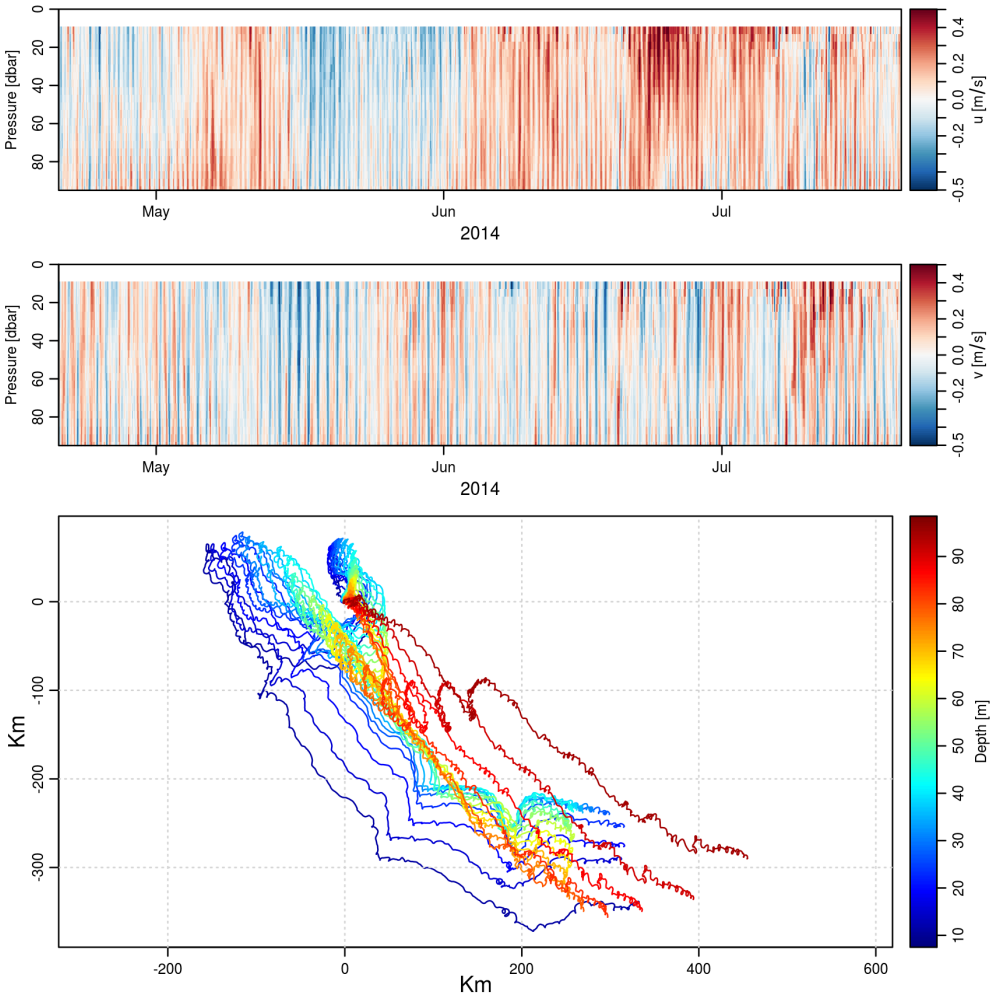

Figure 52: Velocity measurements at STAB-C in 2014, (top) along-isobath, (middle) cross-isobath, and (bottom) a progressive vector diagram from the ADCP measurements.

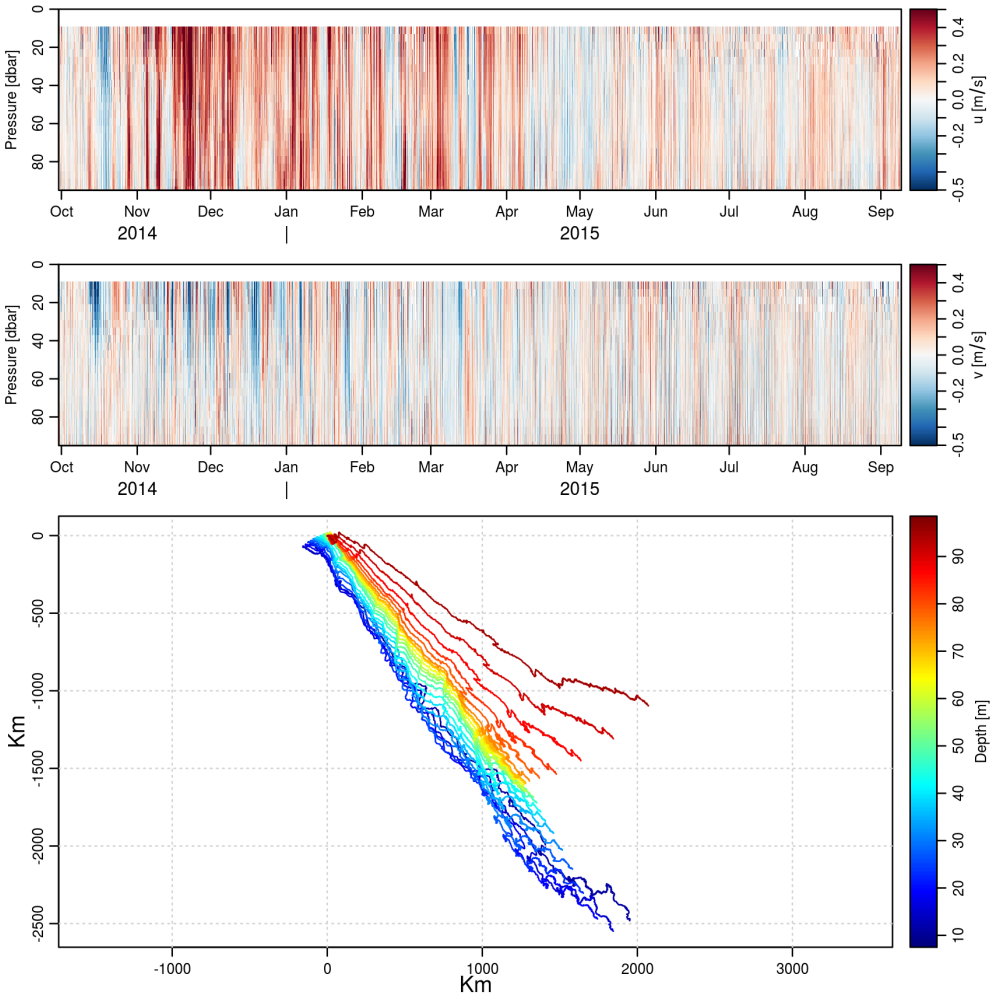

Figure 53: Velocity measurements at STAB-C from fall 2014 to fall 2015, (top) along-isobath, (middle) cross-isobath, and (bottom) a progressive vector diagram from the ADCP measurements.

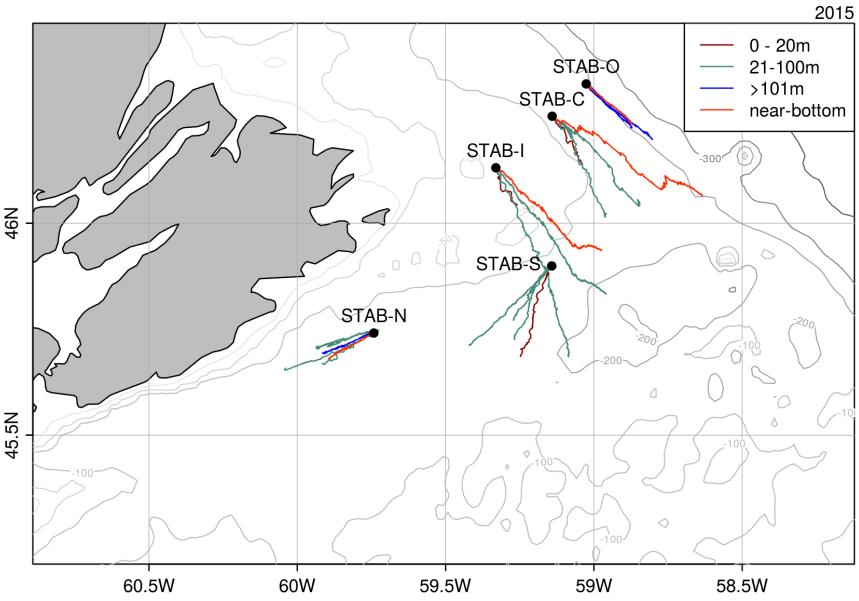

Figure 54: Scaled progressive vectors for all moorings deployed in 2015.

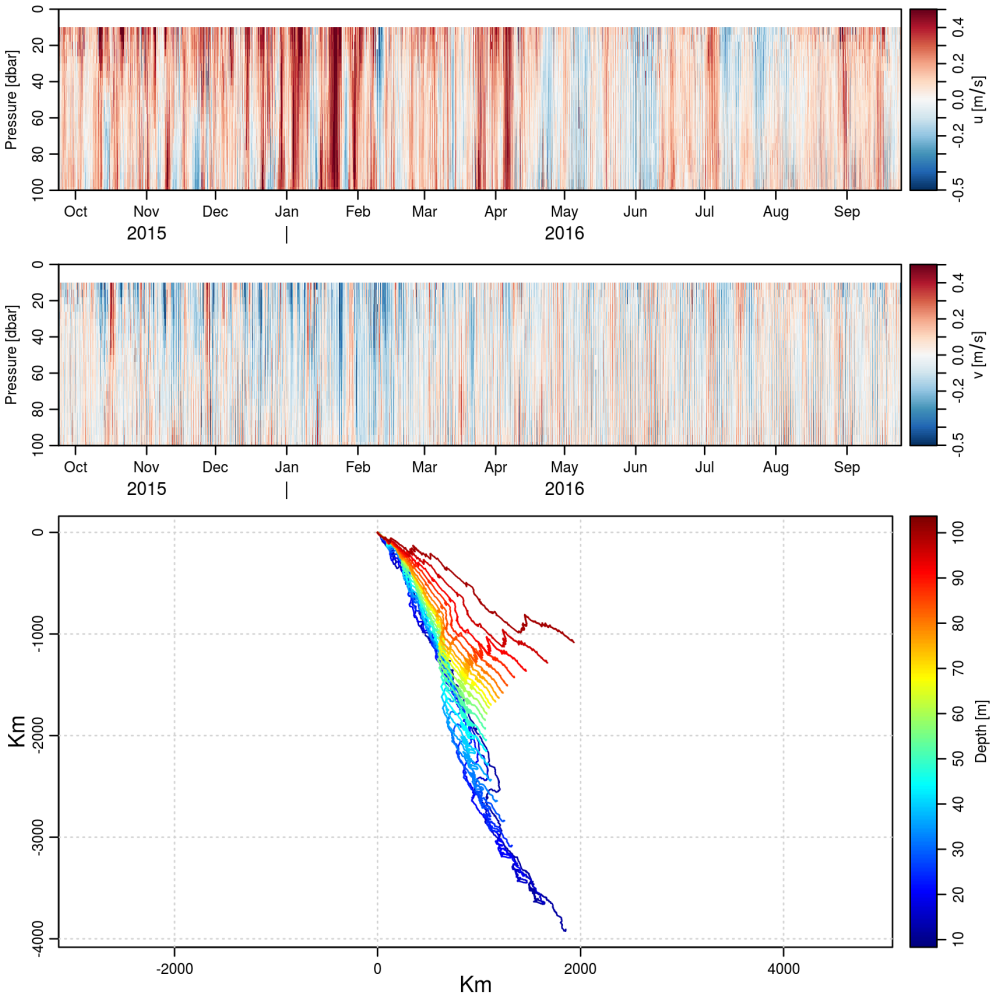

Figure 55: Velocity measurements at STAB-C from fall 2015 to fall 2016, (top) along-isobath, (middle) cross-isobath, and (bottom) a progressive vector diagram from the ADCP measurements.

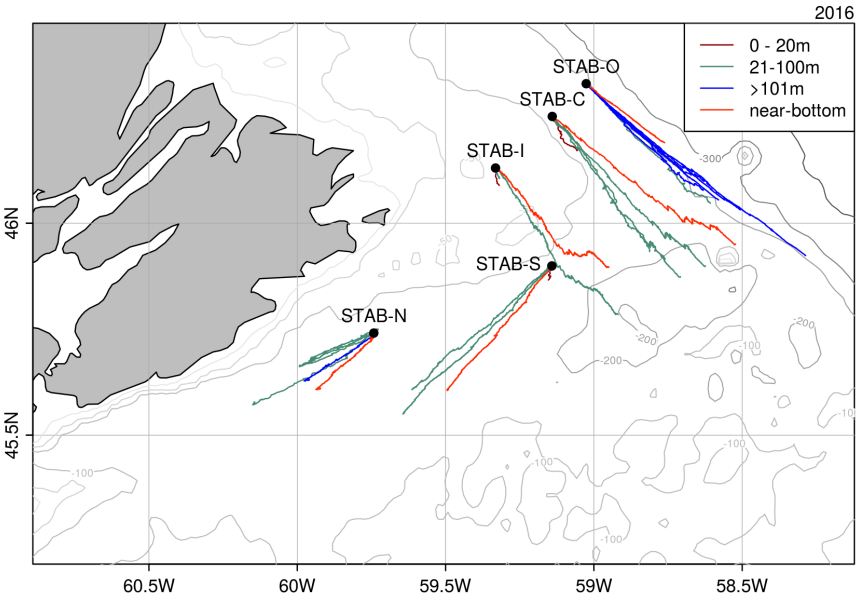

Figure 56: Scaled progressive vectors for all moorings deployed in 2016.

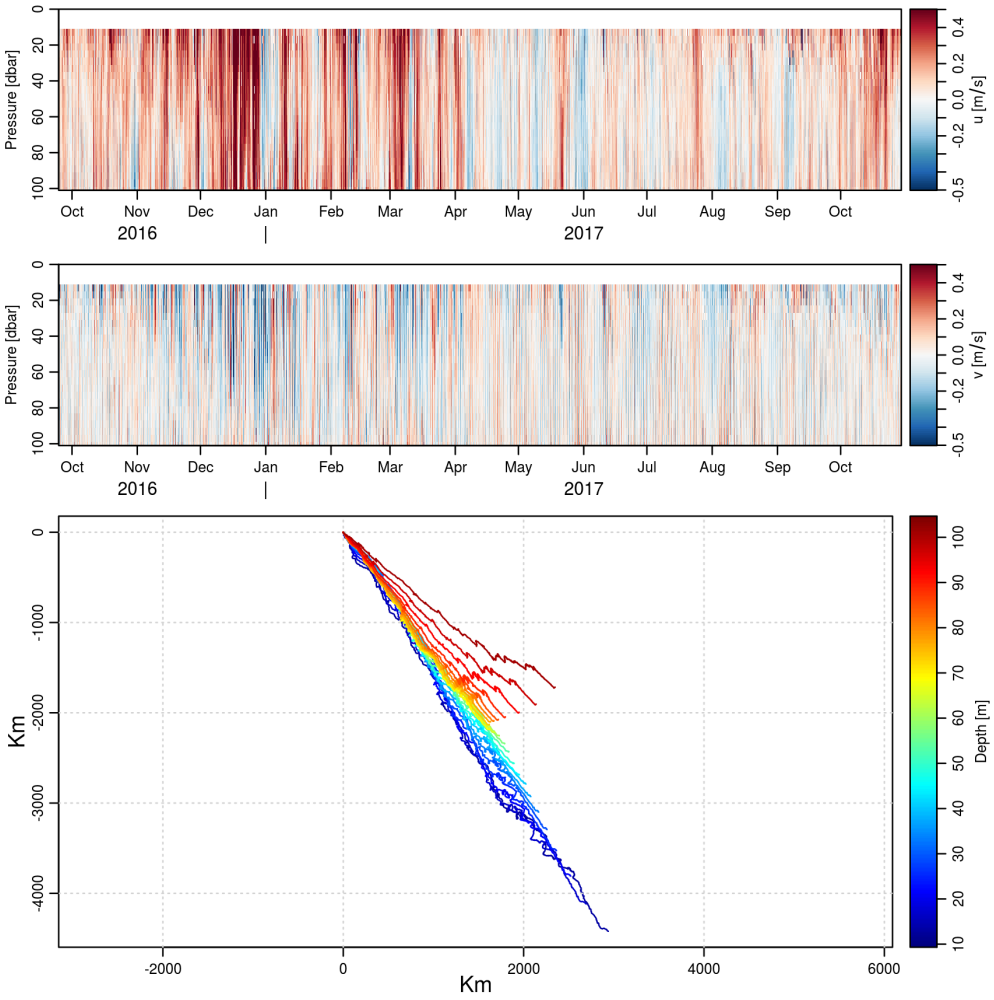

Figure 57: Velocity measurements at STAB-C from fall 2016 to fall 2017, (top) along-isobath, (middle) cross-isobath, and (bottom) a progressive vector diagram from the ADCP measurements.

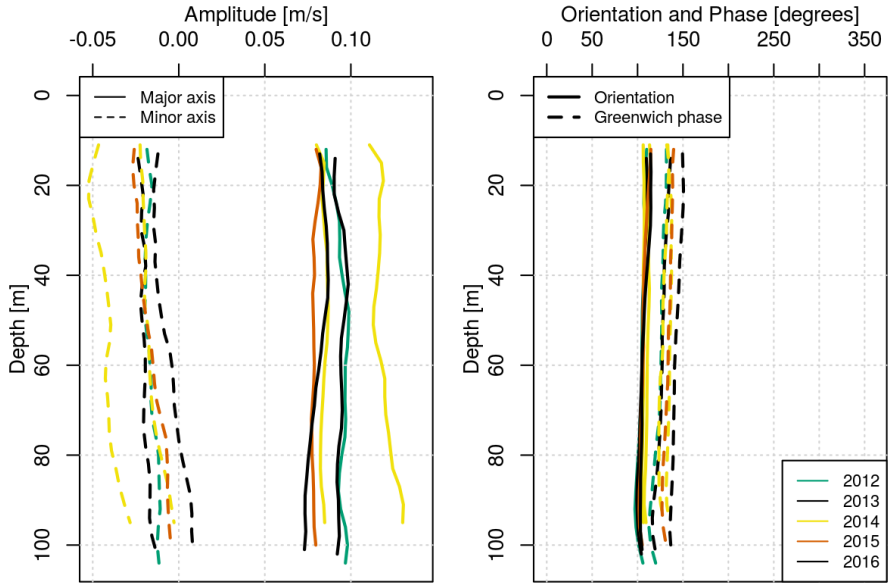

Figure 58: K1 tidal constituent parameters using the ADCP data at STAB-C, (left) major and minor axis, (right) orientation and phase.

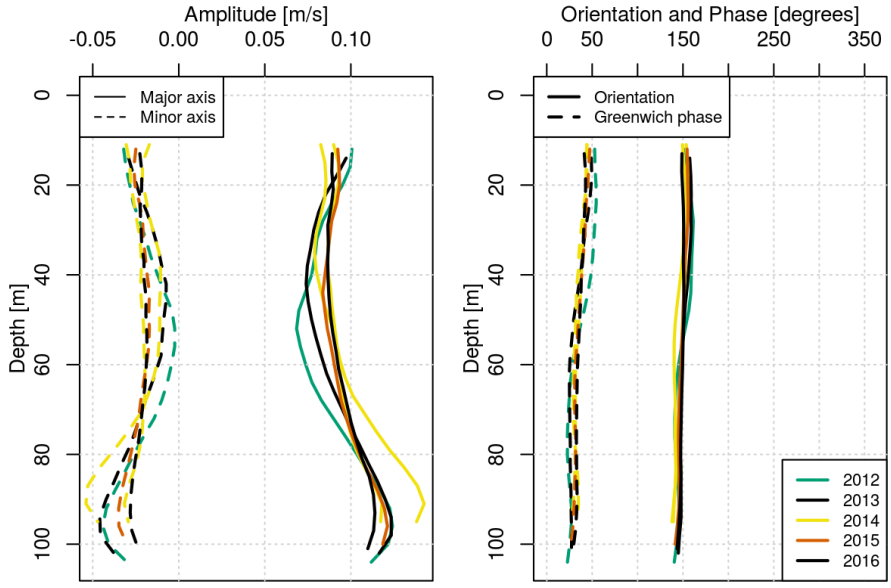

Figure 59: M2 tidal constituent parameters using the ADCP data at STAB-C, (left) major and minor axis, (right) orientation and phase.

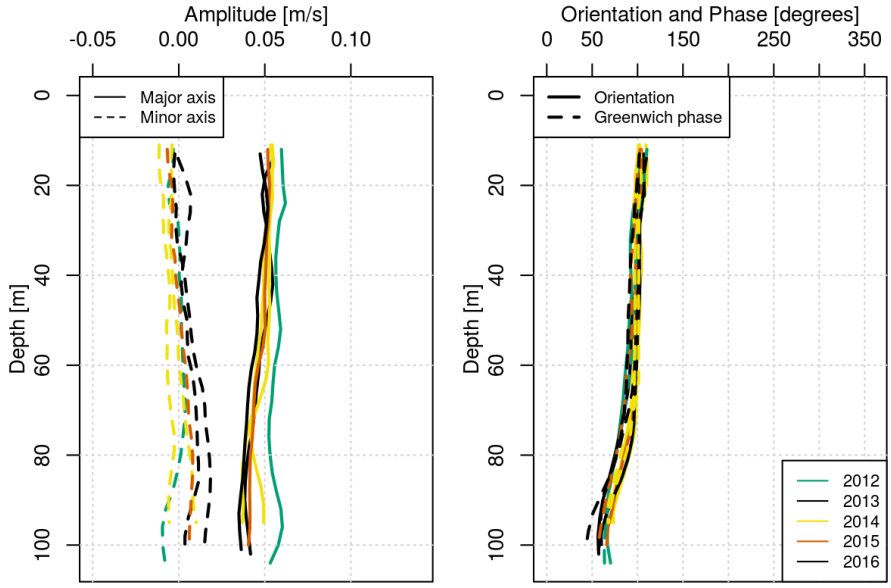

Figure 60: O1 tidal constituent parameters using the ADCP data at STAB-C, (left) major and minor axis, (right) orientation and phase.

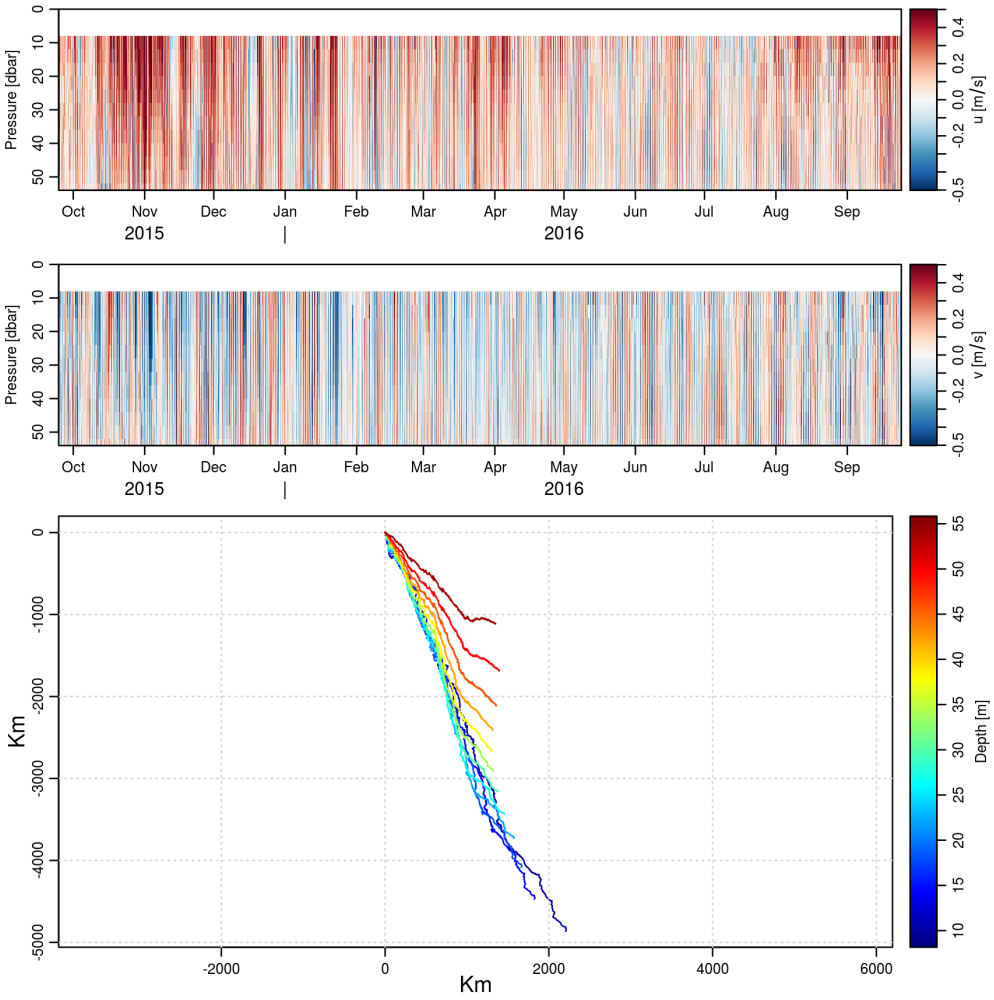

Figure 61: Velocity measurements at STAB-I from fall 2015 to fall 2016, (top) along-isobath, (middle) cross-isobath, and (bottom) a progressive vector diagram from the ADCP measurements.

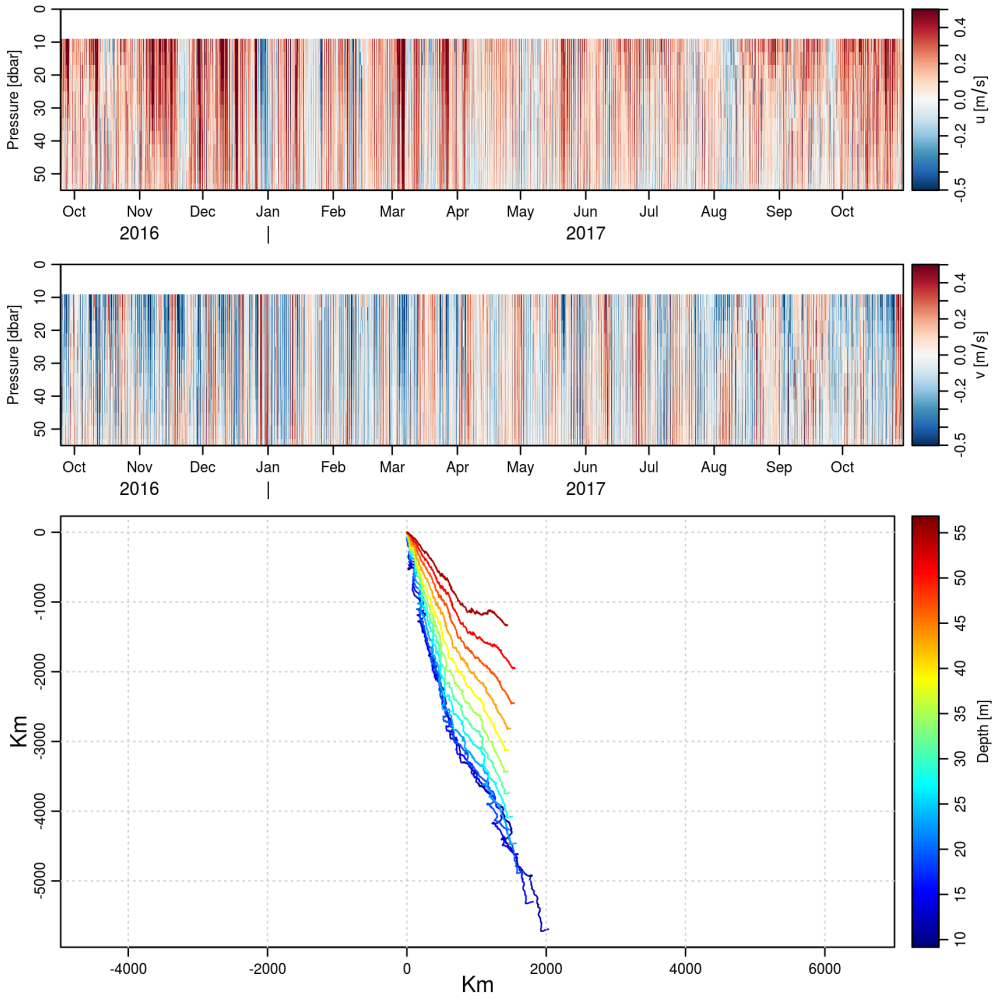

Figure 62: Velocity measurements at STAB-I from fall 2016 to fall 2017, (top) along-isobath, (middle) cross-isobath, and (bottom) a progressive vector diagram from the ADCP measurements.

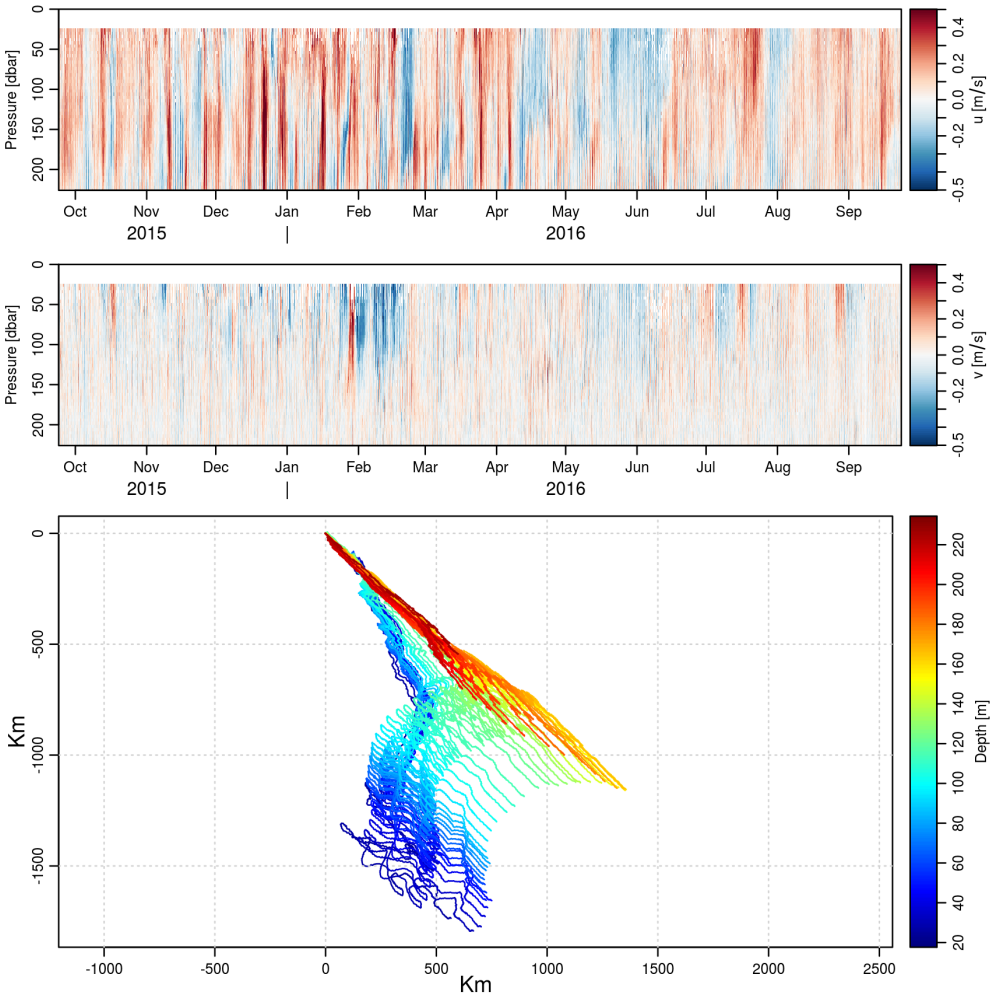

Figure 63: Velocity measurements at STAB-O from fall 2015 to fall 2016, (top) along-isobath, (middle) cross-isobath, and (bottom) a progressive vector diagram from the ADCP measurements.

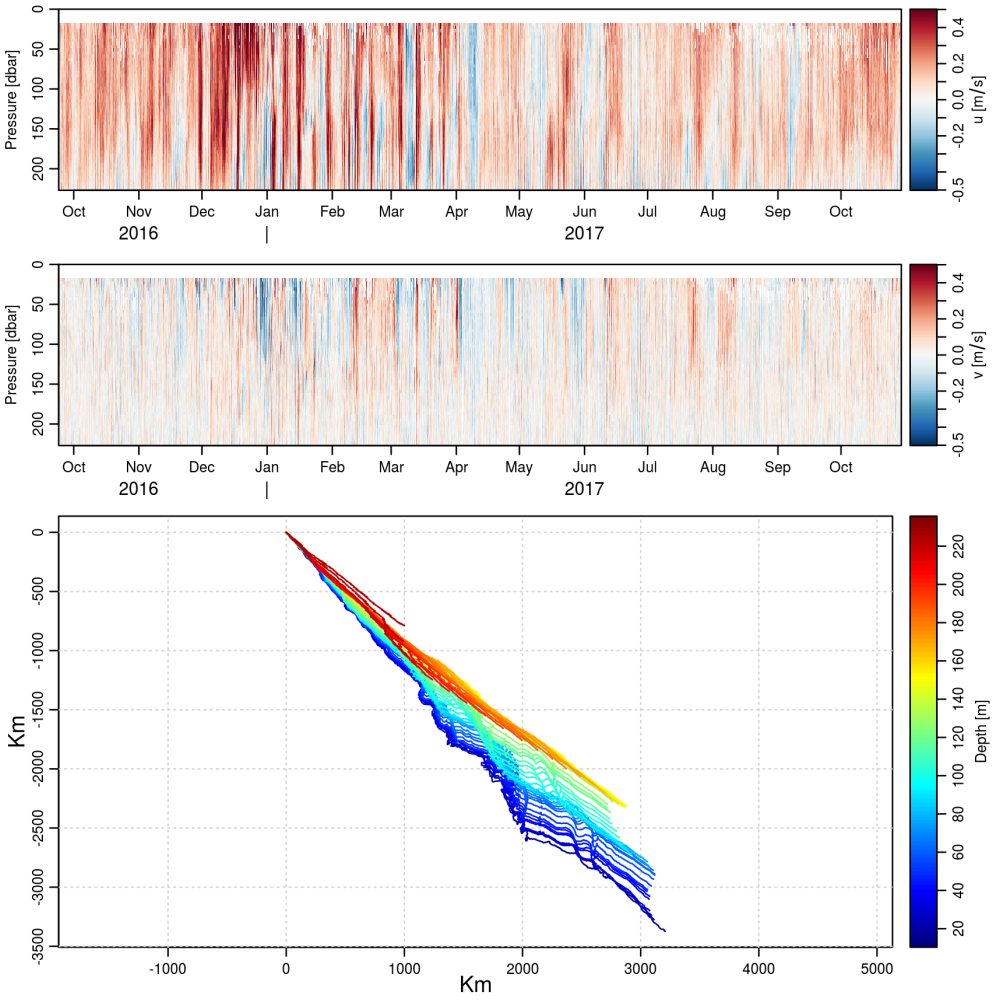

Figure 64: Velocity measurements at STAB-O from fall 2016 to fall 2017, (top) along-isobath, (middle) cross-isobath, and (bottom) a progressive vector diagram from the ADCP measurements.

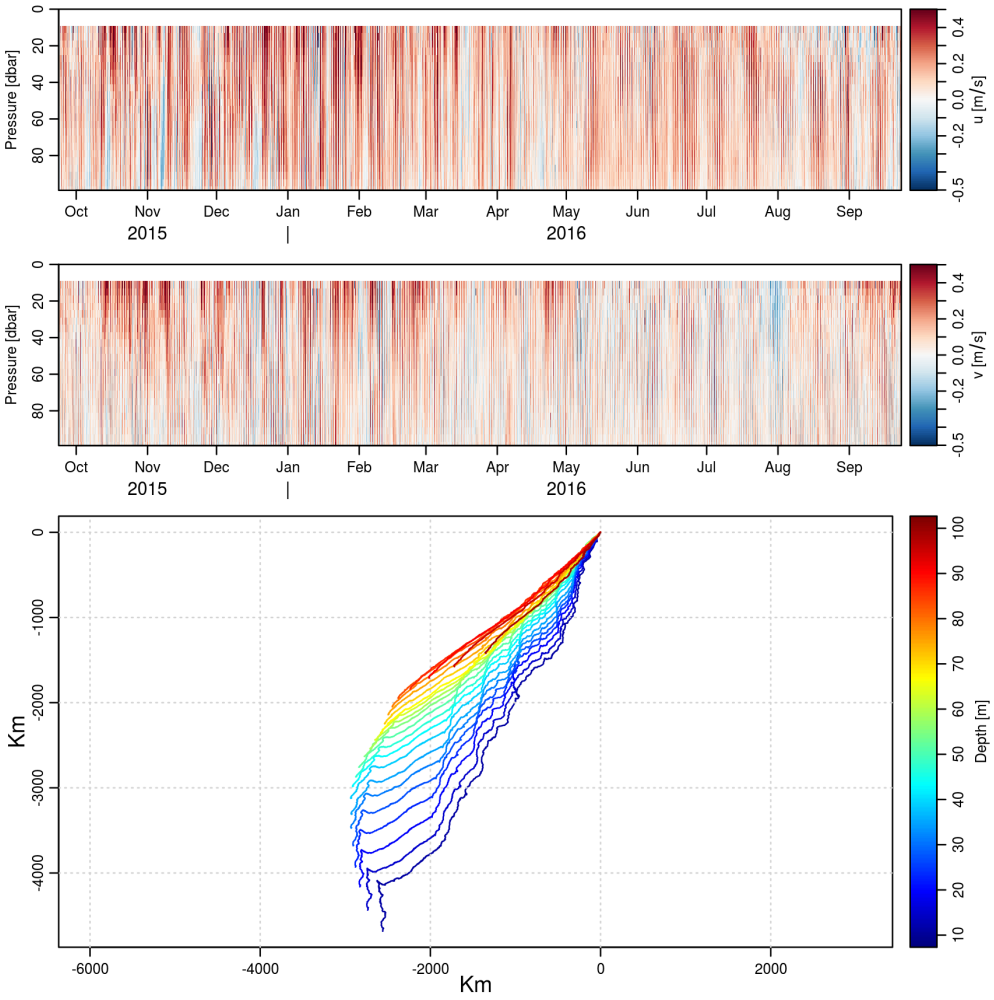

Figure 65: Velocity measurements at STAB-S from fall 2015 to fall 2016, (top) along-isobath, (middle) cross-isobath, and (bottom) a progressive vector diagram from the ADCP measurements.

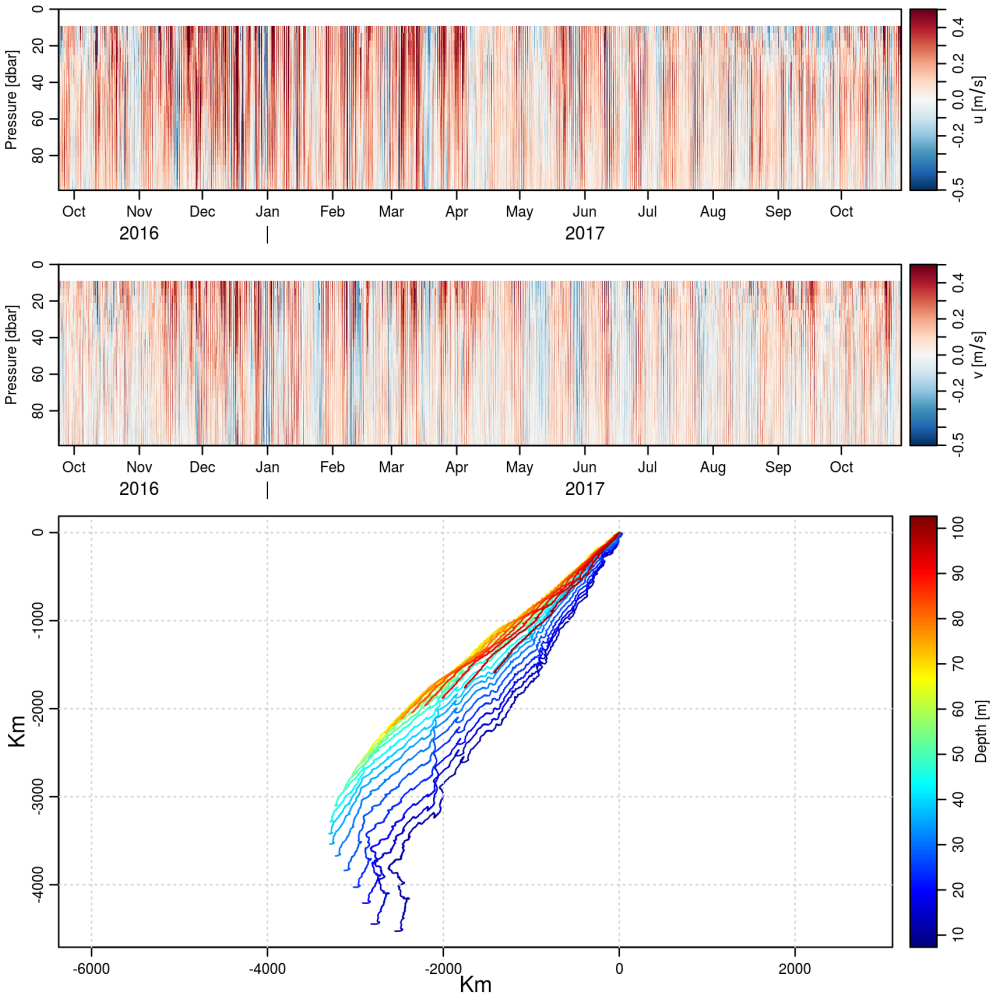

Figure 66: Velocity measurements at STAB-S from fall 2016 to fall 2017, (top) along-isobath, (middle) cross-isobath, and (bottom) a progressive vector diagram from the ADCP measurements.

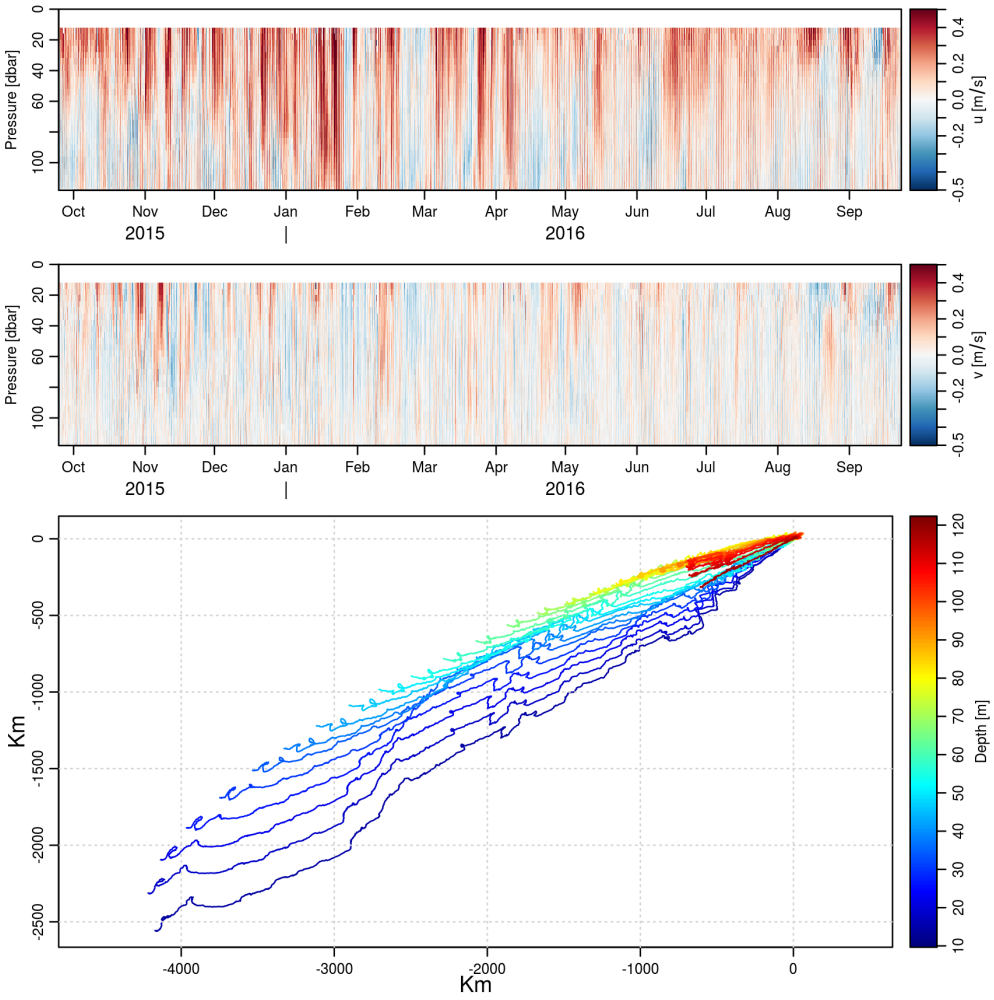

Figure 67: Velocity measurements at STAB-N from fall 2015 to fall 2016, (top) along-isobath, (middle) cross-isobath, and (bottom) a progressive vector diagram from the ADCP measurements.

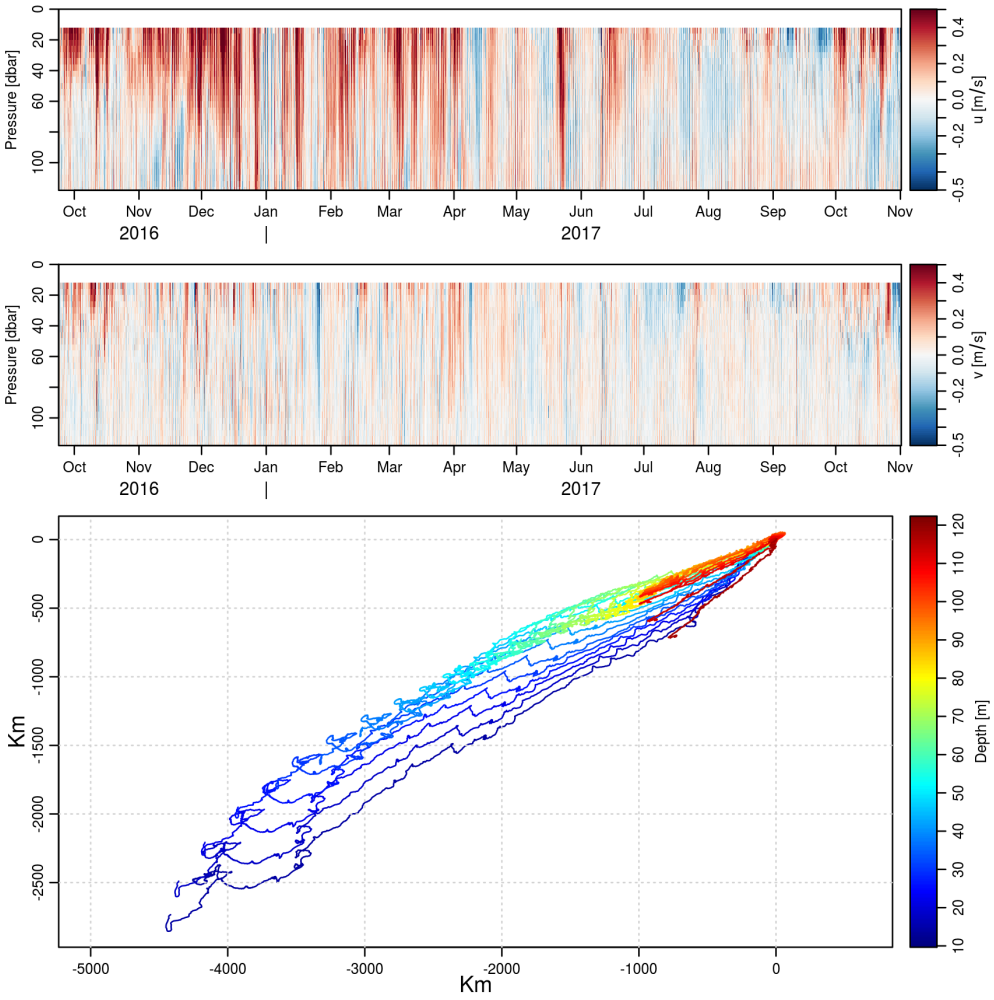

Figure 68: Velocity measurements at STAB-N from fall 2016 to fall 2017, (top) along-isobath, (middle) cross-isobath, and (bottom) a progressive vector diagram from the ADCP measurements.

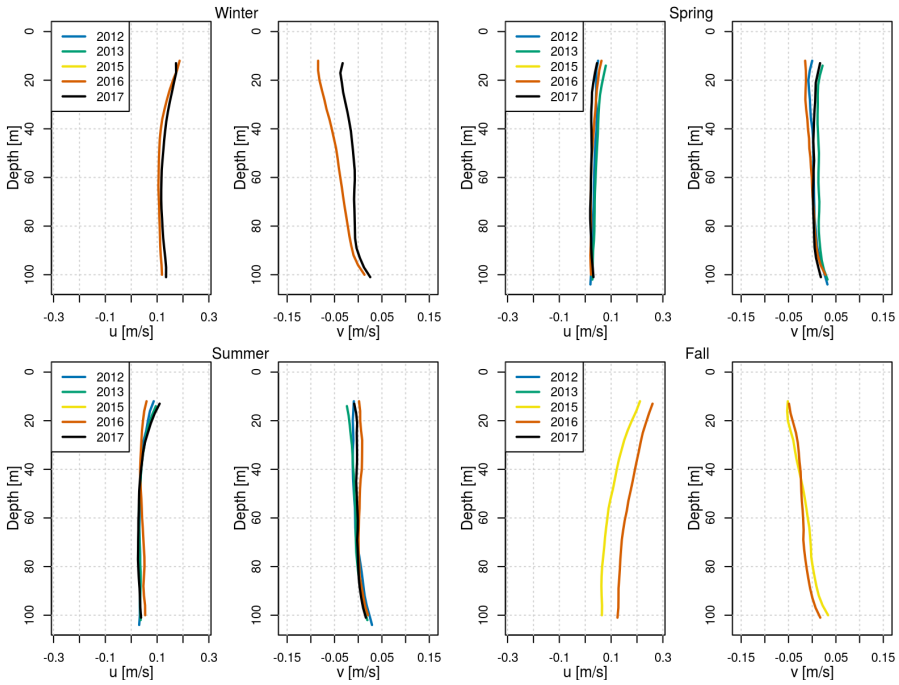

Figure 69: Seasonal average along-isobath and cross-isobath velocity component profiles for (top-left) winter, (top-right) spring, (bottom-left) summer, and (bottom-right) fall at STAB-C.

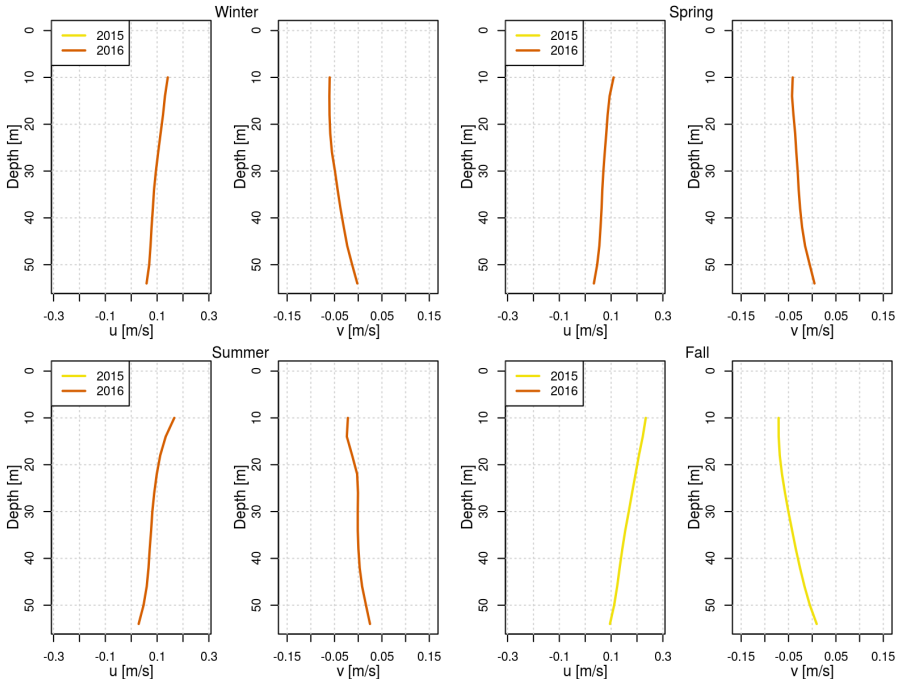

Figure 70: Seasonal average along-isobath and cross-isobath velocity component profiles for (top-left) winter, (top-right) spring, (bottom-left) summer, and (bottom-right) fall at STAB-I.

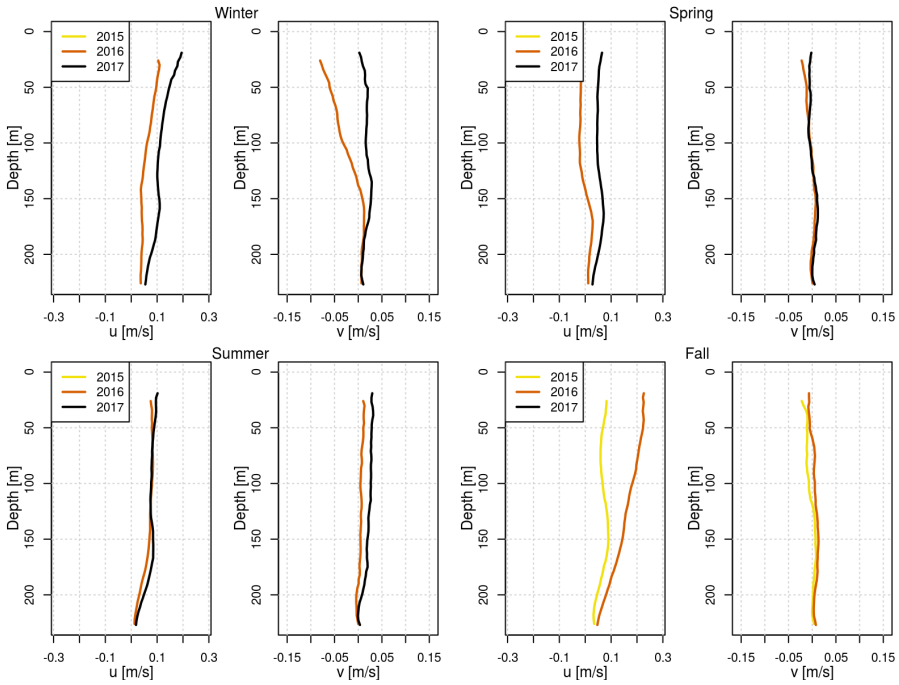

Figure 71: Seasonal average along-isobath and cross-isobath velocity component profiles for (top-left) winter, (top-right) spring, (bottom-left) summer, and (bottom-right) fall at STAB-O.

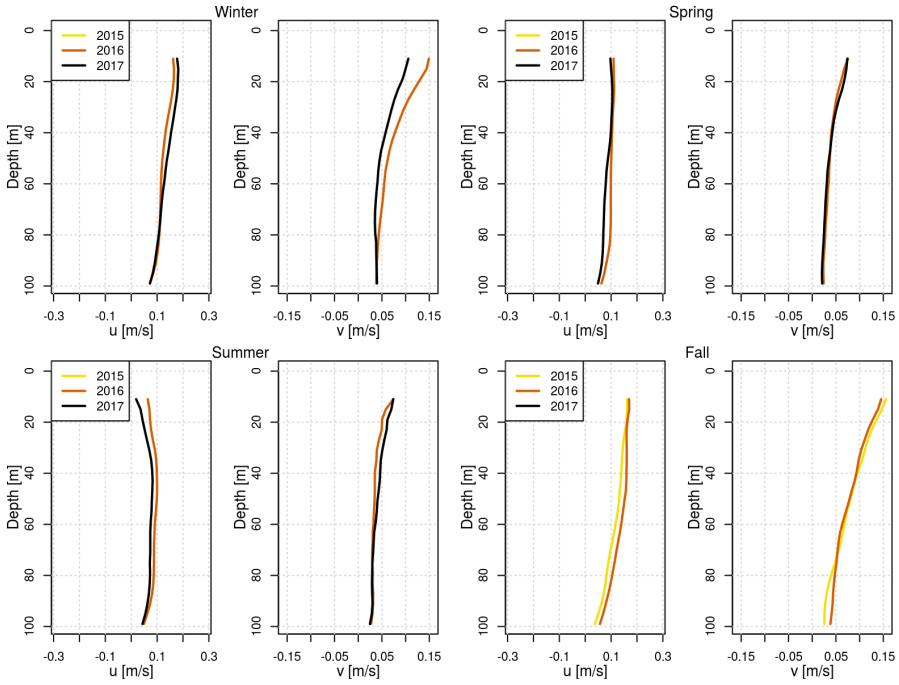

Figure 72: Seasonal average along-isobath and cross-isobath velocity component profiles for (top-left) winter, (top-right) spring, (bottom-left) summer, and (bottom-right) fall at STAB-S.

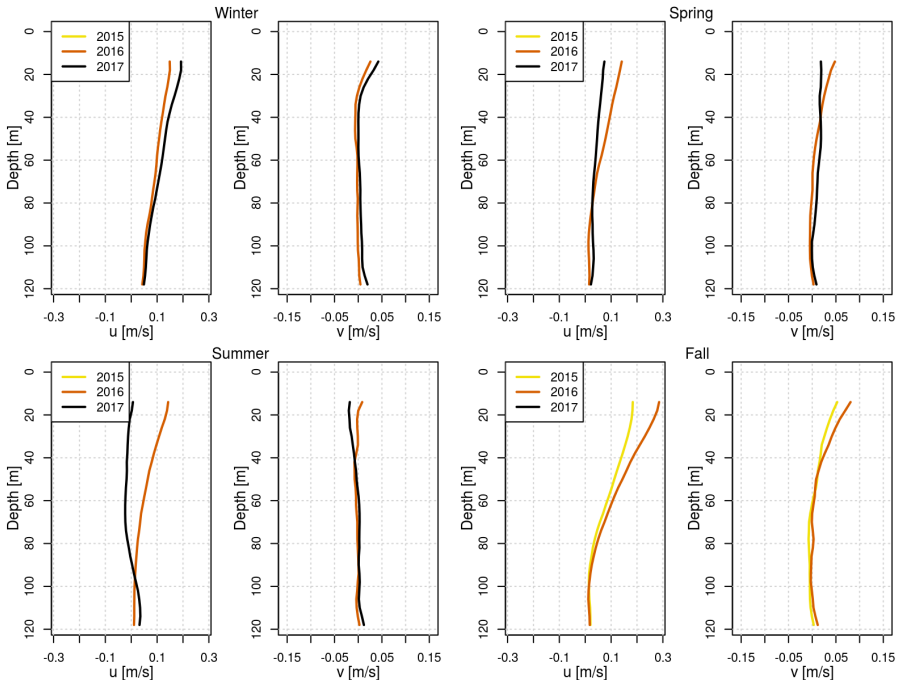

Figure 73: Seasonal average along-isobath and cross-isobath velocity component profiles for (top-left) winter, (top-right) spring, (bottom-left) summer, and (bottom-right) fall at STAB-N.

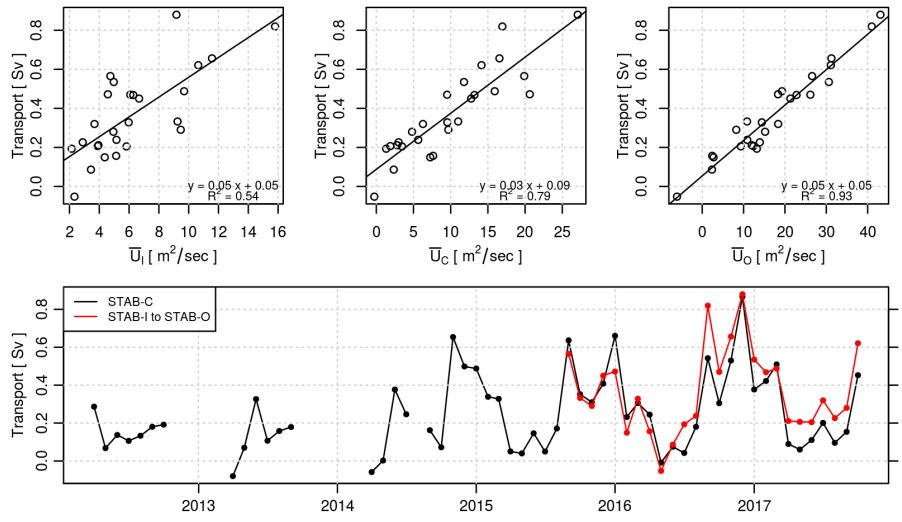

Figure 74: Linear regression of depth integrated along-isobath velocity, $\bar{U}$ at (top left) STAB-I, (top middle) STAB-C, and (top right) STAB-O against total calculated transport using measurements from all three mooring locations. (Bottom) Time-series of total calculated transport across the transect between the mooring locations for two scenario, one using just the depth integrated velocity at STAB-C, and the other using the depth integrated velocity from all three locations.

6 Tables

Table 1: Summary of CTD stations.

Cruise name	Station name	Longitude (decimal degrees)	Latitude (decimal degrees)	Sounding (m)	Maximum Depth (m)	Start time (UTC)
HUD2011043	STAB5	-58.871	46.418	365	365	2011-10-08 11:00:50
	STAB4	-59.069	46.295	155	147	2011-10-08 14:22:55
	STAB3	-59.199	46.216	92	88	2011-10-08 16:03:09
	STAB2	-59.363	46.108	68	63	2011-10-08 17:41:28
	STAB1	-59.529	45.998	60	57	2011-10-08 19:08:04
HUD2012042	STAB1	-59.533	45.996	60	53	2012-10-04 12:16:27
	STAB2	-59.358	46.106	62	60	2012-10-04 14:40:33
	STAB3	-59.200	46.220	88	82	2012-10-04 16:30:59
	STAB4	-59.070	46.300	150	149	2012-10-04 18:10:21
	STAB5	-58.880	46.421	371	366	2012-10-04 20:24:19
HUD2013004	STAB5	-58.878	46.411	363	364	2013-04-19 00:00:05
	STAB4	-59.065	46.298	159	149	2013-04-19 01:43:40
	STAB3	-59.193	46.216	94	89	2013-04-19 03:16:13
	STAB2	-59.361	46.109	68	63	2013-04-19 04:43:49
	STAB1	-59.531	46.001	60	58	2013-04-19 06:11:12
HUD2013037	STAB1	-59.530	45.998	50	51	2013-09-28 05:01:39
	STAB2	-59.363	46.108	59	60	2013-09-28 06:36:11
	STAB3	-59.200	46.219	80	81	2013-09-28 08:02:37
	STAB4	-59.071	46.300	146	149	2013-09-28 12:27:01
	STAB5	-58.876	46.417	375	367	2013-09-28 14:08:50
HUD2014004	STAB5	-58.875	46.419	392	368	2014-04-20 07:20:59
	STAB4	-59.070	46.299	156	150	2014-04-20 10:05:39
	STAB3	-59.198	46.220	88	82	2014-04-20 13:56:53
	STAB2	-59.360	46.108	68	61	2014-04-20 15:26:15
	STAB1	-59.530	46.000	62	52	2014-04-20 16:57:17
HUD2014030	STAB1	-59.533	45.996	52	49	2014-09-29 14:27:59
	STAB2	-59.366	46.105	65	60	2014-09-29 16:22:22
	STAB3	-59.197	46.215	94	88	2014-09-29 18:07:28
	STAB4	-59.066	46.300	152	152	2014-09-29 22:13:24
	STAB5	-58.883	46.416	386	366	2014-09-30 00:56:15
HUD2015004	STAB5	-58.881	46.417	370	367	2015-04-25 09:52:14
	STAB4	-59.069	46.300	150	149	2015-04-25 12:52:02
	STAB3	-59.195	46.217	-99.9	87	2015-04-25 14:47:43
	STAB2	-59.366	46.108	60	59	2015-04-25 16:36:12
	STAB1	-59.534	46.001	60	57	2015-04-25 18:15:40
HUD2015030	STAB5	-58.875	46.416	390	370	2015-09-24 03:45:41
	STAB4	-59.061	46.297	160	153	2015-09-24 06:45:06
	STAB3	-59.193	46.215	95	91	2015-09-24 08:21:01
	STAB2	-59.363	46.108	67.3	62	2015-09-24 10:01:34
	STAB1	-59.534	45.999	-99.9	56	2015-09-24 11:26:34
HUD2016003	STAB5	-58.882	46.415	365	365	2016-04-21 21:21:05
	STAB4	-59.065	46.298	161	153	2016-04-21 23:54:26
	STAB3	-59.194	46.217	94	85	2016-04-22 01:50:25
	STAB2	-59.364	46.108	68	62	2016-04-22 04:00:07
	STAB1	-59.536	45.999	60	53	2016-04-22 05:56:44
HUD2016027	STAB5	-58.880	46.420	388	367	2016-09-23 22:35:19
	STAB4	-59.062	46.301	162	154	2016-09-24 01:52:02
	STAB3	-59.194	46.216	86	85	2016-09-24 03:33:51
	STAB2	-59.367	46.102	60	58	2016-09-24 05:48:49
	STAB1	-59.535	45.996	54	54	2016-09-24 07:18:19
COR2017001	STAB1	-59.527	46.000	56	58	2017-04-27 17:41:04
	STAB2	-59.358	46.105	60	60	2017-04-27 19:27:32
	STAB3	-59.189	46.217	87	85	2017-04-27 21:09:07
	STAB4	-59.058	46.300	157	160	2017-04-27 23:07:48
	STAB5	-58.878	46.417	366	367	2017-04-28 01:38:38
EN2017606	STAB1	-59.536	46.003	66.2	60	2017-12-04 02:04:19
	STAB2	-59.368	46.111	64.5	59	2017-12-04 03:57:45
	STAB3	-59.197	46.214	94.2	89	2017-12-04 05:52:21
	STAB4	-59.066	46.300	156	154	2017-12-04 08:11:37
	STAB5	-58.892	46.414	372	359	2017-12-04 10:47:48

Table 2: Summary of moored CTD instruments.

Mooring	Deployment cruise number	Mooring number	Longitude (decimal degrees)	Latitude (decimal degrees)	Moored depth (m)	Sounding (m)	Start time (UTC)	End time (UTC)	Sampling interval (s)
STAB-C	EGR2012914	1815	-59.142	46.255	112	114	2012-04-26 15:30:00	2012-10-06 13:05:00	300
	HUD2013004	1845	-59.141	46.252	110	112	2013-04-18 13:00:00	2013-09-28 11:01:00	1860
	HUD2014004	1864	-59.151	46.246	104	106	2014-04-20 12:00:00	2014-09-29 19:31:00	1860
	HUD2014030	1896	-59.152	46.246	103	105	2014-09-29 21:05:00	2015-09-23 11:45:00	300
	HUD2015030	1898	-59.141	46.255	7	118	2015-09-23 16:00:00	2016-09-24 17:10:00	600
	HUD2015030	1899	-59.141	46.251	108	114	2015-09-23 17:00:00	2016-09-24 15:31:00	1860
	HUD2016027	1998	-59.140	46.250	109	112	2016-09-24 16:30:00	2017-08-06 13:00:00	1800
	HUD2016027	1997	-59.140	46.254	6.6	115	2016-09-24 19:45:00	2017-10-29 18:10:00	300
STAB-I	HUD2015030	1900	-59.330	46.130	62	68	2015-09-24 16:10:00	2016-09-24 10:20:00	600
STAB-O	HUD2015030	1903	-59.026	46.326	235	239	2015-09-23 18:30:00	2016-09-23 19:40:00	600
	HUD2016027	2002	-59.026	46.327	236	240	2016-09-23 20:30:00	2017-10-29 16:50:00	300
STAB-S	HUD2015030	1902	-59.142	45.899	108	113	2015-09-23 10:00:00	2016-09-23 14:30:00	600
	HUD2016027	2001	-59.142	45.900	107	112	2016-09-23 15:10:00	2017-10-29 12:50:00	600
STAB-N	HUD2015030	1901	-59.742	45.741	126	132	2015-09-24 13:20:00	2016-09-23 11:20:00	600
	HUD2016027	2000	-59.742	45.741	126	131	2016-09-23 12:10:00	2017-11-01 11:05:00	300

Table 3: Summary of ADCP instruments.

Mooring	Deployment cruise number	Mooring number	Longitude (decimal degrees)	Latitude (decimal degrees)	Sounding (m)	Min bin depth (m)	Max bin depth (m)	Bin interval (m)	Start time (UTC)	End time (UTC)	Sampling interval (s)
STAB-C	EGR2012914	1815	-59.142	46.255	114	12	104	4	2012-04-26 15:35:00	2012-10-06 12:55:00	600
	HUD2013004	1845	-59.141	46.252	112	14	102	4	2013-04-18 13:02:30	2013-09-28 10:32:30	1800
	HUD2014004	1864	-59.151	46.246	106	11	95	4	2014-04-20 12:02:36	2014-07-20 07:58:49	1806
	HUD2014030	1896	-59.152	46.246	105	11	95	4	2014-09-29 21:32:15	2015-09-09 08:32:15	1800
	HUD2015030	1899	-59.141	46.251	114	12	100	4	2015-09-23 17:00:30	2016-09-24 15:00:30	3600
	HUD2016027	1998	-59.140	46.250	112	13	101	4	2016-09-24 17:00:30	2017-10-29 19:00:30	3600
STAB-I	HUD2015030	1900	-59.330	46.130	68	10	54	4	2015-09-24 17:00:30	2016-09-24 10:00:30	3600
	HUD2016027	1999	-59.332	46.129	66	11	55	4	2016-09-24 12:00:30	2017-10-29 21:00:30	3600
STAB-O	HUD2015030	1903	-59.026	46.326	239	26	226	4	2015-09-23 19:01:30	2016-09-23 19:01:30	3600
	HUD2016027	2002	-59.026	46.327	240	19	227	4	2016-09-23 21:01:30	2017-10-29 16:01:29	3600
STAB-S	HUD2015030	1902	-59.142	45.899	113	11	99	4	2015-09-23 10:00:30	2016-09-23 14:00:30	3600
	HUD2016027	2001	-59.142	45.900	112	11	99	4	2016-09-23 16:00:30	2017-10-29 12:00:30	3600
STAB-N	HUD2015030	1901	-59.742	45.741	132	14	118	4	2015-09-24 14:00:30	2016-09-23 11:00:30	3600
	HUD2016027	2000	-59.742	45.741	131	14	118	4	2016-09-23 13:00:30	2017-11-01 10:00:30	3600

Table 4: Summary of successfully recovered moored temperature recording instruments which were only used for the STAB-C mooring location.

Deployment cruise number	Mooring number	Longitude (decimal degrees)	Latitude (decimal degrees)	Moored depth (m)	Minimum depth (m)	Maximum depth (m)	Sounding (m)	Start time (UTC)	End time (UTC)	Sampling interval (s)
EGR2012914	1815	-59.142	46.257	3	1	3	120	2012-04-26 16:20:00	2012-10-06 12:00:00	1200
		-59.145	46.254	28	1	29	120	2012-04-26 17:00:00	2012-10-06 11:00:00	1200
		-59.142	46.257	53	1	54	120	2012-04-26 16:40:00	2012-10-06 12:00:00	1200
		-59.145	46.254	75	8	76	120	2012-04-26 17:00:00	2012-10-06 11:20:00	1200
HUD2013004	1845	-59.143	46.256	2			110	2013-04-18 12:00:00	2013-07-22 08:40:00	600
		-59.143	46.256	12	13	23	110	2013-04-18 12:00:00	2013-09-28 10:00:00	1200
		-59.143	46.256	14			110	2013-04-18 12:00:00	2013-09-28 10:00:00	600
		-59.143	46.256	19			110	2013-04-18 12:00:00	2013-09-28 10:00:00	600
		-59.143	46.256	24			110	2013-04-18 12:00:00	2013-09-28 10:00:00	600
		-59.143	46.256	29			110	2013-04-18 12:00:00	2013-09-28 10:00:00	600
		-59.143	46.256	34			110	2013-04-18 12:00:00	2013-09-28 10:00:00	600
		-59.143	46.256	39			110	2013-04-18 12:00:00	2013-09-28 10:00:00	600
		-59.143	46.256	49	52	59	110	2013-04-18 12:00:00	2013-09-28 10:00:00	1200
		-59.143	46.256	59			110	2013-04-18 12:00:00	2013-09-28 10:00:00	600
		-59.143	46.256	74			110	2013-04-18 12:00:00	2013-09-28 10:00:00	600
		-59.143	46.256	89			110	2013-04-18 12:00:00	2013-09-28 10:00:00	600
HUD2015030	1898	-59.141	46.255	10	5	29	118	2015-09-23 16:30:00	2016-09-24 17:00:00	1800
		-59.141	46.255	15			118	2015-09-23 16:30:00	2016-09-24 17:00:00	1800
		-59.141	46.255	20			118	2015-09-23 16:30:00	2016-09-24 17:00:00	1800
		-59.141	46.255	25			118	2015-09-23 16:30:00	2016-09-24 17:00:00	1800
		-59.141	46.255	30			118	2015-09-23 16:30:00	2016-09-24 17:00:00	1800
		-59.141	46.255	60			118	2015-09-23 16:30:00	2016-09-24 17:00:00	1800
		-59.141	46.255	75			118	2015-09-23 16:30:00	2016-09-24 17:00:00	1800
		-59.141	46.255	90			118	2015-09-23 16:30:00	2016-09-24 17:00:00	1800
HUD2016027	1997	-59.140	46.254	8	4	44	115	2016-09-24 20:00:00	2017-10-29 18:00:00	1800
		-59.140	46.254	23			115	2016-09-24 20:00:00	2017-10-29 18:00:00	1800
		-59.140	46.254	28			115	2016-09-24 20:00:00	2017-10-29 18:00:00	1800
		-59.140	46.254	33			115	2016-09-24 20:00:00	2017-10-29 18:00:00	1800
		-59.140	46.254	38			115	2016-09-24 20:00:00	2017-10-29 18:00:00	1800
		-59.140	46.254	48	47	78	115	2016-09-24 20:00:00	2017-10-29 18:00:00	1800
		-59.140	46.254	58			115	2016-09-24 20:00:00	2017-10-29 18:00:00	1800
		-59.140	46.254	73			115	2016-09-24 20:00:00	2017-10-29 18:00:00	1800
		-59.140	46.254	89	89	102	115	2016-09-24 19:45:00	2017-10-29 18:05:00	300